What is inside an electron: the physics of electromagnetic waves that are perceived as quantum mechanical waves

András Kovács, Giorgio Vassallo, Antonino Oscar Di Tommaso, and Francesco Celani

Published by the Zitter Institute (zitter-institute.org). The book content does not necessarily represent a consensus of all Zitter Institute members.

ISBN 978-952-65314-2-7 (softcover)

ISBN 978-952-65314-3-4 (PDF)

Contents

Preface

This book is for all who are curious about our physical world. We present electromagnetism as a proper field theory, and show how electromagnetic fields and charges are both defined by the electromagnetic vector potential. Using this field theory, it becomes possible to quantitatively describe the electron's internal structure. Our work builds upon the ideas of Maxwell, Dirac, and their notable contemporaries such as Einstein, Heisenberg, and De Broglie. We believe that our ideas formulated in chapters 1-3, were already implicit in the theoretical foundations of physics established more than eighty years ago, but for whatever reason were never fully developed afterwards. In a plausible alternative past, our ideas might have been considered self-evident already by the mid-20th century. It is our hope, that as the book becomes more widely known, it will be recognized as a standard tool of modern physics.

We develop our ideas using the powerful tool of geometric algebra and the foundational concepts stemming from Maxwell and Dirac but also contribute something new in our approach. Key mathematical concepts and structures are explained in the first chapters with the aim of making the book accessible to readers who have the interest and the capability for self-study. Nevertheless, it does presuppose a certain level of mathematical skills essential for developing a correct understanding of electromagnetics and its Lagrangian.

To justify our theory, we discuss a large set of validating experimental data coming from mainstream physics which we believe, in contrast to some current theories, can be explained in an insightful and simple way with our approach. We are not interested in imposing ad-hoc rules (such as imposing the Lorenz gauge rule onto electromagnetic equations, or cutting of the counting of electromagnetic field energy at a certain distance from a supposedly point-like electron) and neither in analyzing exotic fringe experiments (such as the study of yet another meson particle with 10^{-22} sec lifetime) but instead, we shall refer to very fundamental data that characterizes electrons.

The history of physics may be viewed as a progression from particle-oriented to wave-oriented concepts to wave-particle duality. A thousand years ago, if one tried to talk about "fields" and "waves", they would have been met with blank stares. Only the concept of matter particles existed at the time, with direct mechanical interactions among them. Waves were only observed on the surface of water, and were neither understood mathematically nor were they thought to be related to anything else. Scientists, at the time, thought of light as a stream of small "light balls". In contrast, today physicists describe light as waves in the electromagnetic field but also exhibiting particle properties. All mechanical and chemical forces are also described as being exerted by such electromagnetic waves. Approximately, a hundred years ago, the notion that elementary matter particles might also be quantum mechanical waves started to gain acceptance. In this sense, our book simply fits into the historic trend, and represents a next step in the understanding of wave-oriented concepts.

It is worth recalling that such steps in the past have usually been met by strong opposition from the scientific community. We illustrate this through the brief history of light model evolution from the original "light balls" description. Around 1687, Newton and Leibnitz independently discovered differential calculus, which is needed to quantitatively describe waves. However, it took one hundred and thirty more years to recognize light as a wave. In 1818, the scientific Académie of France offered a prize for a consistent understanding of light diffraction. At that time, light diffraction experiments were considered an anomaly of the prevailing "light balls" model. One of the participants, civil engineer and optometrist Augustin-Jean Fresnel submitted a thesis in which he explained diffraction from analysis of both the Huygens–Fresnel principle and Young's double slit experiment. This irritated the academic "old guard", who were staunch believers in the particle theory of light and were skeptical of its alternative, the wave theory. Poisson, a member of the Académie, studied Fresnel's theory in detail and looked for a way to prove it wrong. Poisson thought that he had found a flaw when he demonstrated that Fresnel's theory predicts an on-axis bright spot in the shadow of a circular obstacle blocking a point source of light, where the particle-theory of light predicts complete darkness. Poisson argued this was absurd and Fresnel's model was wrong. The head of the committee, Dominique-François-Jean Arago, performed the experiment. To everyone's surprise, he observed the predicted bright spot, which vindicated the wave model. Fresnel won the

competition, and the wave nature of light gained acceptance in mainstream scientific circles. However, the "field" part was still missing, and mainstream physicists now considered light to be a wave in the physical aether, which they believed filled the vacuum. In essence, the traveling "light balls" model was replaced by a "sea of light carrying balls" model, facilitating the waves.

Maxwell's discovery of electromagnetic field equations in 1862 spelled the beginning of the end for this "sea of light carrying balls" model. After Einstein's discovery of relativity in the early 20th century, Silberstein published a seminal book in 1914, titled "The Theory of Relativity". In this book he quantitatively described how light is carried by a relativistic electromagnetic field. The journal, Nature, published a vitriolic review of Silberstein's work. From the perspective of the reviewer, Silberstein's main sin was to have left the aether out of the discussion: "There is scarcely a reference to the longings of the physicist for an objective aether ... Many will read Dr Silberstein's careful and detailed introduction to it, consider his illustrations, and follow his logic, and yet feel there is something lacking. The argument in favor of an aether is not dealt with. The reluctance that Lorentz had to abandon the aether remains. The seeker after a deeper understanding of the physical is apt to fight shy of a principle which cannot be expressed in terms of concepts to which he can give some degree of substantiality." Eventually, the quantitative theory of electromagnetic field waves gave birth to a wide range of new radio technologies, while the theory of aether was of no use to radio engineers. The aether theory was then quietly abandoned by theoretical physicists. Starting from Fresnel's thesis, the whole process took over one hundred years.

The fundamental equations of physics appear to be remarkably straightforward but the set of their possible solutions is anything but simple. This is not a contradiction: simple equations may allow for many classes of solutions, various symmetries and novel interpretations. Our approach of seeing elementary particles as being akin to electromagnetic waves, although it might not initially be widely accepted, is consistent with the standard equations. We hope there will be some modern-day Aragos among readers, who will strive to resolve experimental anomalies, by carefully considering the various options, and by trying to design experiments to test the quantitative predictions of our theory.

In the last part of this introduction we outline our scientific methodology. Scientists like to think of their respective field as an additive process, which advances through the accumulation of ever wiser ideas and ever more elaborate concepts. That is generally true, but one must be careful to retain checks and balances and correct mistakes or oversights that may slip in.

Correcting mistakes often reveals a more fundamental perspective, whereby one realizes that separate physical laws or phenomena are one and the same thing and can be unified. To give an example from a pre-Newtonian era, the celestial motion of planets was accurately and predictively described by Earth-centered epicycloid formulas. The gravitational fall of bodies was accurately and predictively described by a constant acceleration formula. These two phenomenological laws were thought to be completely unrelated, and scientists of the day had no sense of any mistaken assumption: their formulas were predictive and accurate. They were the top theoreticians of the day, drawn from the same gene pool as today's theoreticians. But their thinking was locked into a mistaken paradigm. Once Newton's efforts revealed the mistaken assumptions, the phenomena of celestial motions and falling bodies were unified, although it continued to meet opposition from some who insisted that their model of Earth-centered epicycloid motions was the correct model of reality. One must understand that phenomenological formulas may involve unrealistic models of reality, even while being experimentally correct.

Correcting mistaken historic assumptions is therefore an important aspect of our methodology. The more one reflects on the foundations, the more one understands the obstacles that stand in the way of progress. We hope readers will appreciate our quest for truth. Correcting mistakes is by no way disrespectful of the scientists who worked on the involved problems. We are grateful for the efforts of others, and recognize that without their results this book would be impossible. In particular, we would like to mention the efforts of Marcel Riesz, who pioneered the geometric algebra perspective for studying electromagnetism, and the efforts of H. E. Moses, who first proposed that Maxwell equations may be treated as proper field equations. In case some readers might be wondering why we did not cite or mention others; be assured that we did not have the intention to ignore anyone, and will gladly add names when appropriate. We simply aim to keep the text as self-consistent and focused as possible.

Our book adheres to Occam's razor principle, and demonstrates that a better understanding of electromagnetic wave dynamics leads to an improved understanding of our physical world. We outline below the key physics equations of the book, so that the reader knows what to anticipate. In the following equations, the $\boldsymbol{\partial}$ operator is expressed in terms of space-time basis vectors. The evolution of electromagnetic fields and charges can be equivalently calculated from Maxwell's equation or from the electromagnetic Lagrangian density:

$$\boldsymbol{\partial}^2 \boldsymbol{A}_{\square} = 0 \;\Leftrightarrow\; \mathscr{L} = \frac{1}{2\mu_0} \boldsymbol{\partial} \boldsymbol{A}_{\square} \widetilde{\boldsymbol{\partial} \boldsymbol{A}_{\square}}$$

where the space-time metric is flat. The above equations are the fundamental equations of electrodynamics, but they have not been previously expressed in this simple form because electric charges have been treated as externally added "black box" objects. We identify both longitudinal and transversal electromagnetic wave solutions. We find that the electron dynamics is defined by a Lagrangian action $\mathscr{S}$, which is derived from a longitudinal electromagnetic wave:

$$\mathscr{S} = \int (e\boldsymbol{A} \cdot \boldsymbol{c} - eV)\, dt$$

where V and $\boldsymbol{A}$ are the electromagnetic vector potential components experienced by the electron charge. The above formula for $\mathscr{S}$ remains valid down to the classical electron radius scale. Using these quantities, the electron's mass-energy can be expressed in natural units as $[m_e = eV = eA]_{NU}$. When an electron is observed from a reference frame boosted by a Lorentz boost factor γ_L, its relativistic mass becomes γ_L times larger. We show that this relativistic mass increase is caused by the combination of transversal relativistic Doppler shift and Lorentz contraction; these effects adjust both the electron wavelength and electron size by γ_L^{-1} factor. The shrinking electron size intensifies the electromagnetic fields around the electron charge, and the experienced vector potential becomes proportional to the frequency of electron wave. De Broglie's $mc^2 = \hbar\omega$ relation thus remains valid in any reference frame.

In the absence of noise, the above-mentioned $\mathscr{S}$ action describes a well-defined electron path. However, the electron wave is embedded in a noisy vacuum environment. Specifically, the mean electric and magnetic field energy of vacuum noise is given by the following expression:

$$\varepsilon_0 \bar{E}^2 = \frac{\bar{B}^2}{\mu_0} = \frac{1}{V} \sum \frac{1}{2} \hbar\omega$$

where V is a unit volume element, and the summation runs over all possible frequencies. Essentially, the reduced Planck constant $\hbar$ defines the vacuum noise amplitude. The above infinite summation yields an infinitely large noise energy. The reason why this infinitely large noise effect is not perceived in classical mechanics is that the electron responds to vacuum noise only in a surprisingly tight frequency range: $\frac{\omega_{max}}{\omega_{min}} = 2\pi$. We determine this phenomenological $\frac{\omega_{max}}{\omega_{min}} = 2\pi$ ratio from the Lamb-shift effect, and our work is the first correct evaluation of this ratio as far as we know. At the vacuum noise amplitude defined by $\hbar$, the electron wave is thus transparent to all noise frequencies higher than ω_{max} or lower than ω_{min}: that is the linear electromagnetic regime where all electromagnetic waves pass through each other. I.e. the threshold between linear and non-linear electromagnetic regimes depends on the wave amplitude and wave frequency as well. The higher an electromagnetic wave amplitude is, the more readily it interacts with an electron wave, giving all the well-known electron-light interaction phenomena.

The vacuum noise adds a random walk pattern onto the evolution of the electron wave: the overall electron propagation probability between two points is obtained by calculating and summing up $e^{i\mathscr{S}/\hbar}$ factors for each possible path connecting these points, where $\mathscr{S}$ is the above-mentioned electromagnetic action and the $\hbar$ noise amplitude becomes a diffusion parameter. On the one hand, the electron is subject to a noise-induced random distribution, and on the other hand its electromagnetic wave evolves according to the above-indicated Lagrangian. Regarding this second aspect, the electron's quantum mechanical wavenumber becomes the Lorentz-transformed spatial component of the electromagnetic wave's time evolution, and we derive the Aharonov-Bohm formula describing the evolution of the quantum mechanical phase φ:

$$\varphi = \frac{e}{\hbar} \int \boldsymbol{A} \cdot d\boldsymbol{l} = \frac{e}{\hbar} \int_T V dt$$

where V and $\boldsymbol{A}$ are again the electromagnetic vector potential components experienced by the electron charge. From these considerations, it is possible to derive the Schrödinger and Dirac equations that describe the evolution of the electron wavefunction ψ. Keeping in mind that the electron wavefunction

describes a probability distribution where ψ is strictly scalar valued, the Dirac equation takes on a particularly simple mathematical form, and can be written in two equivalent ways:

$$I\hbar\partial\psi = mc\psi \;\Leftrightarrow\; \hbar\partial\psi = -\boldsymbol{m}c\psi$$

where I is the Clifford pseudoscalar, $I\boldsymbol{m} \equiv m$ is the tri-vector representation of the electron mass, and $\boldsymbol{m}$ is the vector representation of electron mass. The needlessly complicated preceding formulations of the Dirac equation are no longer necessary. Although the Dirac equation is linear, it yields extremely precise energy eigenvalue solutions, not just a linear estimate. This means that the electron mass term of the Dirac equation somehow incorporates non-linearity, and corresponds to a parameter value that stabilizes the underlying non-linear electron wave. In the context of Maxwell's equation, non-linear terḿs appear as a consequence of curved space-time, and it is well known that electromagnetic energy density creates space-time curvature. We show that the electromagnetic energy density energy-momentum density vector $\boldsymbol{w}$ can be expressed as a rotation of the time base vector γ_t :

$$\boldsymbol{w} = \frac{1}{2\mu_0}\left(\boldsymbol{\partial A}_{\square}\gamma_t\widetilde{\boldsymbol{\partial A}_{\square}}\right)$$

where $\boldsymbol{\partial A}_{\square}$ gives the electromagnetic field in a physical sense and it is a rotor in a mathematical sense. The more intense the electromagnetic field is, the more it twists the time basis vector with respect to the spatial basis vectors. Since the Dirac equation's mass term incorporates non-linearity, it must be somehow related to space-time curvature. We refer to the work of Paul O'Hara, who found that the Dirac equation is such an eigenvalue equations where the mass term can be expressed in terms of space-time metric:

$$\frac{\partial\psi}{\partial s} = \frac{mc}{\hbar}\psi$$

where s measures space-time distance, and it is defined as $ds^2 \equiv g_{\mu\nu}dx^\mu dx^\nu$. The above relationship expresses a very interesting property of the electron wave. We propose the following hypothesis on the origin of electron mass value m_e: this value must lead to the $\frac{\partial\psi}{\partial s} = \frac{m_e c}{\hbar}\psi$ relation, which as an apparent condition on particle stability, although we do not yet understand the reason behind this condition.

Any stable electron state is an eigenstate solution of the Dirac equation: such solutions are standing waves characterized by a well-defined energy eigenvalue. We find that all stable electron charge circulations generate a magnetic flux that is quantized in units of h/e. A stable electron state generally involves two such circulations: its orbital current and its spin current.

Our companion book titled "The Bose-Einstein condensation of electrons: a long overdue discovery of how superconductors really work" applies the above outlined concepts to problems of practical interest. It is shown that the well-defined energy eigenstate condition requires that N electrons occupying a quantum mechanical state must be isotropically spin correlated, and in the case of incoherent electrons this condition can be fulfilled only for $N \leq 2$. I.e. the electron spin value has nothing to do with Pauli exclusion, and after 100 years of postulates based approach to the Pauli exclusion principle we shed light on how chemistry really works. For the $N = 2$ case, we show that isotropic spin correlation can be fulfilled for both parallel and anti-parallel spin alignments. The parallel spin alignment of electron pairs is usually energetically unfavorable, and thus rarely observed. Nevertheless, the experimentally confirmed existence of electron pairs' parallel spin alignment confirms our calculations and invalidates the historically embraced postulates about anti-symmetric electron wavefunctions. The practical relevance of electron pairs' parallel spin alignment is that these pairs seed the Bose-Einstein condensation of electron waves. We shows experimental evidence of both delocalized and bound electrons' Bose-Einstein condensation: the delocalized case is the superconductivity phenomena, and the bound case opens up a whole new domain of chemistry.

An introduction to Clifford algebra

Andras Kovacs[1]
[1] ExaFuse. E-mail: andras.kovacs@broadbit.com

We begin by briefly introducing the mathematical language of Clifford algebra, that is used extensively in this book. Beyond this introduction, a complete Clifford algebra tutorial can be found in reference [**1**].

Mathematical nomenclature

The following notations are used throughout the book.

$\boldsymbol{A}_{\square}, A$**:** four-vector in Minkowski spacetime;
$\boldsymbol{A}_{\triangle}, \mathbf{A}$**:** three-vector in physical space;
$\gamma_x, \gamma_{xy}, \gamma_{xyz}, \gamma_{xyzt} \equiv I$**:** Clifford bases for vectors, bi-vectors, tri-vectors, and the pseudo-scalar;
$\widetilde{A}$**:** Clifford reversion of A;
$\bar{C}$**:** the complex conjugate of a complex number C;

0.1. Clifford algebra overview

Clifford algebra is defined by the multiplication rule of its basis elements. The Clifford basis elements are defined to obey the following multiplication rules:

$$\gamma_t^2 = -1, \gamma_x^2 = \gamma_y^2 = \gamma_z^2 = 1 \tag{0.1.1}$$

$$\gamma_i \gamma_j = -\gamma_j \gamma_i \, (i \neq j) \tag{0.1.2}$$

The t index represents the time coordinate, and indices x, y, z represent spatial coordinates. Thus the Clifford algebra basis elements can be identified with the unit vectors spanning our four dimensional space-time.

The above defined algebra of the 3+1 basis elements is referred to as $Cl_{3,1}(\mathbb{R})$ algebra type. In the context of the Dirac equation, the above base vectors are equivalent to the Dirac gamma matrices.

The multiplication of two different base vectors defines a bi-vector, which spans an oriented surface. We use the following notation for bi-vectors: $\gamma_{ij} \equiv \gamma_i \gamma_j$. Similarly, tri-vectors are volume elements, and denoted as: $\gamma_{ijk} \equiv \gamma_i \gamma_j \gamma_k$. The dimensionality of an expression goes up through multiplication of different base vector components.

Based on the above definitions, we observe the following multiplication properties:

$$\gamma_x \gamma_{xyz} = \gamma_{yz}, \; \gamma_y \gamma_{xyz} = -\gamma_{xz}, \; \gamma_z \gamma_{xyz} = \gamma_{xy} \tag{0.1.3}$$

$$\gamma_{yz} \gamma_{xyz} = -\gamma_x, \; \gamma_{zx} \gamma_{xyz} = -\gamma_y, \; \gamma_{xy} \gamma_{xyz} = -\gamma_z \tag{0.1.4}$$

$$-1 = \boldsymbol{\gamma}_{ij}^{\mathbf{2}} = \boldsymbol{\gamma}_{ijk}^{\mathbf{2}} \, (i \neq j \neq k, i \neq t, j \neq t, k \neq t) \tag{0.1.5}$$

The above multiplication examples illustrate how the dimensionality of an expression goes down through the multiplication of same base vector components.

A useful notation for a space-time vector is $Q = (Q_t \gamma_t, \mathbf{Q})$, where the bold capital notation is denoting a spatial vector, i.e. $\mathbf{Q} = q_x \gamma_x + q_y \gamma_y + q_z \gamma_z$. The product of two vectors is:

$$PQ = (P_t \gamma_t, \mathbf{P})(Q_t \gamma_t, \mathbf{Q}) = (-P_t Q_t + \mathbf{P} \cdot \mathbf{Q}) + (-P_t \mathbf{Q} + \mathbf{P} Q_t) \gamma_t + \mathbf{P} \times \mathbf{Q} \gamma_{xyz} \tag{0.1.6}$$

In the above expression the $(-P_tQ_t+\mathbf{P}\cdot\mathbf{Q})$ part is scalar, while the other terms are bi-vectors. However, we wrote the bivector terms by highlighting two spatial vectors: $(-P_t\mathbf{Q}+\mathbf{P}Q_t)$ and $\mathbf{P}\times\mathbf{Q}$. It must be kept in mind that the bold $\mathbf{P}\times\mathbf{Q}$ notation represents a spatial vector.

We define the unitary pseudoscalar as $I\equiv\gamma_{txyz}$, composed of the space-time unit vectors. Algebraically, we can identify the imaginary unit i with the unitary pseudoscalar I. We note that $I\gamma_t=\gamma_{txyz}\gamma_t=\gamma_{xyz}$, and that $I\mathbf{P}=-\mathbf{P}I$ because a vector contains one index same as γ_{txyz}. Because of this commutation rule, multiplying a vector by I is different from numerical multiplication. On the other hand, the multiplication of a scalar or bi-vector by I commutes the same way as numerical multiplication.

0.2. An electromagnetic application example

We define the differentiation operator $\boldsymbol{\partial}$ in space-time algebra:

$$\boldsymbol{\partial}=\gamma_x\frac{\partial}{\partial x}+\gamma_y\frac{\partial}{\partial y}+\gamma_z\frac{\partial}{\partial z}+\gamma_t\frac{1}{c}\frac{\partial}{\partial t}\equiv\nabla+\gamma_t\frac{1}{c}\partial_t, \tag{0.2.1}$$

where $\nabla=\gamma_x\frac{\partial}{\partial x}+\gamma_y\frac{\partial}{\partial y}+\gamma_z\frac{\partial}{\partial z}$ and $c=1/\sqrt{\epsilon_0\mu_0}$).

The electromagnetic vector potential can be written as $A\equiv(A_t\gamma_t,\mathbf{A})$, where $\mathbf{A}$ contains the spatial components of the vector potential.

We apply the $\boldsymbol{\partial}$ operator to A:

$$\begin{aligned}\boldsymbol{\partial}A&=\left(-\frac{1}{c}\partial_tA_t+\nabla\cdot\mathbf{A}\right)+\left(-\frac{1}{c}\partial_t\mathbf{A}+\nabla A_t\right)\gamma_t+\nabla\times\mathbf{A}\gamma_{xyz}=\\&=\left(-\frac{1}{c}\partial_tA_t+\nabla\cdot\mathbf{A}\right)+\mathbf{B}\gamma_{xyz}+\mathbf{E}\gamma_t\end{aligned} \tag{0.2.2}$$

where the terms inside the parenthesis have scalar dimensionality, the magnetic field $\mathbf{B}$ is a spatial vector, and the electric field $\mathbf{E}$ is also a spatial vector.

Equation 0.2.2 essentially means that $\boldsymbol{\partial}A$ yields the electromagnetic fields. Alternatively, the above space-time differentiation can also be written with the following notation:

$$\boldsymbol{\partial}A=\boldsymbol{\partial}\cdot A+\boldsymbol{\partial}\wedge A=S+\boldsymbol{F} \tag{0.2.3}$$

where $S\equiv\left(-\frac{1}{c}\partial_tA_t+\nabla\cdot\mathbf{A}\right)$ contains the scalar result of dot-product differentiation, while the $\boldsymbol{F}\equiv\mathbf{B}\gamma_{xyz}+\mathbf{E}\gamma_t$ bi-vector is the result of wedge-product differentiation and it is known as the anti-symmetric Faraday tensor.

References [**2, 3, 4, 5, 6, 7**] thoroughly explain the practical use of Clifford algebra in physics.

0.3. Clifford reversion and Clifford rotors

We define Clifford reversion as the operator which reverses the order of base vectors. Scalars and vectors thus remain unchanged upon reversion: $\widetilde{S}=S$ and $\widetilde{\gamma_i}=\gamma_i$. Reversion acts as follows on bi-vectors and tri-vectors: $\widetilde{(\gamma_i\gamma_j)}=\gamma_j\gamma_i=-\gamma_i\gamma_j$ and $\widetilde{(\gamma_i\gamma_j\gamma_k)}=\gamma_k\gamma_j\gamma_i=-\gamma_i\gamma_j\gamma_k$.

Consider the $\gamma_x\gamma_y$ plane spanned by the orthogonal unit vectors γ_x and γ_y. As shown in reference [**1**], a rotation in this plane by an angle 2θ can is a linear map r, that is given by:

$$\gamma_y\mapsto r\left(\gamma_y\right)=e^{-\theta\gamma_x\gamma_y}\gamma_ye^{\theta\gamma_x\gamma_y}\equiv\boldsymbol{R}\gamma_y\tilde{\boldsymbol{R}} \tag{0.3.1}$$

where the object $\boldsymbol{R}=e^{-\theta\gamma_x\gamma_y}$ is called a rotor, and it encodes in a compact way both the plane of rotation and the angle.

When the same map is applied to a basis vector which is orthogonal to the rotation plane, it remains unaffected by the rotation:

$$\gamma_z\mapsto r\left(\gamma_z\right)=e^{-\theta\gamma_x\gamma_y}\gamma_ze^{\theta\gamma_x\gamma_y}=\gamma_z \tag{0.3.2}$$

Regarding a rotation around an arbitrary axis, it can be performed by some rotor $\boldsymbol{R}=e^{-\theta\boldsymbol{m}\wedge\boldsymbol{n}}$, where $\boldsymbol{m}\wedge\boldsymbol{n}$ spans the plane in which the rotation is performed, and the angle of rotation is 2θ.

It is important to note that these rotation rules also apply to the four-vectors of the space-time algebra. In particular, rotors with pure spatial bi-vector parts (such as $\gamma_x\gamma_y$) generate ordinary rotations, whereas γ_t containing bi-vectors (such as $\gamma_z\gamma_t$) generate hyperbolic rotations which are the Lorentz boosts. Rotor operations are a very powerful geometric tool for numerous applications.

The group of three dimensional rotations is the $SO(3)$ group. In Clifford algebra, rotation can be represented by two unitary complex numbers. The group of two unitary complex numbers is the $SU(2)$ group. The important point here is that a rotor with angle θ generates physical rotation with angle 2θ. Thus one full circle in the rotor space corresponds to two full circles of physical rotation. This is what mathematicians mean by saying that the $SU(2)$ group is a double cover of the $SO(3)$ group.

Bibliography

[1] Clifford algebra tutorial available at: https://www.worldscientic.com/doi/10.1142/9781800611306_fmatter01

[2] G. Bettini. Clifford Algebra, 3 and 4-Dimensional Analytic Functions with Applications. Manuscripts of the Last Century. Quantum Physics:1–63, 2011

[3] J. M. Chappell, S. P. Drake, C. L. Seidel, L. J. Gunn, A. Iqbal, A. Allison, and D. Abbott. Geometric Algebra for Electrical and Electronic Engineers. Proceedings of the IEEE, 102(9):1340–1363, Sept 2014.

[4] David Hestenes. Spacetime Physics with Geometric Algebra. American Journal of Physics, 71(3):691–714, July 2003.

[5] Justin Dressel, Konstantin Y. Bliokh, and Franco Nori. Spacetime Algebra as a Powerful Tool for Electromagnetism. Physics Reports, 589:1 – 71, 2015

[6] David Hestenes. Reforming the Mathematical Language of Physics. Oersted Medal Lecture, 2002.

[7] Amr M. Shaarawi. Clifford algebra formulation of an electromagnetic charge-current wave theory. Foundations of Physics, 30(11):1911–1941, 2000.

CHAPTER 1

Maxwell's equations and Occam's razor

Francesco Celani[1,2], **Antonino Oscar Di Tommaso**[3] and **Giorgio Vassallo**[2,3]

[1] Istituto Nazionale di Fisica Nucleare (INFN-LNF), Via E. Fermi 56, 00044 Frascati, Roma, Italy. E-mail: francesco.celani@lnf.infn.it.

[2] International Society for Condensed Matter Nuclear Science (ISCMNS)-UK.

[3] Università degli Studi di Palermo - Engineering Department, viale delle Scienze, 90128 Palermo, Italy. E-mail: antoninooscar.ditommaso@unipa.it, giorgio.vassallo@unipa.it.

Nomenclature

Symbol, name, SI units, natural units (NU).

$\boldsymbol{A}_{\square}$: electromagnetic four-potential $[\mathrm{V}\cdot\mathrm{s}\cdot\mathrm{m}^{-1}]$, [eV];
$\boldsymbol{r}_{\square}$: four-position vector [m], $[\mathrm{eV}^{-1}]$;
$\boldsymbol{G}$: electromagnetic field $[\mathrm{V}\cdot\mathrm{s}\cdot\mathrm{m}^{-2}]$, $[\mathrm{eV}^2]$;
$\boldsymbol{F}$: electromagnetic field bivector $[\mathrm{V}\cdot\mathrm{s}\cdot\mathrm{m}^{-2}]$, $[\mathrm{eV}^2]$;
$\boldsymbol{B}$: flux density field $[\mathrm{V}\cdot\mathrm{s}\cdot\mathrm{m}^{-2}] = [\mathrm{T}]$, $[\mathrm{eV}^2]$;
$\boldsymbol{E}$: electric field $[\mathrm{V}\cdot\mathrm{m}^{-1}]$, $[\mathrm{eV}^2]$;
S: scalar field $[\mathrm{V}\cdot\mathrm{s}\cdot\mathrm{m}^{-2}]$, $[\mathrm{eV}^2]$;
$\boldsymbol{J}_{\square e}$: four-current density field $[\mathrm{A}\cdot\mathrm{m}^{-2}]$, $[\mathrm{eV}^3]$;
$\boldsymbol{v}_{\square}$: four-velocity vector $[\mathrm{m}\cdot\mathrm{s}^{-1}]$, [1];
$\boldsymbol{A}'$: electromagnetic eight-potential $[\mathrm{V}\cdot\mathrm{s}\cdot\mathrm{m}^{-1}]$, [eV];
P: pseudoscalar field $[\mathrm{V}\cdot\mathrm{s}\cdot\mathrm{m}^{-2}]$, $[\mathrm{eV}^2]$;
$\boldsymbol{J}_{\square m}$: magnetic four-current density field $[\mathrm{A}\cdot\mathrm{s}\cdot\mathrm{m}^{-3}]$, $[\mathrm{eV}^3]$;
ρ: charge density $[\mathrm{A}\cdot\mathrm{s}\cdot\mathrm{m}^{-3} = \mathrm{C}\cdot\mathrm{m}^{-3}]$, $[\mathrm{eV}^3]$;
ρ_m: magnetic charge density $[\mathrm{A}\cdot\mathrm{m}^{-2}]$, $[\mathrm{eV}^3]$;
x, y, z: space coordinates [m], $[\mathrm{eV}^{-1}]$, $[1.973\,270\,5\cdot10^{-7}\ \mathrm{m} = 1\ \mathrm{eV}^{-1}]$;
t: time variable [s], $[\mathrm{eV}^{-1}]$, $[6.582\,122\cdot10^{-16}\ \mathrm{s} = 1\ \mathrm{eV}^{-1}]$;
c: light speed in vacuum $[2.997\,924\,58\cdot10^{8}\ \mathrm{m}\cdot\mathrm{s}^{-1}]$, [1];
μ_0: permeability of vacuum $[4\pi\cdot10^{-7}\ \mathrm{V}\cdot\mathrm{s}\cdot\mathrm{A}^{-1}\cdot\mathrm{m}^{-1}]$, $[4\pi]$;
ϵ_0: dielectric constant of vacuum $[8.854\,187\,817\cdot10^{-12}\ \mathrm{A}\cdot\mathrm{s}\cdot\mathrm{V}^{-1}\cdot\mathrm{m}^{-1}]$, $[\frac{1}{4\pi}]$;
$\boldsymbol{P}_{\square}$: electromagnetic four-momentum $[\mathrm{kg}\cdot\mathrm{m}\cdot\mathrm{s}^{-1}]$, [eV];
$\mathfrak{S}$: generalized Poynting vector $[\mathrm{W}\cdot\mathrm{m}^{-2}]$, $[\mathrm{eV}^4]$.
w: specific energy $[\mathrm{J}\cdot\mathrm{m}^{-3}]$, $[\mathrm{eV}^4]$.

1.1. Introduction

Science is based on the creation and validation of models of abstract concepts and experimental data. For this reason it is important to examine the rules used to evaluate the quality of a model. Occam's razor principle emphasizes the simplicity and conciseness of the model: among different models that fit experimental data, the simplest one must be preferred, *i.e.* the model that does not introduce concepts or entities that are not strictly necessary. The following sentences in Latin [**2**] briefly illustrate this principle:

Pluralitas non est ponenda sine necessitate.

Frustra fit per plura quod potest fieri per pauciora.

Entia non sunt multiplicanda praeter necessitatem.

which can be translated respectively as "plurality should not be posited without necessity.", "it is futile to do with more things that which can be done with fewer" and "entities must not be multiplied beyond necessity".

According to this principle, the model quality can be measured by means of two fundamental parameters:

(1) Good agreement of model's predictions with experimental data and/or with other expected results;

(2) The model's simplicity: a value that is inversely related to the amount of information, concepts, entities, exceptions, postulates, parameters and variables used by the model itself.

These rules are universal, and can be applied in many contexts [**16**]. In this chapter, we apply Occam's razor principle to Maxwell's equations.

We introduce and use the space-time Clifford algebra, showing that only one fundamental physical entity is sufficient to describe the origin of electromagnetic fields, charges and currents*:* the electromagnetic four-potential. The vector potential should not be viewed only as a mathematical tool but as a real physical entity, as suggested by the Aharonov-Bohm effect, a quantum mechanical phenomenon in which a charged particle is affected by the electromagnetic potentials in regions in which the electromagnetic fields are null [**1**]. Actually, many papers deal with the application of geometric algebra to Maxwell's equation (see [**3, 4, 5, 7, 19**] and many others), but few of them deal with the concept of scalar field. Among the most interesting works we can find a paper by Giuliano Bettini [**3**], two papers written by K. J. van Vlaenderen [**21, 22**] and two papers of Lee M. Hively [**14, 15**].

In this work we propose a reinterpretation of Maxwell's equations which does not use any gauge: the unique constraint is that the electromagnetic four-potential must be represented by a *harmonic* function, as proposed by G. Bettini [**3**]. A mistaken application of the so called "Lorenz gauge" in Maxwell's equations *denies the status of real physical entity* to a scalar field that, although not directly observable, has a gradient in space-time with clear physical meaning: the microscopic four-current density field. As a consequence of our approach, a spinor field that encodes the electromagnetic fields and the derivative of a scalar field emerges from Maxwell's equations. The scalar field will be here investigated and it will be shown that its existence has many implications and consequences on the microscopic structure of electrical charges and currents. It points towards a particular *Zitterbewegung* model for charged elementary particles.

This chapter is composed of the following parts: Section 1.2 illustrates how Maxwell's equations can be derived only from the electromagnetic four potential; Section 1.3 deals with the main properties of the electromagnetic field, the derivation of Maxwell's equations from the Lagrangian density, the generalized Poynting vector, the symmetrical Maxwell's equations and, finally, in Section 1.4 some essential points are summarized.

1.2. Gaugeless electrodynamics as a proper field theory

The behavior of electromagnetic waves was described in 1865 by James Clerk Maxwell in his work "Dynamical Theory of the Electromagnetic Field". Maxwell's equations are a system of partial differential equations, where different concepts are employed: electric field, flux density (or magnetic) field, charge density and current density [**3, 4, 7**].

In order to study the undulatory behavior of particles, the concept of wave function was introduced. Following the interpretation of Born, the "square" of this function represents the probability density to find a particle in a point of the space, just like the undulatory theory of light, whose intensity is given by the square of the electromagnetic wave amplitude. Now, following the principle of Occam's razor, which suggests carefulness in the introduction of new concepts, we consider two interesting possibilities:

(1) find a common origin of the conceptual entities used in Maxwell's equations;
(2) consider the wave function as a particular reformulation of concepts/entities already present in Maxwell's equations.

1.2.1. The Electromagnetic Four Potential. Maxwell's equations can be reinterpreted by means of a unique entity, namely, the electromagnetic four potential, as defined by the following equation:

$$\boldsymbol{A}_{\square}\left(\boldsymbol{r}_{\square}\right)=\gamma_{x}A_{x}\left(\boldsymbol{r}_{\square}\right)+\gamma_{y}A_{y}\left(\boldsymbol{r}_{\square}\right)+\gamma_{z}A_{z}\left(\boldsymbol{r}_{\square}\right)+\gamma_{t}A_{t}\left(\boldsymbol{r}_{\square}\right), \tag{1.2.1}$$

where each of the vector potential components A_x, A_y, A_z and A_t are functions of the space-time coordinates and $\boldsymbol{r}_{\square}\left(x,y,z,t\right)=\gamma_{x}x+\gamma_{y}y+\gamma_{z}z-\gamma_{t}ct=\boldsymbol{r}_{\triangle}-\gamma_{t}ct$ is the position vector in space-time. The γ_i unit vectors are the basis elements of $Cl_{3,1}$ Clifford algebra. From now on, in the four-potential and in other field quantities the variable $\boldsymbol{r}_{\square}$ will be omitted for simplicity. The four-potential has dimension in SI units equal to $[V\cdot s\cdot m^{-1}]$. Two basic assumptions are made:

(1) the vector potential field $\boldsymbol{A}_{\square}$ is represented by a *harmonic* function;
(2) the space is homogeneous, linear and isotropic.

Therefore, we assume a function that links a vector of four components to each point of the space-time as the unique source of Maxwell's equations entities.

We use the following definition of the operator $\boldsymbol{\partial}$ in space-time algebra

$$\boldsymbol{\partial} = \gamma_x \frac{\partial}{\partial x} + \gamma_y \frac{\partial}{\partial y} + \gamma_z \frac{\partial}{\partial z} + \gamma_t \frac{1}{c}\frac{\partial}{\partial t} = \nabla + \gamma_t \frac{1}{c}\frac{\partial}{\partial t}, \tag{1.2.2}$$

where $\nabla = \gamma_x \frac{\partial}{\partial x} + \gamma_y \frac{\partial}{\partial y} + \gamma_z \frac{\partial}{\partial z}$ and $c = 1/\sqrt{\epsilon_0 \mu_0}$).

If $\boldsymbol{A}_\square$ is the vector potential defined by (1.2.1) the following expression can be written:

$$\boldsymbol{\partial}\boldsymbol{A}_\square = \boldsymbol{\partial} \cdot \boldsymbol{A}_\square + \boldsymbol{\partial} \wedge \boldsymbol{A}_\square = S + \boldsymbol{F} = \boldsymbol{G}, \tag{1.2.3}$$

where

$$\boldsymbol{G}(x,y,z,t) = S + \gamma_x\gamma_t F_{xt} + \gamma_y\gamma_t F_{yt} + \gamma_z\gamma_t F_{zt} + \gamma_y\gamma_z F_{yz} + \gamma_x\gamma_z F_{xz} + \gamma_x\gamma_y F_{xy}. \tag{1.2.4}$$

Expanding (1.2.3), by considering the products as shown in Table 1 and by collecting all terms with the same blade, the following set of equations is found:

$$\boldsymbol{\partial} \cdot \boldsymbol{A}_\square = S = \frac{\partial A_x}{\partial x} + \frac{\partial A_y}{\partial y} + \frac{\partial A_z}{\partial z} - \frac{1}{c}\frac{\partial A_t}{\partial t} \tag{1.2.5}$$

$$\gamma_x\gamma_t F_{xt} = \gamma_x\gamma_t \frac{1}{c} E_x = \gamma_x\gamma_t \left(\frac{\partial A_t}{\partial x} - \frac{1}{c}\frac{\partial A_x}{\partial t} \right) \tag{1.2.6}$$

$$\gamma_y\gamma_t F_{yt} = \gamma_y\gamma_t \frac{1}{c} E_y = \gamma_y\gamma_t \left(\frac{\partial A_t}{\partial y} - \frac{1}{c}\frac{\partial A_y}{\partial t} \right) \tag{1.2.7}$$

$$\gamma_z\gamma_t F_{zt} = \gamma_z\gamma_t \frac{1}{c} E_z = \gamma_z\gamma_t \left(\frac{\partial A_t}{\partial z} - \frac{1}{c}\frac{\partial A_z}{\partial t} \right) \tag{1.2.8}$$

$$\gamma_y\gamma_z F_{yz} = \gamma_y\gamma_z B_x = \gamma_y\gamma_z \left(\frac{\partial A_z}{\partial y} - \frac{\partial A_y}{\partial z} \right) \tag{1.2.9}$$

$$\gamma_x\gamma_z F_{xz} = -\gamma_x\gamma_z B_y = \gamma_x\gamma_z \left(\frac{\partial A_z}{\partial x} - \frac{\partial A_x}{\partial z} \right) \tag{1.2.10}$$

$$\gamma_x\gamma_y F_{xy} = \gamma_x\gamma_y B_z = \gamma_x\gamma_y \left(\frac{\partial A_y}{\partial x} - \frac{\partial A_x}{\partial y} \right), \tag{1.2.11}$$

where $S = S_1 + S_2 + S_3 + S_4$ is a scalar field, whose meaning will be clarified later. It is to be noted that equating (1.2.5) to zero, *i.e.* $S = 0$, gives an expression that takes the form of the "Lorenz gauge" condition if $A_t = -\frac{\varphi}{c}$, where φ is the scalar potential of the electric field [**4, 20, 22**].

TABLE 1. Products $\boldsymbol{\partial}\boldsymbol{A}_\square$.

$\boldsymbol{\partial}\boldsymbol{A}_\square$	$\gamma_x A_x$	$\gamma_y A_y$	$\gamma_z A_z$	$\gamma_t A_t$
$\gamma_x \frac{\partial}{\partial x}$	$\frac{\partial A_x}{\partial x}$	$\gamma_x\gamma_y \frac{\partial A_y}{\partial x}$	$\gamma_x\gamma_z \frac{\partial A_z}{\partial x}$	$\gamma_x\gamma_t \frac{\partial A_t}{\partial x}$
$\gamma_y \frac{\partial}{\partial y}$	$-\gamma_x\gamma_y \frac{\partial A_x}{\partial y}$	$\frac{\partial A_y}{\partial y}$	$\gamma_y\gamma_z \frac{\partial A_z}{\partial y}$	$\gamma_y\gamma_t \frac{\partial A_t}{\partial y}$
$\gamma_z \frac{\partial}{\partial z}$	$-\gamma_x\gamma_z \frac{\partial A_x}{\partial z}$	$-\gamma_y\gamma_z \frac{\partial A_y}{\partial z}$	$\frac{\partial A_z}{\partial z}$	$\gamma_z\gamma_t \frac{\partial A_t}{\partial z}$
$\gamma_t \frac{1}{c}\frac{\partial}{\partial t}$	$-\gamma_x\gamma_t \frac{1}{c}\frac{\partial A_x}{\partial t}$	$-\gamma_y\gamma_t \frac{1}{c}\frac{\partial A_y}{\partial t}$	$-\gamma_z\gamma_t \frac{1}{c}\frac{\partial A_z}{\partial t}$	$-\frac{1}{c}\frac{\partial A_t}{\partial t}$

Equation (1.2.5) can be rewritten as

$$S = \nabla \cdot \boldsymbol{A}_\triangle - \frac{1}{c}\frac{\partial A_t}{\partial t} \tag{1.2.12}$$

were $\boldsymbol{A}_\triangle = \gamma_x A_x + \gamma_y A_y + \gamma_z A_z$ is the usual three components vector potential.

Using the so called "Lorenz gauge" the scalar field S is considered zero everywhere, *denying its status of a real physical entity* [**3**]. Same consideration can be done for the "Coulomb gauge" that assign zero value to each addendum S_i. We simply do not apply any "gauge", apart from defining $\boldsymbol{A}_\square$ as a harmonic function. According to our point of view, both Lorenz and Coulomb "gauges" should be considered just

as boundary conditions and the scalar field S, although not directly observable, has a gradient in space-time with a clear physical meaning. Similar considerations are normally presented in electromagnetism to introduce the concept of vector potential, that is a not directly measurable field. The components of the geometric product $\boldsymbol{\partial A}_{\square}$ are shown in Table 1. An electromagnetic field $\boldsymbol{G}$ with seven components emerges, composed by one scalar and six bivectors.

The set of equations from (1.2.6) to (1.2.11) can be rewritten also in the following way:

$$E_x = c\frac{\partial A_t}{\partial x} - \frac{\partial A_x}{\partial t} \tag{1.2.13}$$

$$E_y = c\frac{\partial A_t}{\partial y} - \frac{\partial A_y}{\partial t} \tag{1.2.14}$$

$$E_z = c\frac{\partial A_t}{\partial z} - \frac{\partial A_z}{\partial t} \tag{1.2.15}$$

$$B_x = \frac{\partial A_z}{\partial y} - \frac{\partial A_y}{\partial z} \tag{1.2.16}$$

$$B_y = -\frac{\partial A_z}{\partial x} + \frac{\partial A_x}{\partial z} \tag{1.2.17}$$

$$B_z = \frac{\partial A_y}{\partial x} - \frac{\partial A_x}{\partial y}, \tag{1.2.18}$$

where

$$\boldsymbol{E} = \gamma_x E_x + \gamma_y E_y + \gamma_z E_z = c\nabla A_t - \frac{\partial \boldsymbol{A}_{\triangle}}{\partial t}, \tag{1.2.19}$$

$$\boldsymbol{B} = \gamma_x B_x + \gamma_y B_y + \gamma_z B_z = \nabla \times \boldsymbol{A}_{\triangle}. \tag{1.2.20}$$

The sum of all diagonal elements in Table 1 represents the scalar product

$$S = \boldsymbol{\partial} \cdot \boldsymbol{A}_{\square}, \tag{1.2.21}$$

whereas the sum of all extra-diagonal elements gives the six components of electromagnetic bivector F

$$\boldsymbol{F} = \boldsymbol{\partial} \wedge \boldsymbol{A}_{\square}. \tag{1.2.22}$$

Referring to the function $\boldsymbol{G}$, it is possible to note that the "electromagnetic field" is characterized by seven values: three for the electric field, three for the flux density field and one for the scalar field S.

Table 2 represents the relation between the fundamental electromagnetic entities and the space-time components of the vector potential $\boldsymbol{A}_{\square}$.

TABLE 2. Relation between electromagnetic entities and the vector potential $\boldsymbol{A}_{\square}$.

$\boldsymbol{\partial A}_{\square}$	$\gamma_x A_x$	$\gamma_y A_y$	$\gamma_z A_z$	$\gamma_t A_t$
$\gamma_x \frac{\partial}{\partial x}$	S_1	B_{z1}	$-B_{y1}$	$\frac{1}{c} \cdot E_{x1}$
$\gamma_y \frac{\partial}{\partial y}$	B_{z2}	S_2	B_{x1}	$\frac{1}{c} \cdot E_{y1}$
$\gamma_z \frac{\partial}{\partial z}$	$-B_{y2}$	B_{x2}	S_3	$\frac{1}{c} \cdot E_{z1}$
$\gamma_t \frac{1}{c} \frac{\partial}{\partial t}$	$\frac{1}{c} E_{x2}$	$\frac{1}{c} E_{y2}$	$\frac{1}{c} E_{z2}$	S_4

With reference to Table 2 the electromagnetic field $\boldsymbol{G}$ can also be expressed as

$$\begin{aligned}\boldsymbol{G}(x,y,z,t) = S + \boldsymbol{F} = S + \gamma_x\gamma_t\frac{E_x}{c} + \gamma_y\gamma_t\frac{E_y}{c} + \gamma_z\gamma_t\frac{E_z}{c} + \gamma_y\gamma_z B_x - \gamma_x\gamma_z B_y + \gamma_x\gamma_y B_z = \\ = S + \frac{1}{c}\boldsymbol{E}\gamma_t + I\boldsymbol{B}\gamma_t = S + \frac{1}{c}(\boldsymbol{E} + Ic\boldsymbol{B})\gamma_t,\end{aligned} \tag{1.2.23}$$

where

$$I = \gamma_x\gamma_y\gamma_z\gamma_t \tag{1.2.24}$$

is the unitary pseudoscalar and

$$\boldsymbol{F} = \frac{1}{c}\boldsymbol{E}\gamma_t + I\boldsymbol{B}\gamma_t = \frac{1}{c}(\boldsymbol{E} + Ic\boldsymbol{B})\gamma_t. \tag{1.2.25}$$

On the other hand, with reference to Table 1, the electromagnetic field $\boldsymbol{G}$ can be expressed in the following compact form

$$\boldsymbol{G}(x,y,z,t) = \nabla\cdot\boldsymbol{A}_\triangle - \frac{1}{c}\frac{\partial A_t}{\partial t} + \nabla A_t\gamma_t - \frac{1}{c}\frac{\partial \boldsymbol{A}_\triangle}{\partial t}\gamma_t + I\nabla\times\boldsymbol{A}_\triangle\gamma_t, \tag{1.2.26}$$

which again results in equations (1.2.12), (1.2.19) and (1.2.20) by taking (1.2.23) into account.

1.2.2. Maxwell's Equations. Now, by applying the operator $\boldsymbol{\partial}$ to the multivector $\boldsymbol{G}$ (1.2.3) and equating it to zero, a new expression is found, *i.e.*

$$\boldsymbol{\partial}\boldsymbol{G} = \boldsymbol{\partial}^2\boldsymbol{A}_\square = 0, \tag{1.2.27}$$

whose components are shown in Table 3. The equation $\boldsymbol{\partial}\boldsymbol{G} = 0$ *can be seen as an extension in four dimensions of the Cauchy-Riemann conditions for analytic functions of a complex (two dimensional) variable* [**3, 11**]. In [**11**] Hestenes writes: *"Members of this audience will recognize* $\square\psi_0 = 0$ *as a generalization of the Cauchy-Riemann equations to spacetime, so we can expect it to have a rich variety of solutions. The problem is to pick out those solutions with physical significance."*. In fact, if $\boldsymbol{A}_\square$ is harmonic then

$$\boldsymbol{\partial}^2\boldsymbol{A}_\square = \nabla^2\boldsymbol{A}_\square - \frac{1}{c^2}\frac{\partial^2\boldsymbol{A}_\square}{\partial t^2} = 0, \tag{1.2.28}$$

which represents the wave equation of the four-potential and where

$$\boldsymbol{\partial}^2 = \frac{\partial^2}{\partial x^2} + \frac{\partial^2}{\partial y^2} + \frac{\partial^2}{\partial z^2} - \frac{1}{c^2}\frac{\partial^2}{\partial t^2} = \nabla^2 - \frac{1}{c^2}\frac{\partial^2}{\partial t^2}.$$

It should be noted that in our case, considering the scalar field $S \neq 0$ and $\boldsymbol{A}_\square$ harmonic, (1.2.28) is always homogeneous.

TABLE 3. Products $\boldsymbol{\partial}\boldsymbol{G} = \boldsymbol{\partial}\left(\boldsymbol{\partial}\boldsymbol{A}_\square\right)$. $\gamma_{ij} = \gamma_i\gamma_j$, $\gamma_{ijk} = \gamma_i\gamma_j\gamma_k$.

$\boldsymbol{\partial}^2\boldsymbol{A}_\square$	S	$\gamma_{xt}\frac{1}{c}E_x$	$\gamma_{yt}\frac{1}{c}E_y$	$\gamma_{zt}\frac{1}{c}E_z$
$\gamma_x\frac{\partial}{\partial x}$	$\gamma_x\frac{\partial S}{\partial x}$	$\gamma_t\frac{1}{c}\frac{\partial E_x}{\partial x}$	$\gamma_{xyt}\frac{1}{c}\frac{\partial E_y}{\partial x}$	$\gamma_{xzt}\frac{1}{c}\frac{\partial E_z}{\partial x}$
$\gamma_y\frac{\partial}{\partial y}$	$\gamma_y\frac{\partial S}{\partial y}$	$-\gamma_{xyt}\frac{1}{c}\frac{\partial E_x}{\partial y}$	$\gamma_t\frac{1}{c}\frac{\partial E_y}{\partial y}$	$\gamma_{yzt}\frac{1}{c}\frac{\partial E_z}{\partial y}$
$\gamma_z\frac{\partial}{\partial z}$	$\gamma_z\frac{\partial S}{\partial z}$	$-\gamma_{xzt}\frac{1}{c}\frac{\partial E_x}{\partial z}$	$-\gamma_{yzt}\frac{1}{c}\frac{\partial E_y}{\partial z}$	$\gamma_t\frac{1}{c}\frac{\partial E_z}{\partial z}$
$\gamma_t\frac{1}{c}\frac{\partial}{\partial t}$	$\gamma_t\frac{1}{c}\frac{\partial S}{\partial t}$	$\gamma_x\frac{1}{c^2}\frac{\partial E_x}{\partial t}$	$\gamma_y\frac{1}{c^2}\frac{\partial E_y}{\partial t}$	$\gamma_z\frac{1}{c^2}\frac{\partial E_z}{\partial t}$
$\boldsymbol{\partial}^2\boldsymbol{A}_\square$	S	$\gamma_{yz}B_x$	$-\gamma_{xz}B_y$	$\gamma_{xy}B_z$
$\gamma_x\frac{\partial}{\partial x}$	$\gamma_x\frac{\partial S}{\partial x}$	$\gamma_{xyz}\frac{\partial B_x}{\partial x}$	$-\gamma_z\frac{\partial B_y}{\partial x}$	$\gamma_y\frac{\partial B_z}{\partial x}$
$\gamma_y\frac{\partial}{\partial y}$	$\gamma_y\frac{\partial S}{\partial y}$	$\gamma_z\frac{\partial B_x}{\partial y}$	$\gamma_{xyz}\frac{\partial B_y}{\partial x}$	$-\gamma_x\frac{\partial B_z}{\partial y}$
$\gamma_z\frac{\partial}{\partial z}$	$\gamma_z\frac{\partial S}{\partial z}$	$-\gamma_y\frac{\partial B_x}{\partial z}$	$\gamma_x\frac{\partial B_y}{\partial z}$	$\gamma_{xyz}\frac{\partial B_z}{\partial z}$
$\gamma_t\frac{1}{c}\frac{\partial}{\partial t}$	$\gamma_t\frac{1}{c}\frac{\partial S}{\partial t}$	$\gamma_{yzt}\frac{1}{c}\frac{\partial B_x}{\partial t}$	$-\gamma_{xzt}\frac{1}{c}\frac{\partial B_y}{\partial t}$	$\gamma_{xyt}\frac{1}{c}\frac{\partial B_z}{\partial t}$

By collecting all common factors contained in Table 3 the following equations are derived:

$$\gamma_x \left(\frac{\partial S}{\partial x} - \frac{\partial B_z}{\partial y} + \frac{\partial B_y}{\partial z} + \frac{1}{c^2} \frac{\partial E_x}{\partial t} \right) = 0 \tag{1.2.29}$$

$$\gamma_y \left(\frac{\partial B_z}{\partial x} + \frac{\partial S}{\partial y} - \frac{\partial B_x}{\partial z} + \frac{1}{c^2} \frac{\partial E_y}{\partial t} \right) = 0 \tag{1.2.30}$$

$$\gamma_z \left(-\frac{\partial B_y}{\partial x} + \frac{\partial B_x}{\partial y} + \frac{\partial S}{\partial z} + \frac{1}{c^2} \frac{\partial E_z}{\partial t} \right) = 0 \tag{1.2.31}$$

$$\gamma_t \frac{1}{c} \left(\frac{\partial E_x}{\partial x} + \frac{\partial E_y}{\partial y} + \frac{\partial E_z}{\partial z} + \frac{\partial S}{\partial t} \right) = 0 \tag{1.2.32}$$

$$\gamma_y \gamma_z \gamma_t \frac{1}{c} \left(\frac{\partial E_z}{\partial y} - \frac{\partial E_y}{\partial z} + \frac{\partial B_x}{\partial t} \right) = 0 \tag{1.2.33}$$

$$\gamma_x \gamma_z \gamma_t \frac{1}{c} \left(\frac{\partial E_z}{\partial x} - \frac{\partial E_x}{\partial z} - \frac{\partial B_y}{\partial t} \right) = 0 \tag{1.2.34}$$

$$\gamma_x \gamma_y \gamma_t \frac{1}{c} \left(\frac{\partial E_y}{\partial x} - \frac{\partial E_x}{\partial y} + \frac{\partial B_z}{\partial t} \right) = 0 \tag{1.2.35}$$

$$\gamma_x \gamma_y \gamma_z \left(\frac{\partial B_x}{\partial x} + \frac{\partial B_y}{\partial y} + \frac{\partial B_z}{\partial z} \right) = 0. \tag{1.2.36}$$

Rearranging all equations from (1.2.29) to (1.2.36) the following are derived:

$$\frac{\partial B_z}{\partial y} - \frac{\partial B_y}{\partial z} = \frac{\partial S}{\partial x} + \frac{1}{c^2} \frac{\partial E_x}{\partial t} \tag{1.2.37}$$

$$\frac{\partial B_x}{\partial z} - \frac{\partial B_z}{\partial x} = \frac{\partial S}{\partial y} + \frac{1}{c^2} \frac{\partial E_y}{\partial t} \tag{1.2.38}$$

$$\frac{\partial B_y}{\partial x} - \frac{\partial B_x}{\partial y} = \frac{\partial S}{\partial z} + \frac{1}{c^2} \frac{\partial E_z}{\partial t} \tag{1.2.39}$$

$$\frac{\partial E_x}{\partial x} + \frac{\partial E_y}{\partial y} + \frac{\partial E_z}{\partial z} = -\frac{\partial S}{\partial t} \tag{1.2.40}$$

$$\frac{\partial E_z}{\partial y} - \frac{\partial E_y}{\partial z} = -\frac{\partial B_x}{\partial t} \tag{1.2.41}$$

$$\frac{\partial E_x}{\partial z} - \frac{\partial E_z}{\partial x} = -\frac{\partial B_y}{\partial t} \tag{1.2.42}$$

$$\frac{\partial E_y}{\partial x} - \frac{\partial E_x}{\partial y} = -\frac{\partial B_z}{\partial t} \tag{1.2.43}$$

$$\frac{\partial B_x}{\partial x} + \frac{\partial B_y}{\partial y} + \frac{\partial B_z}{\partial z} = 0, \tag{1.2.44}$$

which are coincident with Maxwell's equations if

$$\frac{\partial S}{\partial x} = \mu_0 J_{ex} = \mu_0 \frac{\partial q}{\partial y \partial z \partial t} = \mu_0 \frac{\partial q \partial x}{\partial x \partial y \partial z \partial t} = \mu_0 \rho v_x \tag{1.2.45}$$

$$\frac{\partial S}{\partial y} = \mu_0 J_{ey} = \mu_0 \frac{\partial q}{\partial x \partial z \partial t} = \mu_0 \frac{\partial q \partial y}{\partial x \partial y \partial z \partial t} = \mu_0 \rho v_y \tag{1.2.46}$$

$$\frac{\partial S}{\partial z} = \mu_0 J_{ez} = \mu_0 \frac{\partial q}{\partial x \partial y \partial t} = \mu_0 \frac{\partial q \partial z}{\partial x \partial y \partial z \partial t} = \mu_0 \rho v_z \tag{1.2.47}$$

$$\frac{1}{c}\frac{\partial S}{\partial t} = \mu_0 J_{et} = -\mu_0 c \frac{\partial q}{\partial x \partial y \partial z} = -\mu_0 c \rho, \tag{1.2.48}$$

where ∂q is the differential of a generic charge [**4, 20**]. Equation (1.2.48) can be also written as

$$\frac{\partial S}{\partial t} = c\mu_0 J_{et} = -\mu_0 c \frac{\partial q}{\partial x \partial y \partial z} = -\mu_0 c^2 \rho = -\frac{\rho}{\epsilon_0}. \tag{1.2.49}$$

By taking into account (1.2.45), (1.2.46), (1.2.47) and (1.2.48), the following relation holds for the current density field,

$$\frac{1}{\mu_0}\boldsymbol{\partial} S = \frac{1}{\mu_0}\left(\gamma_x \frac{\partial S}{\partial x} + \gamma_y \frac{\partial S}{\partial y} + \gamma_z \frac{\partial S}{\partial z} + \gamma_t \frac{1}{c}\frac{\partial S}{\partial t}\right) = \boldsymbol{J}_{\square e}, \tag{1.2.50}$$

where

$$\begin{aligned} \boldsymbol{J}_{\square e} &= \gamma_x J_{ex} + \gamma_y J_{ey} + \gamma_z J_{ez} + \gamma_t J_{et} = \gamma_x J_{ex} + \gamma_y J_{ey} + \gamma_z J_{ez} - \gamma_t c\rho = \\ &= \boldsymbol{J}_{\triangle} - \gamma_t c\rho = \rho\left(\boldsymbol{v}_{\triangle} - \gamma_t c\right) \end{aligned} \tag{1.2.51}$$

is the four-current vector,

$$\boldsymbol{v}_{\square} = \gamma_x v_x + \gamma_y v_y + \gamma_z v_z - \gamma_t c = \boldsymbol{v}_{\triangle} - \gamma_t c \tag{1.2.52}$$

is a four-velocity vector and $\boldsymbol{v}_{\triangle}$ is the speed in the ordinary space.

In this formulation the partial derivatives of the scalar field S with respect to time and space coordinates can be interpreted as charge density and current density, respectively. As a matter of fact (1.2.37), (1.2.38) and (1.2.39) represent the spatial components of Ampere's law, *i.e.*

$$\nabla \times \boldsymbol{B} = \mu_0 \boldsymbol{J}_{\triangle} + \frac{1}{c^2}\frac{\partial \boldsymbol{E}}{\partial t}, \tag{1.2.53}$$

where $\boldsymbol{J}_{\triangle} = \gamma_x J_{ex} + \gamma_y J_{ey} + \gamma_z J_{ez}$ is the three component vector of current density, (1.2.40) is the Gauss's law for the electric field

$$\nabla \cdot \boldsymbol{E} = \frac{\rho}{\epsilon_0}, \tag{1.2.54}$$

(1.2.41), (1.2.42) and (1.2.43) represent the spatial components of the Faraday-Neumann-Maxwell-Lenz law

$$\nabla \times \boldsymbol{E} = -\frac{\partial \boldsymbol{B}}{\partial t} \tag{1.2.55}$$

and (1.2.44) the Gauss's law for the flux density field

$$\nabla \cdot \boldsymbol{B} = 0. \tag{1.2.56}$$

Finally, by applying the $\boldsymbol{\partial}\cdot$ operator to (1.2.50) and setting the result to zero, the equation representing the law of electric charge conservation is obtained

$$\frac{1}{\mu_0}\boldsymbol{\partial} \cdot (\boldsymbol{\partial} S) = \boldsymbol{\partial} \cdot \boldsymbol{J}_{\square e} = \frac{\partial J_{ex}}{\partial x} + \frac{\partial J_{ey}}{\partial y} + \frac{\partial J_{ez}}{\partial z} + \frac{\partial \rho}{\partial t} = 0. \tag{1.2.57}$$

It is important to note that the wave equation of the scalar field S can be deduced from the charge-current conservation law:

$$\boldsymbol{\partial} \cdot (\boldsymbol{\partial} S) = \boldsymbol{\partial}^2 S = \frac{\partial^2 S}{\partial x^2} + \frac{\partial^2 S}{\partial y^2} + \frac{\partial^2 S}{\partial z^2} - \frac{1}{c^2}\frac{\partial^2 S}{\partial t^2} = \nabla^2 S - \frac{1}{c^2}\frac{\partial^2 S}{\partial t^2} = 0. \tag{1.2.58}$$

Now, by applying the time derivative to (1.2.58) and remembering (1.2.49), the wave equation of a

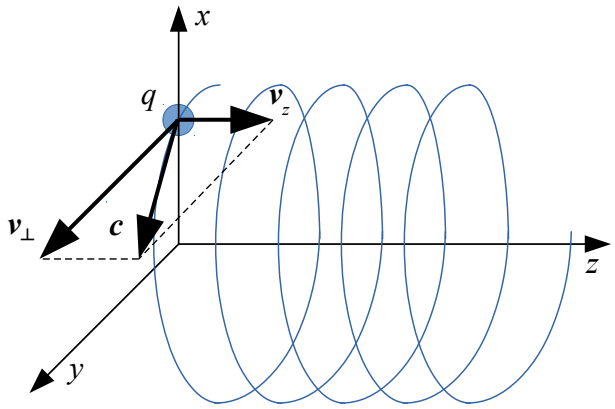

FIGURE 1.2.1. Helical motion of an elementary charge q moving at the speed of light, with $v_z^2 + v_\perp^2 = c^2$.

massless charge field $\rho\left(\boldsymbol{r}_\square\right)$ can also be deduced, *i.e.*

$$\frac{\partial}{\partial t}\left(\boldsymbol{\partial}^2 S\right) = \boldsymbol{\partial}^2\left(\frac{\partial S}{\partial t}\right) = \boldsymbol{\partial}^2\left(-\mu_0 c^2 \rho\right) = -\mu_0 c^2 \boldsymbol{\partial}^2 \rho = 0, \tag{1.2.59}$$

which gives

$$\boldsymbol{\partial}^2 \rho = \nabla^2 \rho - \frac{1}{c^2}\frac{\partial^2}{\partial t^2}\rho = 0. \tag{1.2.60}$$

Clearly, both (1.2.58) and (1.2.60) represent, respectively, fields (S and ρ) that must necessary propagate at the speed of light [**17, 20**]. Equation (1.2.50) means also that the 4-vector current density field can be derived directly from the scalar field S. The hypothesis of existence of scalar waves has been recently explored at the Oak Ridge laboratories: *"The new theory predicts a new charge-fluctuation-driven scalar wave, having energy but not momentum for zero magnetic and electric fields. The scalar wave can co-exist with a longitudinal-electric wave, having energy and momentum. The new theory in 4-vector form is relativistically covariant. New experimental tests are needed to confirm this theory."* [**15**].

The proposed reinterpretation of Maxwell's equations in this work is in agreement with the principle of Occam's razor: the concepts of charge and current density are not inserted "ad hoc" but are deduced from a single more fundamental entity, the four dimensional vector potential field $\boldsymbol{A}_\square\left(\boldsymbol{r}_\square\right) = \boldsymbol{A}_\square\left(x, y, z, t\right)$.

In fact, a big advantage of our perspective on Maxwell's equations is the ability to simply specify both current density and charge density distributions and then see what fields result. Nevertheless, the added constraint on the charge and current density seems to imply that one is no longer free to specify charge and current density distributions at will, because this information is indeed included within the electromagnetic four potential $\boldsymbol{A}_\square$.

Equation (1.2.60) imposes a precise condition on charge dynamics, describing only distributions of charge density moving in vacuum at the speed of light c. At first glance, this result seems to be incompatible with experimental observations, with the usual concepts of charge and current, and with the traditional way of working with Maxwell's equations. A skeptic might ask: "What does a light-speed moving and massless charge field have to do with the electron?" In the following chapters, we precisely derive how this light-speed moving $\rho\left(\boldsymbol{r}_\square\right)$ field is perceived as a massive electron particle and as a quantum mechanical wavefunction. To reach this discovery, we use nothing else than Maxwell's equations and General Relativity.

As will be shown later, we can interpret equation (1.2.60) as a constraint for the definition of models of elementary charged particles. This constraint, however, can be removed when considering macroscopic electromagnetic systems or even the dynamics of a single elementary charge at a spatial scale greater than the particle Compton wavelength λ_c and at a time scale greater than the Compton period $\frac{\lambda_c}{c}$. In this case "static" elementary charges can be seen as charge density distributions moving at the speed of light on a closed trajectory but with a zero average speed (this generalization would be consistent with static charge densities, electrets, dielectrics), whereas currents can be considered as an ordered motion of charge density distributions moving with an absolute velocity equal to the speed of light but with an arbitrary average speed lower than c . As an example, referring to Fig. 1.2.1, the electromagnetic effects generated by an elementary charge q, moving at instantaneous speed c in a helical motion of radius $\leq \frac{\lambda_c}{2\pi}$

with average velocity v_z along the helix axis z and tangential velocity $v_\perp$, can be approximated, on a spatial scale $\gg \lambda_c$ and a temporal scale $\gg \frac{\lambda_c}{c}$, to those produced by the same elementary charge q moving at uniform velocity v_z, creating the current density

$$\boldsymbol{J}_z = J_z\gamma_z \approx \frac{q}{\delta x\delta y\delta z}\frac{dz}{dt}\gamma_z = \frac{q}{\delta V}\frac{dz}{dt}\gamma_z = \rho v_z\gamma_z = \rho\boldsymbol{v}_z, \tag{1.2.61}$$

where $\delta V = \delta x\delta y\delta z \approx \lambda_c^3$. In this view and at a macroscopic level the here proposed new interpretation of Maxwell's equations remains compatible with the traditional way of working with them, i.e. by assigning the sources and determining, as a consequence, both the electric and the flux density (magnetic) field.

The new formulation of Maxwell's equations expressed by (1.2.27) is quite similar to the Dirac-Hestenes equation for $m = 0$ (Weyl equation). In all cases the solution is a *spinor* field. A spinor is a mathematical object that in space-time algebra is simply a multivector of even grade components. The motion of a massless charge that moves at speed of light can be described using a composition of a rotation in the $\gamma_x\gamma_y$ plane followed by a scaled hyperbolic rotation in the $\gamma_z\gamma_t$ plane and can be encoded in real $Cl_{3,1}$ algebra with a single spinor.

At this point, we encourage the reader by an interesting sentence of P. A. M. Dirac. In fact, in his Nobel lecture [**6**], held in 1933, Dirac proposed an electron model in which a charge moves at the speed of light: *"It is found that an electron which seems to us to be moving slowly, must actually have a very high frequency oscillatory motion of small amplitude superposed on the regular motion which appears to us. As a result of this oscillatory motion, the velocity of the electron at any time equals the velocity of light."*.

1.3. Properties of the Electromagnetic Field

In this section, the main properties of the electromagnetic field will be presented and discussed by means of $Cl_{3,1}$ Clifford algebra.

1.3.1. Derivation of Maxwell's Equations from Lagrangian Density. Maxwell's equations can be derived considering the following Lagrangian density, in form of a composition of a scalar and a pseudoscalar part:

$$\begin{aligned}\boldsymbol{L} &= \frac{1}{2\mu_0}\boldsymbol{\partial A}_{\square}\widetilde{\boldsymbol{\partial A}_{\square}} = \frac{1}{2\mu_0}\boldsymbol{G}\widetilde{\boldsymbol{G}} = \frac{1}{2\mu_0}\left\|\boldsymbol{G}\right\|^2 = \frac{1}{2\mu_0}\left(S+\boldsymbol{F}\right)\left(S-\boldsymbol{F}\right) = \frac{1}{2\mu_0}\left(S^2-\boldsymbol{F}^2\right) = \\ &= \frac{1}{2\mu_0}\left(-\frac{E^2}{c^2}+B^2+S^2-\frac{2}{c}I\boldsymbol{E}\cdot\boldsymbol{B}\right),\end{aligned} \tag{1.3.1}$$

where, bearing (1.2.25) in mind,

$$\boldsymbol{F} = \frac{1}{c}\boldsymbol{E}\gamma_t + I\boldsymbol{B}\gamma_t = \frac{1}{c}\left(\boldsymbol{E}+Ic\boldsymbol{B}\right)\gamma_t \tag{1.3.2}$$

is the bivector part of the electromagnetic field and $\widetilde{\ }$ represents the Clifford reversion operator, as defined in the Mathematical Preliminaries chapter. Essentially, equation 1.3.1 equates Lagrangian density with the electromagnetic field's norm-square.

Expanding (1.3.1), and taking equations from (1.2.12) to (1.2.18) into account, we obtain the Lagrangian density as a function of the derivatives of the electromagnetic four-potential components, *i.e.*

$$\begin{aligned}\boldsymbol{L} = \frac{1}{2\mu_0}\Bigg\{&-\left(\frac{\partial A_t}{\partial x}-\frac{1}{c}\frac{\partial A_x}{\partial t}\right)^2-\left(\frac{\partial A_t}{\partial y}-\frac{1}{c}\frac{\partial A_y}{\partial t}\right)^2-\left(\frac{\partial A_t}{\partial z}-\frac{1}{c}\frac{\partial A_z}{\partial t}\right)^2+\\ &+\left(\frac{\partial A_z}{\partial y}-\frac{\partial A_y}{\partial z}\right)^2+\left(\frac{\partial A_x}{\partial z}-\frac{\partial A_z}{\partial x}\right)^2+\left(\frac{\partial A_y}{\partial x}-\frac{\partial A_x}{\partial y}\right)^2+\\ &+\left(\frac{\partial A_x}{\partial x}+\frac{\partial A_y}{\partial y}+\frac{\partial A_z}{\partial z}-\frac{1}{c}\frac{\partial A_t}{\partial t}\right)^2+\\ &-2I\left[\left(\frac{\partial A_t}{\partial x}-\frac{1}{c}\frac{\partial A_x}{\partial t}\right)\left(\frac{\partial A_z}{\partial y}-\frac{\partial A_y}{\partial z}\right)+\left(\frac{\partial A_t}{\partial y}-\frac{1}{c}\frac{\partial A_y}{\partial t}\right)\left(\frac{\partial A_x}{\partial z}-\frac{\partial A_z}{\partial x}\right)+\right.\\ &\left.+\left(\frac{\partial A_t}{\partial z}-\frac{1}{c}\frac{\partial A_z}{\partial t}\right)\left(\frac{\partial A_y}{\partial x}-\frac{\partial A_x}{\partial y}\right)\right]\Bigg\}.\end{aligned} \tag{1.3.3}$$

In $Cl_{3,1}$ algebra the Euler-Lagrange equations can be expressed, considering as variables the electromagnetic four-potential components $A_x(x,y,z,t)$, $A_y(x,y,z,t)$, $A_z(x,y,z,t)$ and $A_t(x,y,z,t)$, in the following way:

$$\sum_{j=x,y,z,t}\left(\sum_{i=x,y,z,t}\gamma_i\frac{\partial}{\partial i}\left(\frac{\partial \boldsymbol{L}}{\gamma_i\gamma_j\partial\left(\frac{\partial A_j}{\partial i}\right)}\right)-\frac{\partial \boldsymbol{L}}{\gamma_j\partial A_j}\right)=0 \tag{1.3.4}$$

which reduces itself to

$$\sum_{j=x,y,z,t}\left(\sum_{i=x,y,z,t}\gamma_i\frac{\partial}{\partial i}\left(\frac{\partial \boldsymbol{L}}{\gamma_i\gamma_j\partial\left(\frac{\partial A_j}{\partial i}\right)}\right)\right)=0, \tag{1.3.5}$$

considering that in this case

$$\sum_{j=x,y,z,t}\left(\frac{\partial \boldsymbol{L}}{\gamma_j\partial A_j}\right)=0, \tag{1.3.6}$$

because in (1.3.3) only the derivative terms of the four-potential ($\frac{\partial A_j}{\partial i}$) appear. By expanding (1.3.5), for example with $j=t$, we achieve, after some trivial calculation steps,

$$\begin{aligned}-\gamma_t\frac{\partial \boldsymbol{L}}{\partial A_t}&=-\gamma_t\frac{\partial}{\partial x}\frac{\partial \boldsymbol{L}}{\partial\left(\frac{\partial A_t}{\partial x}\right)}-\gamma_t\frac{\partial}{\partial y}\frac{\partial \boldsymbol{L}}{\partial\left(\frac{\partial A_t}{\partial y}\right)}-\gamma_t\frac{\partial}{\partial z}\frac{\partial \boldsymbol{L}}{\partial\left(\frac{\partial A_t}{\partial z}\right)}-\gamma_t\frac{\partial}{\partial t}\frac{\partial \boldsymbol{L}}{\partial\left(\frac{\partial A_t}{\partial t}\right)}=\\&=\gamma_t\frac{1}{\mu_0}\left(\frac{1}{c}\frac{\partial E_x}{\partial x}+I\frac{\partial B_x}{\partial x}+\frac{1}{c}\frac{\partial E_y}{\partial y}+I\frac{\partial B_y}{\partial y}+\frac{1}{c}\frac{\partial E_z}{\partial z}+I\frac{\partial B_z}{\partial z}+\frac{1}{c}\frac{\partial S}{\partial t}\right)=0,\end{aligned} \tag{1.3.7}$$

and this equation returns Gauss's laws for the electric field (see eq. (1.2.32)) and for the flux density field (see eq. (1.2.36)), respectively:

$$\gamma_t\frac{1}{c}\left(\frac{\partial E_x}{\partial x}+\frac{\partial E_y}{\partial y}+\frac{\partial E_z}{\partial z}+\frac{\partial S}{\partial t}\right)=0,$$

$$\gamma_x\gamma_y\gamma_z\left(\frac{\partial B_x}{\partial x}+\frac{\partial B_y}{\partial y}+\frac{\partial B_z}{\partial z}\right)=0.$$

Now, if we expand (1.3.5) with $j=x$, we obtain

$$\begin{aligned}\gamma_x\frac{\partial \boldsymbol{L}}{\partial A_x}&=\gamma_x\frac{\partial}{\partial x}\frac{\partial \boldsymbol{L}}{\partial\left(\frac{\partial A_x}{\partial x}\right)}+\gamma_x\frac{\partial}{\partial y}\frac{\partial \boldsymbol{L}}{\partial\left(\frac{\partial A_x}{\partial y}\right)}+\gamma_x\frac{\partial}{\partial z}\frac{\partial \boldsymbol{L}}{\partial\left(\frac{\partial A_x}{\partial z}\right)}+\gamma_x\frac{\partial}{\partial t}\frac{\partial \boldsymbol{L}}{\partial\left(\frac{\partial A_x}{\partial t}\right)}=\\&=\gamma_x\frac{1}{\mu_0}\left(\frac{\partial S}{\partial x}-\frac{\partial B_z}{\partial y}+\frac{I}{c}\frac{\partial E_z}{\partial y}+\frac{\partial B_y}{\partial z}-\frac{I}{c}\frac{\partial E_y}{\partial z}+\frac{1}{c^2}\frac{\partial E_x}{\partial t}+\frac{I}{c}\frac{\partial B_x}{\partial t}\right)=0.\end{aligned} \tag{1.3.8}$$

Equation (1.3.8) gives (1.2.29) and (1.2.33):

$$\gamma_x\left(\frac{\partial B_y}{\partial z}-\frac{\partial B_z}{\partial y}+\frac{\partial S}{\partial x}+\frac{1}{c^2}\frac{\partial E_x}{\partial t}\right)=0,$$

$$\gamma_y\gamma_z\gamma_t\frac{1}{c}\left(\frac{\partial E_z}{\partial y}-\frac{\partial E_y}{\partial z}+\frac{\partial B_x}{\partial t}\right)=0.$$

If we carry on the above procedures with $j=y$ and $j=z$ the other remaining components of Maxwell's equation can be determined, i.e (1.2.30), (1.2.34), (1.2.31) and (1.2.35):

$$\begin{aligned}\gamma_y\frac{\partial \boldsymbol{L}}{\partial A_y}&=\gamma_y\frac{\partial}{\partial x}\frac{\partial \boldsymbol{L}}{\partial\left(\frac{\partial A_y}{\partial x}\right)}+\gamma_y\frac{\partial}{\partial y}\frac{\partial \boldsymbol{L}}{\partial\left(\frac{\partial A_y}{\partial y}\right)}+\gamma_y\frac{\partial}{\partial z}\frac{\partial \boldsymbol{L}}{\partial\left(\frac{\partial A_y}{\partial z}\right)}+\gamma_y\frac{\partial}{\partial t}\frac{\partial \boldsymbol{L}}{\partial\left(\frac{\partial A_y}{\partial t}\right)}=\\&=\gamma_y\frac{1}{\mu_0}\left(\frac{\partial B_z}{\partial x}-\frac{I}{c}\frac{\partial E_z}{\partial x}+\frac{\partial S}{\partial y}-\frac{\partial B_x}{\partial z}+\frac{I}{c}\frac{\partial E_x}{\partial z}+\frac{1}{c^2}\frac{\partial E_y}{\partial t}+\frac{I}{c}\frac{\partial B_y}{\partial t}\right)=0,\end{aligned} \tag{1.3.9}$$

$$\begin{aligned}\gamma_z\frac{\partial \boldsymbol{L}}{\partial A_z} &= \gamma_z\frac{\partial}{\partial x}\frac{\partial \boldsymbol{L}}{\partial\left(\frac{\partial A_z}{\partial x}\right)} + \gamma_z\frac{\partial}{\partial y}\frac{\partial \boldsymbol{L}}{\partial\left(\frac{\partial A_z}{\partial y}\right)} + \gamma_z\frac{\partial}{\partial z}\frac{\partial \boldsymbol{L}}{\partial\left(\frac{\partial A_z}{\partial z}\right)} + \gamma_z\frac{\partial}{\partial t}\frac{\partial \boldsymbol{L}}{\partial\left(\frac{\partial A_z}{\partial t}\right)} = \\ &= \gamma_z\frac{1}{\mu_0}\left(-\frac{\partial B_y}{\partial x} + \frac{I}{c}\frac{\partial E_y}{\partial x} + \frac{\partial B_x}{\partial y} - \frac{I}{c}\frac{\partial E_x}{\partial y} + \frac{\partial S}{\partial z} + \frac{1}{c^2}\frac{\partial E_z}{\partial t} + \frac{I}{c}\frac{\partial B_z}{\partial t}\right) = 0,\end{aligned} \tag{1.3.10}$$

that give, as expected, respectively

$$\begin{aligned}\gamma_y\left(\frac{\partial B_z}{\partial x} + \frac{\partial S}{\partial y} - \frac{\partial B_x}{\partial z} + \frac{1}{c^2}\frac{\partial E_y}{\partial t}\right) = 0,\\ \gamma_x\gamma_z\gamma_t\frac{1}{c}\left(\frac{\partial E_z}{\partial x} - \frac{\partial E_x}{\partial z} - \frac{\partial B_y}{\partial t}\right) = 0,\\ \gamma_z\left(\frac{\partial B_x}{\partial y} + \frac{\partial S}{\partial z} - \frac{\partial B_y}{\partial x} + \frac{1}{c^2}\frac{\partial E_z}{\partial t}\right) = 0,\\ \gamma_x\gamma_y\gamma_t\frac{1}{c}\left(\frac{\partial E_y}{\partial x} - \frac{\partial E_x}{\partial y} + \frac{\partial B_z}{\partial t}\right) = 0.\end{aligned}$$

By analyzing the above reported equations it is possible to reach some conclusions. First of all the Lagrangian density, as defined in (1.3.1), can be divided in the sum of two parts

$$\boldsymbol{L} = L_{field} + L_{int}. \tag{1.3.11}$$

The first part

$$L_{field} = \frac{1}{2\mu_0}\left(-\frac{E^2}{c^2} + B^2\right) = -\frac{1}{2\mu_0}\left(\boldsymbol{F}\cdot\boldsymbol{F}\right) \tag{1.3.12}$$

represents the "field part" of the Lagrangian density, as known in literature, and the second

$$L_{int} = \frac{1}{2\mu_0}\left(S^2 - \frac{2}{c}I\boldsymbol{E}\cdot\boldsymbol{B}\right) \tag{1.3.13}$$

represents the "interaction term" of the Lagrangian density, that takes the interaction of the electromagnetic field with the sources into account, remembering, in addition, that the derivatives of the scalar field S, with respect to the four dimensional space coordinates x, y, z and t, are bounded respectively to the sources J_{ex}, J_{ey}, J_{ez} and $J_{et} = -c\rho$ (see eq. (1.2.50)). Indeed, by deriving only the interaction terms of the Lagrangian density with respect to the four-potential, *i.e.* by performing the operation $\frac{\partial L_{int}}{\partial A_j}$, it is possible to derive the term $\boldsymbol{J}_{\square e}\cdot\boldsymbol{A}_{\square}$. In fact, for the component along γ_t we find

$$\begin{aligned}-\gamma_t\frac{\partial L_{int}}{\partial A_t} &= -\gamma_t\frac{\partial}{\partial x}\frac{\partial L_{int}}{\partial\left(\frac{\partial A_t}{\partial x}\right)} - \gamma_t\frac{\partial}{\partial y}\frac{\partial L_{int}}{\partial\left(\frac{\partial A_t}{\partial y}\right)} - \gamma_t\frac{\partial}{\partial z}\frac{\partial L_{int}}{\partial\left(\frac{\partial A_t}{\partial z}\right)} - \gamma_t\frac{\partial}{\partial t}\frac{\partial L_{int}}{\partial\left(\frac{\partial A_t}{\partial t}\right)} = \\ &= \frac{\gamma_t}{\mu_0}\left(I\frac{\partial B_x}{\partial x} + I\frac{\partial B_y}{\partial y} + I\frac{\partial B_z}{\partial z} + \frac{1}{c}\frac{\partial S}{\partial t}\right) = \frac{\gamma_t}{\mu_0}\left(I\nabla\cdot\boldsymbol{B} + \frac{1}{c}\frac{\partial S}{\partial t}\right) = \\ &= \frac{\gamma_t}{\mu_0 c}\frac{\partial S}{\partial t} = \gamma_t J_{et} = -\gamma_t c\rho.\end{aligned} \tag{1.3.14}$$

Integration of (1.3.14) yields

$$L_{int}|_t = \int\frac{\partial L_{int}}{\partial A_t}dA_t = \int\frac{1}{\mu_0 c}\frac{\partial S}{\partial t}dA_t = \frac{1}{\mu_0 c}\frac{\partial S}{\partial t}A_t = -\frac{1}{\mu_0}\mu_0 c\rho A_t = -c\rho A_t = J_{et}A_t. \tag{1.3.15}$$

For the component along γ_x we find

$$\begin{aligned}\gamma_x\frac{\partial L_{int}}{\partial A_x} &= \gamma_x\frac{\partial}{\partial x}\frac{\partial L_{int}}{\partial\left(\frac{\partial A_x}{\partial x}\right)} + \gamma_x\frac{\partial}{\partial y}\frac{\partial L_{int}}{\partial\left(\frac{\partial A_x}{\partial y}\right)} + \gamma_x\frac{\partial}{\partial z}\frac{\partial L_{int}}{\partial\left(\frac{\partial A_x}{\partial z}\right)} + \gamma_x\frac{\partial}{\partial t}\frac{\partial L_{int}}{\partial\left(\frac{\partial A_x}{\partial t}\right)} = \\ &= \frac{\gamma_x}{\mu_0}\left(\frac{\partial S}{\partial x} + \frac{I}{c}\frac{\partial E_z}{\partial y} - \frac{I}{c}\frac{\partial E_y}{\partial z} + \frac{I}{c}\frac{\partial B_x}{\partial t}\right) = \frac{\gamma_x}{\mu_0}\frac{\partial S}{\partial x} = \gamma_x J_{ex}.\end{aligned} \tag{1.3.16}$$

Integration of (1.3.16) yields

$$L_{int}|_x = \int \left(\frac{\partial L_{int}}{\partial A_x}\right) dA_x = \int \frac{1}{\mu_0}\frac{\partial S}{\partial x} dA_x = \frac{1}{\mu_0}\frac{\partial S}{\partial x} A_x = J_{ex} A_x. \tag{1.3.17}$$

The same procedure is clearly valid also for the components in γ_y and γ_z. Finally, by integration of (1.3.6), we get the Lagrangian density interaction term as

$$L_{int} = \sum_{j=x,y,z,t} \int \left(\frac{\partial L_{int}}{\partial A_j}\right) dA_j = J_{ex}A_x + J_{ey}A_y + J_{ez}A_z - c\rho A_t = \boldsymbol{J}_{\square e} \cdot \boldsymbol{A}_{\square}, \tag{1.3.18}$$

which is the usual "source" term that is added in traditional Lagrangian theory for classical electricity and magnetism in order to obtain the complete set of Maxwell's equations [**5, 7, 20**]. The scalar product $\boldsymbol{J}_{\square e} \cdot \boldsymbol{A}_{\square}$ has a dimension of energy per volume ($J \cdot m^{-3}$); in particular, the contribution of the spatial components of vectors $\boldsymbol{J}_{\square e}$ and $\boldsymbol{A}_{\square}$ (the scalar product $\boldsymbol{J}_{\triangle} \cdot \boldsymbol{A}_{\triangle}$) can be considered as the specific "kinetic" energy of the electromagnetic field, whereas the term $J_{et}A_t = -c\rho A_t$ the "potential" energy. By virtue of (1.3.13), (1.3.18) becomes

$$L_{int} = \frac{1}{2\mu_0}\left(S^2 - \frac{2}{c} I\boldsymbol{E} \cdot \boldsymbol{B}\right) = \boldsymbol{J}_{\square e} \cdot \boldsymbol{A}_{\square}. \tag{1.3.19}$$

By inspection of (1.3.14) and (1.3.16), and generalizing, it is possible to define the four-current vector $\boldsymbol{J}_{\square e}$ from the interaction Lagrangian term:

$$\begin{aligned} \sum_{j=x,y,z,t} \left(\frac{\partial L_{int}}{\gamma_j \partial A_j}\right) &= \gamma_x \frac{\partial L_{int}}{\partial A_x} + \gamma_y \frac{\partial L_{int}}{\partial A_y} + \gamma_z \frac{\partial L_{int}}{\partial A_z} - \gamma_t \frac{\partial L_{int}}{\partial A_t} = \\ &= \gamma_x J_{ex} + \gamma_y J_{ey} + \gamma_z J_{ez} + \gamma_t J_{et} = \boldsymbol{J}_{\square e}. \end{aligned} \tag{1.3.20}$$

and, again, by virtue of the Noether's theorem, the law of current and charge conservation

$$\boldsymbol{\partial} \cdot \left[\sum_{j=x,y,z,t} \left(\frac{\partial L_{int}}{\gamma_j \partial A_j}\right)\right] = \boldsymbol{\partial} \cdot \boldsymbol{J}_{\square e} = 0, \tag{1.3.21}$$

which returns, consequently, the wave equations (1.2.58) and (1.2.60), respectively.

As can be seen the definition of the electromagnetic field $\boldsymbol{G}$ is complete and it includes itself the information of both action and interaction, without the need of any additional term: this is in full accordance with the principle of Occam's razor.

Thanks to the $Cl_{3,1}$ Clifford algebra the Euler-Lagrange equations can be conveniently defined in in a very compact form:

$$\boldsymbol{\partial}\left(\frac{\partial L}{\partial\left(\boldsymbol{\partial} \wedge \boldsymbol{A}_{\square}\right)}\right) - \frac{\partial L}{\partial \boldsymbol{A}_{\square}} = \boldsymbol{\partial}\left(\frac{\partial L}{\partial \boldsymbol{F}}\right) - \frac{\partial L}{\partial \boldsymbol{A}_{\square}} = 0, \tag{1.3.22}$$

where, now, the scalar Lagrangian density is

$$L = L_{field} + L_{int} = -\frac{1}{2\mu_0}\boldsymbol{F} \cdot \boldsymbol{F} + \boldsymbol{J}_{\square e} \cdot \boldsymbol{A}_{\square}. \tag{1.3.23}$$

Substituting (1.3.23) in (1.3.22) one can achieve directly Maxwell's equations in $Cl_{3,1}$ in the form shown in the previous sections (see eq. (1.2.27)), *i.e.*

$$\boldsymbol{\partial}\left(\frac{\partial\left(-\frac{1}{2\mu_0}\boldsymbol{F} \cdot \boldsymbol{F} + \boldsymbol{J}_{\square e} \cdot \boldsymbol{A}_{\square}\right)}{\partial \boldsymbol{F}}\right) - \frac{\partial\left(-\frac{1}{2\mu_0}\boldsymbol{F} \cdot \boldsymbol{F} + \boldsymbol{J}_{\square e} \cdot \boldsymbol{A}_{\square}\right)}{\partial \boldsymbol{A}_{\square}} = -\frac{1}{\mu_0}\boldsymbol{\partial}\boldsymbol{F} - \boldsymbol{J}_{\square e} = 0, \tag{1.3.24}$$

which yields

$$\boldsymbol{\partial}\boldsymbol{F} + \mu_0 \boldsymbol{J}_{\square e} = \boldsymbol{\partial}\boldsymbol{F} + \boldsymbol{\partial} S = \boldsymbol{\partial}\left(\boldsymbol{F} + S\right) = \boldsymbol{\partial}\boldsymbol{G} = 0. \tag{1.3.25}$$

1.3.2. Energy of the Electromagnetic Field. The light-like energy-momentum density vector of the field $\boldsymbol{G}$ can be represented by a rotation of the base vector γ_t :

$$\boldsymbol{w} = \frac{1}{2\mu_0}\left(\boldsymbol{G}\gamma_t\widetilde{\boldsymbol{G}}\right)$$

$$\boldsymbol{G} = S + \boldsymbol{F} = S + \frac{1}{c}\left(\boldsymbol{E} + Ic\boldsymbol{B}\right)\gamma_t$$

$$\boldsymbol{G}\gamma_t = S\gamma_t + \boldsymbol{F}\gamma_t = S\gamma_t - \frac{1}{c}\left(\boldsymbol{E} + Ic\boldsymbol{B}\right)$$

$$\boldsymbol{w} = \frac{1}{2\mu_0}\left[S\gamma_t - \frac{1}{c}\left(\boldsymbol{E} + Ic\boldsymbol{B}\right)\right]\left[S - \frac{1}{c}\left(\boldsymbol{E} + Ic\boldsymbol{B}\right)\gamma_t\right]$$

$$\boldsymbol{w} = \frac{S^2}{2\mu_0}\gamma_t + \frac{\epsilon_0\boldsymbol{E}^2}{2}\gamma_t + \frac{\boldsymbol{B}^2}{2\mu_0}\gamma_t - \frac{1}{c\mu_0}I\boldsymbol{E}\wedge\boldsymbol{B}\gamma_t + \frac{S\boldsymbol{E}}{c\mu_0}$$

$$\boldsymbol{w} = \left(\frac{S^2}{2\mu_0} + \frac{\epsilon_0\boldsymbol{E}^2}{2} + \frac{\boldsymbol{B}^2}{2\mu_0}\right)\gamma_t - \frac{1}{c\mu_0}\left(\boldsymbol{E}\times\boldsymbol{B} - S\boldsymbol{E}\right) \tag{1.3.26}$$

Using natural units, the above equation takes the following form:

$$\left[\boldsymbol{w} = \frac{1}{4\pi}\left(\frac{1}{2}\left(S^2 + E^2 + B^2\right)\gamma_t - \left(\boldsymbol{E}\times\boldsymbol{B} - S\boldsymbol{E}\right)\right)\right]_{NU} \tag{1.3.27}$$

$$\boldsymbol{w} = \left(w_s + w_e + w_m\right)\gamma_t - \frac{1}{c}\cdot\boldsymbol{\mathfrak{S}},$$

where $w_s = \frac{S^2}{2\mu_0} = \boldsymbol{J}_{\square e}\cdot\boldsymbol{A}_{\square}$, $w_e = \epsilon_0\frac{\boldsymbol{E}^2}{2}$ and $w_m = \frac{\boldsymbol{B}^2}{2\mu_0}$ are the specific energies of the scalar, the electric and the magnetic flux density fields, and where

$$\boldsymbol{\mathfrak{S}} = \frac{1}{\mu_0}\left(\boldsymbol{E}\times\boldsymbol{B} - S\boldsymbol{E}\right) \tag{1.3.28}$$

is the generalized Poynting vector. It contains the usual $\boldsymbol{E}\times\boldsymbol{B}$ term, regardless of the scalar field presence. The poynting vector's sign depends on the field polarization type.

1.3.3. Electric Charge, Antimatter and Time Direction. R. Feynman proposed to interpret the positron (a particle which is identical to the electron but with a positive charge) as an electron traveling back in time [**8, 9**]. Such an interpretation seems to be perfectly compatible with the definition of electric charge density given in (1.2.48):

$$\frac{\partial S}{\partial t} = \frac{-\rho}{\epsilon_0}. \tag{1.3.29}$$

By multiplying both sides of (1.3.29) by -1 we obtain

$$-\frac{\partial S}{\partial t} = \frac{\rho}{\epsilon_0}$$

or, equivalently

$$\frac{\partial S}{\partial(-t)} = \frac{\rho}{\epsilon_0}. \tag{1.3.30}$$

However, traveling back in time is unphysical. Analogously, it can be shown that the Dirac equation's negative energy solutions correspond to a reversal of time direction, which is also unphysical.

The obvious positron solution is to reverse the sign of S, while time keeps moving forward in the positive direction. The positron then has positive charge and positive energy. The positron's positive energy is experimentally measured: electron-positron annihilation experiments show that $2\cdot 511$ keV energy is radiated away.

1.3.4. Magnetic Charges and Currents. Starting from an hypothetical eight component "vector potential" that includes the four pseudovectors (Trivectors) $\boldsymbol{T}$ of space-time algebra, symmetrical Maxwell's equations emerge. This new set of equations now include the magnetic charge and magnetic current densities that are the time and spatial derivatives of a pseudoscalar field P. By considering (1.2.1) and the four pseudovectors defined as

$$\boldsymbol{T} = \gamma_y\gamma_z\gamma_t T_x + \gamma_x\gamma_z\gamma_t T_y + \gamma_x\gamma_y\gamma_t T_z + \gamma_x\gamma_y\gamma_z T_t \tag{1.3.31}$$

a new vector potential can be defined as

$$\boldsymbol{A'} = \gamma_x A_x + \gamma_y A_y + \gamma_z A_z + \gamma_t A_t + \gamma_y\gamma_z\gamma_t T_x + \gamma_x\gamma_z\gamma_t T_y + \gamma_x\gamma_y\gamma_t T_z + \gamma_x\gamma_y\gamma_z T_t \tag{1.3.32}$$

from which we obtain

$$\boldsymbol{\partial}(\boldsymbol{A'}) = \boldsymbol{\partial}\left(\boldsymbol{A}_{\square} + \boldsymbol{T}\right) = S + \boldsymbol{F} + P. \tag{1.3.33}$$

Using SI units and following the same procedure as shown in Section 1.2 we can write:

$$S = \frac{\partial A_x}{\partial x} + \frac{\partial A_y}{\partial y} + \frac{\partial A_z}{\partial z} - \frac{1}{c}\frac{\partial A_t}{\partial t}$$

$$\gamma_x\gamma_t\frac{1}{c}E_x = \gamma_x\gamma_t\left(\frac{\partial A_t}{\partial x} - \frac{\partial T_z}{\partial y} - \frac{\partial T_y}{\partial z} - \frac{1}{c}\frac{\partial A_x}{\partial t}\right)$$

$$\gamma_y\gamma_t\frac{1}{c}E_y = \gamma_y\gamma_t\left(\frac{\partial T_z}{\partial x} + \frac{\partial A_t}{\partial y} - \frac{\partial T_x}{\partial z} - \frac{1}{c}\frac{\partial A_y}{\partial t}\right)$$

$$\gamma_z\gamma_t\frac{1}{c}E_z = \gamma_z\gamma_t\left(\frac{\partial T_y}{\partial x} + \frac{\partial T_x}{\partial y} + \frac{\partial A_t}{\partial z} - \frac{1}{c}\frac{\partial A_z}{\partial t}\right)$$

$$\gamma_x\gamma_y\gamma_z\gamma_t P = \gamma_x\gamma_y\gamma_z\gamma_t\left(\frac{\partial T_x}{\partial x} - \frac{\partial T_y}{\partial y} + \frac{\partial T_z}{\partial z} - \frac{1}{c}\frac{\partial T_t}{\partial t}\right)$$

$$\gamma_y\gamma_z B_x = \gamma_y\gamma_z\left(\frac{\partial T_t}{\partial x} + \frac{\partial A_z}{\partial y} - \frac{\partial A_y}{\partial z} - \frac{1}{c}\frac{\partial T_x}{\partial t}\right)$$

$$\gamma_x\gamma_z B_y = \gamma_x\gamma_z\left(-\frac{\partial A_z}{\partial x} + \frac{\partial T_t}{\partial y} + \frac{\partial A_x}{\partial z} + \frac{1}{c}\frac{\partial T_y}{\partial t}\right)$$

$$\gamma_x\gamma_y B_z = \gamma_x\gamma_y\left(\frac{\partial A_y}{\partial x} - \frac{\partial A_x}{\partial y} + \frac{\partial T_t}{\partial z} - \frac{1}{c}\frac{\partial T_z}{\partial t}\right).$$

By applying again the $\boldsymbol{\partial}$ operator to (1.3.33) and equating to zero:

$$\boldsymbol{\partial}^2\boldsymbol{A'} = \boldsymbol{\partial}\left(S + \boldsymbol{F} + P\right) = \boldsymbol{0}. \tag{1.3.34}$$

Here

$$\boldsymbol{\partial F} = -\boldsymbol{\partial}S - \boldsymbol{\partial}P = \mu_0\boldsymbol{J}_{\square e} + \frac{1}{\epsilon_0}\boldsymbol{J}_{\square m}, \tag{1.3.35}$$

where $\boldsymbol{J}_{\square e}$ is the four-current as defined in (1.2.50), $\boldsymbol{J}_{\square m} = \gamma_x J_{mx} + \gamma_y J_{my} + \gamma_z J_{mz} + \gamma_t J_{mt} = \gamma_x J_{mx} + \gamma_y J_{my} + \gamma_z J_{mz} - \gamma_t\frac{1}{c}\rho_m$ is the magnetic four-current vector and ρ_m the magnetic charge. By carrying out all calculation in (1.3.34) the following set of equations is obtained:

$$\gamma_x\left(\frac{\partial S}{\partial x} - \frac{\partial B_z}{\partial y} + \frac{\partial B_y}{\partial z} + \frac{1}{c^2}\frac{\partial E_x}{\partial t}\right) = 0$$

$$\gamma_y\left(\frac{\partial B_z}{\partial x} + \frac{\partial S}{\partial y} - \frac{\partial B_x}{\partial z} + \frac{1}{c^2}\frac{\partial E_y}{\partial t}\right) = 0$$

$$\gamma_z\left(-\frac{\partial B_y}{\partial x} + \frac{\partial B_x}{\partial y} + \frac{\partial S}{\partial z} + \frac{1}{c^2}\frac{\partial E_z}{\partial t}\right) = 0$$

$$\gamma_t\frac{1}{c}\left(\frac{\partial E_x}{\partial x} + \frac{\partial E_y}{\partial y} + \frac{\partial E_z}{\partial z} + \frac{\partial S}{\partial t}\right) = 0$$

$$\gamma_y\gamma_z\gamma_t\frac{1}{c}\left(\frac{\partial P}{\partial x}+\frac{\partial E_z}{\partial y}-\frac{\partial E_y}{\partial z}+\frac{\partial B_x}{\partial t}\right)=0$$
$$\gamma_x\gamma_z\gamma_t\frac{1}{c}\left(\frac{\partial E_z}{\partial x}-\frac{\partial P}{\partial y}-\frac{\partial E_x}{\partial z}-\frac{\partial B_y}{\partial t}\right)=0$$
$$\gamma_x\gamma_y\gamma_t\frac{1}{c}\left(\frac{\partial E_y}{\partial x}-\frac{\partial E_x}{\partial y}+\frac{\partial P}{\partial z}+\frac{\partial B_z}{\partial t}\right)=0$$
$$\gamma_x\gamma_y\gamma_z\left(\frac{\partial B_x}{\partial x}+\frac{\partial B_y}{\partial y}+\frac{\partial B_z}{\partial z}+\frac{\partial P}{\partial t}\right)=0.$$

This set of equations represents the symmetrical Maxwell's equations considering the hypothesis of existing magnetic currents and charges. This hypothesis was experimentally proven by several independent experiments, which we discuss in a later chapter on magnetic monopoles.

1.4. Conclusions

Simplicity is an important and concrete value in scientific research. Connections between very different concepts in physics can be evidenced if we use the language of geometric algebra. The application of Occam's Razor principle to Maxwell's equations highlights some essential concepts:

(1) Clifford algebra is by far the most appropriate, simple and intuitive mathematical language for encoding in general the laws of physics and here, particularly, for the laws of electromagnetism;
(2) a scalar field derives from the definition of "harmonic" electromagnetic four-potential and is at the origin of charges and currents;
(3) the charge density derived from the scalar field follows the wave equation with a propagation speed equal to the speed of light.

In particular, the important element emerging from the present work is that (1.2.60) imposes a precise condition on charge dynamics, describing distributions of charge density moving in vacuum at the speed of light.

In the model proposed here, the added constraint on the charge and current density seems to imply that one is no longer free to specify charge and current density distributions at will, because this information is indeed included within the definition of the four-potential $\boldsymbol{A}_{\square}$. However, this constraint can be removed when considering macroscopic electromagnetic systems or even the dynamics of a single elementary charge at a spatial scale greater than the particle Compton wavelength λ_c and at a time scale greater than the Compton period $\frac{\lambda_c}{c}$. In this case static elementary charges can be visualized as charge density distributions moving at the speed of light on a closed trajectory but with a zero average speed (this generalization would be consistent with static charge densities, dielectrics), whereas currents can be considered as an ordered motion of charge density distributions moving with an absolute velocity equal to the speed of light but with an arbitrary absolute average speed lower than c. *This observation favors a pure electromagnetic model of elementary particles based on a particular Zitterbewegung interpretation of quantum mechanics* [**10, 12**]. Therefore, the free electron, and perhaps all other elementary charged particles, can be viewed as a charge distribution that rotates at the speed of light along a circumference whose length is equal to its Compton wavelength [**18**].

Finally, it has been demonstrated that Maxwell's equations can be explicitly derived in a simple way directly from a Lagrangian density of the electromagnetic bivector and the scalar field. An interesting consequence is also that the specific energy of the scalar field is deeply connected to the interaction term of the Lagrangian density and, therefore, both to the electromagnetic four-potential and the four-current density.

Bibliography

[1] Aharonov, Y. and Bohm, D. Significance of Electromagnetic Potentials in the Quantum Theory. Physical Review, 115:485–491, 1959.

[2] L. Bauer. The Linguistics Student's Handbook. Edinburgh University Press, 2007.

[3] G. Bettini. Clifford Algebra, 3 and 4-Dimensional Analytic Functions with Applications. Manuscripts of the Last Century. viXra.org, Quantum Physics:1–63, 2011. http://vixra.org/abs/1107.0060.

[4] J. M. Chappell, S. P. Drake, C. L. Seidel, L. J. Gunn, A. Iqbal, A. Allison, and D. Abbott. Geometric Algebra for Electrical and Electronic Engineers. Proceedings of the IEEE, 102(9):1340–1363, Sept 2014.

[5] J. M. Chappell, A. Iqbal, and D. Abbott. A simplified approach to electromagnetism using geometric algebra. ArXiv e-prints, oct 2010. https://arxiv.org/pdf/1010.4947.pdf.

[6] Paul A. M. Dirac. Nobel Lecture: Theory of electrons and positrons. Nobel Lectures, Physics 1922-1941, 1965.

[7] Justin Dressel, Konstantin Y. Bliokh, and Franco Nori. Spacetime Algebra as a Powerful Tool for Electromagnetism. Physics Reports, 589:1 – 71, 2015

[8] R. P. Feynman. Nobel Lecture: The Development of the Space-Time View of Quantum Electrodynamics. Nobel Lectures, Physics 1963-1970, 1972

[9] R. P. Feynman. QED: The Strange Theory of Light and Matter. Penguin Books. Penguin, 1990.

[10] David Hestenes. Quantum Mechanics from Self-interaction. Foundations of Physics, 15(1):63–87, 1985.

[11] David Hestenes. Clifford Algebra and the Interpretation of Quantum Mechanics, pages 321–346. Springer Netherlands, Dordrecht, 1986.

[12] David Hestenes. Zitterbewegung Modeling. Foundations of Physics, 23(3):365–387, 1993.

[13] David Hestenes. Reforming the Mathematical Language of Physics. Oersted Medal Lecture 2002, 2002.

[14] Lee M. Hively. Implications of a new electrodynamic theory. July 2015. at https://www.researchgate.net

[15] Lee M Hively and G. C. Giakos. Toward a more complete electrodynamic theory. International Journal of Signals and Imaging Systems Engineering, 5(1), Jan 2012.

[16] G. Pilato and G. Vassallo. TSVD as a Statistical Estimator in the Latent Semantic Analysis Paradigm. IEEE Transactions on Emerging Topics in Computing, 3(2):185–192, June 2015

[17] A. Rathke. A critical analysis of the hydrino model. New Journal of Physics, 7:127, 2005.

[18] F. Santandrea and P. Cirilli. Unificazione elettromagnetica, concezione elettronica dello spazio, dell'energia e della materia. Atlante di numeri e lettere, Laboratorio di ricerca industriale, pages 1–8, 2006. http://www.atlantedinumerielettere.it/energia2006/pdf/labor.pdf.

[19] Amr M. Shaarawi. Clifford algebra formulation of an electromagnetic charge-current wave theory. Foundations of Physics, 30(11):1911–1941, 2000.

[20] Karoly Simonyi. Theoretische Elektrotechnik. Hochschulbücher für Physik. VEB Deutscher Verlag der Wissenschaften, Berlin, Germany, 9th edition, 1989.

[21] K. J. van Vlaenderen. A generalisation of classical electrodynamics for the prediction of scalar field effects. ArXiv Physics e-prints, May 2003. https://arxiv.org/pdf/physics/0305098.pdf.

[22] K. J. van Vlaenderen and A. Waser. Generalization of Classical Electrodynamics to Admit a Scalar Field and Longitudinal Waves. Hadronic Journal, 24:609–628, 2001.

CHAPTER 2

The self-stabilizing electron wave

Andras Kovacs[1]
[1] ExaFuse. E-mail: andras.kovacs@broadbit.com

2.1. The electromagnetic wave that generates the quantum mechanical wave

> "According to our present conceptions the elementary particles of matter are, in their essence, nothing else than condensations of the electromagnetic field" Einstein in 1920

This chapter serves as a bridge between the improved understanding of Maxwell's equation, which was developed in chapter 1, and our study of the electron's particle aspect in the following chapters. With the emergence of quantum mechanics in the early 20$^{\text{th}}$ century, it has become recognized that the electron is some kind of a wave. The electron's wave aspect is very dramatically demonstrated in electron double-slit experiments, where the observed interference pattern proves that the electron passes through both slits simultaneously, despite their macroscopic separation.

Historically, quantum mechanics has been established over a set of experimentally motivated postulates. This set of postulates includes also paradoxical properties, such as the instantaneous wavefunction collapse or the intrinsic electron spin. An intense philosophical debate ensued over the past 100 years regarding the physical interpretation of these postulates. Einstein, Schrödinger, and Dirac were of the opinion that the electron comprises some kind of entrapped electromagnetic wave. At that time, attempts to model the electron as an electromagnetic wave were not successful. Therefore, since the mid-20$^{\text{th}}$ century, the quantum mechanical wavefunction has been taken as the starting point for any electron discussion, and most scientists abandoned exploring the relationship between quantum mechanical and electromagnetic waves. Our goal is to progress beyond this 20$^{\text{th}}$ century detour, and to develop a proper field theory that clarifies the electromagnetic wave nature of an electron. To progress towards this goal, we start by considering how the electron's wavefunction is generated.

Consider an electron moving at speed v. In relation to light-speed, its speed is characterized by $\beta = \frac{v}{c}$, $\gamma_L = \left(1-\beta^2\right)^{-\frac{1}{2}}$ and rapidity w defined as $\gamma_L = \cosh w$. It follows that $\cosh^2 w - \sinh^2 w = 1$, $\tanh w = \beta$, and $\sinh w = \gamma_L \beta$.

A relativistic boost rotates the time and space axes into each other according to the following hyperbolic rotation matrix:

$$\begin{pmatrix} ct' \\ x' \end{pmatrix} = \begin{pmatrix} \cosh w & -\sinh w \\ -\sinh w & \cosh w \end{pmatrix} \begin{pmatrix} ct \\ x \end{pmatrix}$$

Therefore, the time-wise Zitterbewegung wave evolution of the rest frame acquires a spatial oscillation component in the boosted reference frame. Specifically, the Zitterbewegung frequency of the rest frame is $\frac{\omega}{2\pi} = \frac{m_0 c^2}{h}$, and the corresponding wavenumber in the boosted frame is:

$$\frac{k}{2\pi} = \frac{\omega}{2\pi}\frac{\sinh w}{c}$$

Evaluating the right side of the above equation, we obtain:

$$\frac{k}{2\pi} = \frac{m_0 c^2}{h}\frac{\gamma_L v}{c^2}$$

Rearranging the above equation, we finally obtain:

$$\hbar k = \left(\gamma_L m_0\right) v = mv = p_{kinetic}$$

We recognize the above result as the basic postulate of quantum mechanics. However, it is no longer a postulate in our case: the appearing quantum mechanical wave is simply the Lorentz transformed component of the electron's Zitterbewegung oscillation. The next step is to understand what comprises the Zitterbewegung wave.

2.2. The longitudinal electromagnetic wave that carries the Zitterbewegung current

The electron is found where its current density $\boldsymbol{J}_{\square}$ is non-zero. How could this Zitterbewegung current density be an electromagnetic wave? We showed shown via equation 1.3.19 that $\boldsymbol{J}_{\square} \cdot \boldsymbol{A}_{\square}$ is equivalent to the electromagnetic $\frac{1}{2\mu_0}\left(S^2 - \frac{2}{c}\mathcal{I}\boldsymbol{E}\cdot\boldsymbol{B}\right)$ expression.

Let us find such a wave solution to Maxwell's equation that its Lagrangian density is given by the $\frac{1}{2\mu_0}\left(S^2 - \frac{2}{c}\mathcal{I}\boldsymbol{E}\cdot\boldsymbol{B}\right)$ expression. Here, the $\boldsymbol{E}\cdot\boldsymbol{B}$ term indicates that the electric and magnetic fields are parallel. The gaugeless Maxwell equation is simply $\boldsymbol{\partial}^2\boldsymbol{A}_{\square} = 0$, and we look for its longitudinal wave solutions. One trivial solution transforms electric and scalar field energies into each other, with the electric field pointing along the direction of propagation. For a longitudinal wave traveling along the z direction, the trivial longitudinal solution is:

$$E_z = E_0 \sin(\omega t - kz)\,,\; S = S_0 \sin(\omega t - kz)$$

where $S_0 = E_0$ in Natural units, and the wave is propagating at the speed of light along the z direction.

An other trivial solution transforms magnetic and scalar field energies into each other, with the magnetic field pointing along the direction of propagation. For a longitudinal wave traveling along the z direction, the trivial longitudinal solution is:

$$B_z = B_0 \cos(\omega t - kz)\,,\; S = \mathcal{I}S_0 \cos(\omega t - kz)$$

where $\mathcal{I}$ is the Clifford pseudo-scalar, $S_0 = B_0$ in Natural units, and the wave is propagating at the speed of light into the z direction.

Recall from chapter 1 that the complete electromagnetic Lagrangian density is:

$$\mathscr{L} = \frac{1}{2\mu_0}\left(-\frac{E^2}{c^2} + B^2 + S^2 - \frac{2}{c}\mathcal{I}\boldsymbol{E}\cdot\boldsymbol{B}\right)$$

We note that the trivial transversal wave solution corresponds to $-\frac{E^2}{c^2} + B^2 = 0$. The above described trivial longitudinal solutions correspond to either $-\frac{E^2}{c^2} + S^2 = 0$ with no magnetic field or $B^2 + S^2 = 0$ with no electric field. Since electromagnetic wave solutions can be superposed, we can combine the trivial longitudinal wave solutions. Adding the above-written electric and magnetic wave expressions, we get a longitudinal wave where the out-of-phase electric and magnetic field energies rotate into each other with scalar field mediation.

Let us now consider adding the trivial electric and magnetic longitudinal waves with the same $\sin(\omega t - kz)$ phase. The amplitude of the scalar wave part becomes $S_0^2(1+\mathcal{I})^2 = S_0^2 \cdot 2\mathcal{I}$. Multiplying the in-phase electric and magnetic fields gives a combined wave amplitude of $E_0 B_0 = S_0^2$. Clearly, we have found the longitudinal wave solution that corresponds to $S^2 - \frac{2}{c}\mathcal{I}\boldsymbol{E}\cdot\boldsymbol{B} = 0$, with parallel oriented electric and magnetic fields. In natural units, the longitudinal wave solution corresponding to $\boldsymbol{J}_{\square}\cdot\boldsymbol{A}_{\square}$ is:

$$\left\{ \begin{array}{c} E_z = E_0 \sin(\omega t - kz)\,,\; B_z = \pm B_0 \sin(\omega t - kz) \\ S = S_0 \sin(\omega t - kz) \pm \mathcal{I}S_0 \sin(\omega t - kz) \end{array} \right\} \tag{2.2.1}$$

where $\mathcal{I}$ is the Clifford pseudo-scalar, $S_0 = E_0 = B_0$ in Natural units, and this electric current-carrying wave is propagating at the speed of light into the z direction. In this simple plane wave case the electric and magnetic fields have no x, y components. The reason why this longitudinal wave solution has not been recognized in the past is its non-zero scalar field component.

At last, we can model the electron's Zitterbewegung current as a proper electromagnetic wave. Since electron's Zitterbewegung current forms a circulating loop, its mathematical formulation is more complex than the linear solution. Nevertheless, the identified longitudinal wave concept remains the same.

For an ordinary transversal wave, the associated wave energy is calculated by integrating the field energy density within the given wave. However, the longitudinal wave that comprises electric charge and current density, which induces electric and magnetic fields around the Zitterbewegung current loop. The energy associated energy with these external fields is defined by the vector potential experienced by the Zitterbewegung current loop. As will be shown in the following chapter, the associated wave energy is given by the $\iiint_V JA\,dV$ expression, which integrates over the volume where this longitudinal wave is present.

2.3. The electromagnetic formulation of quantum mechanical action

The evolution of a quantum mechanical electron wave is captured by the well-known Schrödinger equation:

$$i\hbar\frac{\partial\psi}{\partial t} = -\frac{\hbar^2}{2m}\frac{\partial^2\psi}{\partial x^2} + V(x)\cdot\psi \tag{2.3.1}$$

Expressing the wavefunction in the $\psi = e^{i\mathscr{S}/\hbar}$ harmonic wave form, the Schrödinger equation becomes:

$$-\frac{\partial\mathscr{S}}{\partial t} = -\frac{i\hbar}{2m}\frac{\partial^2\mathscr{S}}{\partial x^2} + \frac{1}{2m}\left(\frac{\partial\mathscr{S}}{\partial x}\right)^2 + V(x) \tag{2.3.2}$$

When we neglect the first term on the right hand side, the above equation reduces exactly to the classical Hamilton–Jacobi equation, where $\mathscr{S}$ is the classical action and $\frac{1}{2m}\left(\frac{\partial\mathscr{S}}{\partial x}\right)^2 + V(x)$ is the Hamiltonian giving the electron energy. With this formulation, we can see right away that quantum mechanics converges to classical mechanics in the $\hbar \to 0$ limit.

In equation 2.3.2, the $-\frac{i\hbar}{2m}\frac{\partial^2\mathscr{S}}{\partial x^2}$ term generates the interferences of the electron wavefunction. Let us take an analogy from optics: when observed from far away, light travels in the form of rays, whose trajectory is defined by the local propagation speed. That is the classic trajectory of light rays. Only when we look close enough, we see that light propagation is in fact governed by Maxwell's equation, and see the wave interference patterns emerging around slits or obstacles.

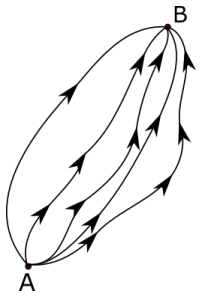

FIGURE 2.3.1. An illustration of the path integral formulation of quantum mechanics. The figure shows five of the infinitely many paths available for an electron wave to move from point A at time t to point B at time t'. An action $\mathscr{S}$ can be calculated for each path.

The above analysis demonstrates that the electron wavefunction ψ is determined by a quantum mechanical action function $\mathscr{S}$, and the $\psi = e^{i\mathscr{S}/\hbar}$ formula expresses the relationship between them. While the classical electron movement follows a single trajectory, the movement of a quantum mechanical electron wave can be treated as simultaneous propagation over a very large number of different trajectories. This methodology is referred to as the path integral formulation of quantum mechanics; it was firstly formulated by Dirac and then further developed by Feynman. The overall electron propagation probability between points A and B is obtained by calculating and summing up the $e^{i\mathscr{S}/\hbar}$ factors for each possible path. Some exemplary paths are illustrated in figure 2.3.1.

To properly understand how a longitudinal electromagnetic wave generates the quantum mechanical wave, one must find the corresponding electromagnetic formulation of $\mathscr{S}$. This important task is accomplished in chapter 4; starting from the above-discussed $\boldsymbol{J}_{\square}\cdot\boldsymbol{A}_{\square}$ formulation of the longitudinal electromagnetic wave, the following $\mathscr{S}$ formulation is obtained:

$$\mathscr{S} = \int (e\boldsymbol{A}\cdot\boldsymbol{c} - eV)\,dt \tag{2.3.3}$$

where e is the elementary charge, $(V\gamma_t, \boldsymbol{A}) \equiv \boldsymbol{A}_{\square}$ is the vector potential experienced by the charge-carrying longitudinal wave, $\boldsymbol{c}$ is the speed vector of the longitudinal wave, and dt is the elapsed infinitesimal time along its path. In this context, $\boldsymbol{A}_{\square}$ is the sum of the externally applied and electron-internal vector potential fields. The beauty of this action formula is that it is valid from femtometer-scale all the way to macroscopic scale, and hence it describes the electron wave's evolution at a more fundamental level than the quantum mechanical wavefunction. In other words, starting from the $\boldsymbol{J}_{\square}$ and $\boldsymbol{A}_{\square}$ functions

we can calculate ψ, but starting from ψ we cannot calculate the picometer-scale Zitterbewegung structure of $\boldsymbol{J}_{\square}$ and $\boldsymbol{A}_{\square}$. Besides establishing a deeper understanding of the electron wave, the electromagnetic formulation of $\mathscr{S}$ becomes relevant when electron spin interactions play a stabilizing role. Chapter 4 gives some examples of electron interaction phenomena where equation 2.3.3 provides new insights.

In essence, we may now distinguish three regimes of electron description:

(1) The classical regime, where the interferences of the electron wavefunction are negligible. This regime corresponds to the $\hbar \to 0$ limit of equation 2.3.2.

(2) The quantum mechanical regime, where the presence of electron wavefunction is relevant, but spin interactions can be neglected. This regime corresponds to equation 2.3.2, with $\mathscr{S}$ remaining a scalar parameter.

(3) The spin interaction regime, where the electron's wavefunction and spin interactions are both relevant. This regime corresponds to equation 2.3.2, with $\mathscr{S}$ being defined by equation 2.3.3.

Our work is of course not the first one to address electron spin interactions; up to now spin interactions have been evaluated mainly via the Dirac equation. One may then wonder how the Dirac equation relates to longitudinal electromagnetic waves. There must be a deep connection, after all Schrödinger identified the Zitterbewegung phenomenon by studying the Dirac equation. This topic is explored in chapter 5 and section 7.4, where we unpack the true meaning of the energy-momentum eigenvalues encoded by the Dirac equation.

Lastly, let us consider the minimization condition expressed in equation 2.3.3. Take an analogy from optics; a light ray propagates over a path that minimizes the travel time between points A and B. This travel time minimization condition is expressed via the following action:

$$\mathscr{S}_{optics} = \int_A^B n\frac{ds}{c} = \int n \cdot dt \tag{2.3.4}$$

where ds is infinitesimal displacement, and n is the index of light refraction along the trajectory; this index may vary from point to point. Here, n is a macroscopic parameter that is determined by the underlying atomic structure. Light rays propagate paths that minimize the integral of n.

Similarly, the elementary charge value e is a "macroscopic" parameter in the context of equation 2.3.3; it is generated by the underlying longitudinal wave structure. This underlying structure shall be determined in chapter 3. The $e\boldsymbol{A} \cdot \boldsymbol{c}$ term of equation 2.3.3 represents magnetic field induction, and the eV term represents electric field induction. In any electromagnetic wave, the magnetic and electric field inductions are in balance. The minimization of $(e\boldsymbol{A} \cdot \boldsymbol{c} - eV)$ thus represents the stable condition of electromagnetic wave propagation. An electron encounters disturbances to this stable condition along its path. For example, its electric field is disturbed as it approaches a highly charged nucleus. The minimized $(e\boldsymbol{A} \cdot \boldsymbol{c} - eV)$ condition means that the electron finds such stable states that minimize the averaged disturbances to its electromagnetic wave induction. This is the essential feature of a self-stabilizing electromagnetic wave.

2.4. The electron state before and during quantum mechanical state transitions

We use quantum mechanical state transition examples to further illustrate electrons' electromagnetic wave aspect. For an elementary particle to emit electromagnetic wave energy at the angular frequency ω, its charge must be oscillating at this frequency. This statement is a direct consequence of Maxwell's equation, and therefore it remains true under any circumstance. Since the kinetic oscillation of charges is described by the quantum mechanical wavefunction Ψ, light-matter interaction is a process between an electromagnetic angular frequency ω and the same kinetic oscillation frequency.

One the one hand, it is a direct consequence of Maxwell's equation that a quantum mechanical state transition process must last for a certain duration and must involve the transient presence of an ω angular frequency charge oscillation. On the other hand, the current axioms of quantum mechanics completely bypass Maxwell's equation. These axioms state that a quantum mechanical state transition is a timewise discontinuous "jump" process, which releases a so-called "photon particle". This hypothetical photon particle is characterized by the frequency ω, which is presumably never present in the photon-emitting particle wavefunction. Such polar opposite perspective makes one wonder about the origin of the "photon particle" concept, which dates back to more than 100 years ago. In his first quantum mechanics related publication, Einstein was trying to explain the experimental observation that the probability of a quantum mechanical state transition depends on the frequency of incident light, and not on its amplitude. It has been generally assumed in those days that light amplitude plays no role; it was only much later discovered that even low-frequency light causes quantum mechanical state transition when

the light amplitude is sufficiently high [**2**]. Regrettably, Einstein chose to go against the historic trend of exploring electromagnetic waves, and introduced the notion of "light particles" which are presently referred to as photons. At that time, most physicists believed in the reality of "aether particles" which supposedly permeate all space. In that pioneering era, the notion of a second type of light carrying particle appeared to be the simplest explanation of experiments. While it was mathematically clear from the start that a single-frequency electromagnetic emission implies an infinite wavefunction size of the hypothetical "photon particle", Einstein's contemporaries chose to ignore this mathematical paradox. Bohr complemented Einstein's postulate by an additional axiom stating that the release of a photon particle coincides with an abrupt jump between quantum mechanical states. But some years later Einstein was taken aback by the paradoxical implications of these axioms, and then fought against them till the end of his career. He felt that there is some hidden reality behind quantum mechanics, which is occulted by all these axioms. Schrödinger was also unhappy with Bohr's quantum jump postulate, and preferred to seek a proper wave-oriented description of state transitions: "I believe that the spectral lines do not arise from jumps, but from the beating between two stationary solutions of the wave equation".

Until recently, there was no experimental evidence to determine whether a quantum mechanical state transition is a smooth process of a certain duration or a sudden jump process. In a recent seminal experiment, the authors of [**3**] experimentally proved that quantum mechanical state transitions do have a characteristic duration. The authors of [**3**] distinguish the trigger event of quantum mechanical state transitions, which is stochastic, and the subsequent state transition process. They found that a triggered light emission or absorption process is deterministic and has a well-defined duration. Furthermore, figure 2.4.1 demonstrates a deterministic control over the completion or reversal of an already ongoing quantum mechanical state transition process. An electromagnetic pulse is employed for gaining such deterministic control over the outcome of an ongoing quantum mechanical state transition process. It is clear from these results that understanding light-matter interactions requires finding analytic solutions of Maxwell's equation in the microscopic limit. Ad-hoc axioms, which bypass all equations of electromagnetism, can only lead to misunderstandings.

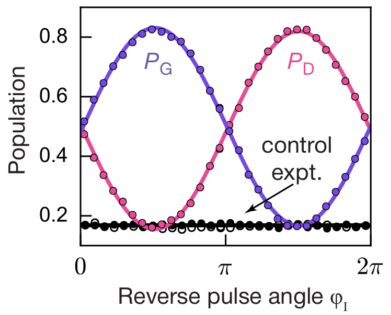

FIGURE 2.4.1. External control over the outcome of a quantum mechanical transition, which was applied at mid-point in the transition process. By definition, at this mid-point half of the particles are still in the ground state while the other half are already in the destination state. The applied external pulse angle determines whether the ongoing quantum mechanical transition completes or reverses itself. P_G denotes the probability of finding the particle in the ground state, while P_D denotes the probability of finding the particle in the excited destination state. In the control experiment the same pulse is applied at a random time, i.e. not at the mid-point of an ongoing quantum mechanical transition process. Reproduced from [**3**].

Quantum mechanical measurements have been also axiomatized as discontinuous "jump" processes, involving instantaneous wavefunction collapse. This leads to paradoxical assumptions of instantaneous communications, supposedly achieved by measuring entangled photons. Regarding such assumptions, which would violate causality, a refuting experiment is reported in reference [**4**]. Its author suggests that the observed Bell inequality violation is related to standing electromagnetic waves that arise between the source and detector already before the measurement. The random nature of quantum measurement outcomes is caused by the electromagnetic vacuum noise, into which the electron is embedded. How to understand measurement outcomes in a noisy environment? This simple sounding question does not have a trivial answer, and leads to the long-standing challenge of interpreting quantum mechanics. Reference [**5**] aims to clarify what quantum mechanical measurements really mean. In our work, we focus on clarifying the fundamental nature of the electron wave, which is then subject to electromagnetic vacuum

noise. Once the foundations are well-defined, the study of stochastic processes in noisy environments is a follow-on step.

In summary, the above examples illustrate that by properly understanding the electron's electromagnetic wave aspect we may clarify the foundations of quantum mechanics, which lays the foundation for further progress.

Bibliography

[1] B. Houchmandzadeh "The Hamilton–Jacobi equation: An alternative approach", American Journal of Physics, volume 88.5 (2020)

[2] T. F. Gallagher "Ionization in linearly and circularly polarized microwave fields", book chapter in "The Electron - New Theory and Experiment" (1991)

[3] Z. K. Minev et al "To catch and reverse a quantum jump mid-flight", Nature (2019)

[4] M. Fleury "Observations of Bell inequality violations with causal isolation between source and detectors", Entropy, volume 24.9 (2022)

[5] J. Lindgren "On the Unitarity of the Stueckelberg Wave Equation and Measurement as Bayesian Update from Maximum Entropy Prior Distribution" (2025)

CHAPTER 3

The Zitterbewegung geometry of the electron wave, and electron mass calculation from electromagnetic field energy

Andras Kovacs[1]
[1] ExaFuse. E-mail: andras.kovacs@broadbit.com

Nomenclature

Symbol, name, SI units, natural units (NU).

$\boldsymbol{A}_{\square}$: electromagnetic four-potential $[\mathrm{V}\cdot\mathrm{s}\cdot\mathrm{m}^{-1}]$, [eV];
$\boldsymbol{A}_{\triangle}$: electromagnetic vector potential $[\mathrm{V}\cdot\mathrm{s}\cdot\mathrm{m}^{-1}]$, [eV];
$\boldsymbol{G}$: electromagnetic field $[\mathrm{V}\cdot\mathrm{s}\cdot\mathrm{m}^{-2}]$, $[\mathrm{eV}^2]$;
$\boldsymbol{F}$: electromagnetic field bivector $[\mathrm{V}\cdot\mathrm{s}\cdot\mathrm{m}^{-2}]$, $[\mathrm{eV}^2]$;
$\boldsymbol{B}$: flux density field $[\mathrm{V}\cdot\mathrm{s}\cdot\mathrm{m}^{-2}] = [\mathrm{T}]$, $[\mathrm{eV}^2]$;
$\boldsymbol{E}$: electric field $[\mathrm{V}\cdot\mathrm{m}^{-1}]$, $[\mathrm{eV}^2]$;
S: scalar field $[\mathrm{V}\cdot\mathrm{s}\cdot\mathrm{m}^{-2}]$, $[\mathrm{eV}^2]$;
$\boldsymbol{J}_{\square e}$: four-current density field $[\mathrm{A}\cdot\mathrm{m}^{-2}]$, $[\mathrm{eV}^3]$;
$\boldsymbol{J}_{\triangle}$: current density field $[\mathrm{A}\cdot\mathrm{m}^{-2}]$, $[\mathrm{eV}^3]$;
$\boldsymbol{v}_{\square}$: four-velocity vector $[\mathrm{m}\cdot\mathrm{s}^{-1}]$, [1];
$\boldsymbol{v}_{\triangle}$: velocity vector $[\mathrm{m}\cdot\mathrm{s}^{-1}]$, [1];
ρ: charge density $[\mathrm{A}\cdot\mathrm{s}\cdot\mathrm{m}^{-3} = \mathrm{C}\cdot\mathrm{m}^{-3}]$, $[\mathrm{eV}^3]$;
x, y, z: space coordinates [m], $[\mathrm{eV}^{-1}]$, $[1.9732705\cdot10^{-7}\ \mathrm{m} \approx 1\ \mathrm{eV}^{-1}]$;
t: time variable [s], $[\mathrm{eV}^{-1}]$, $[6.5821220\cdot10^{-16}\ \mathrm{s} \approx 1\ \mathrm{eV}^{-1}]$;
c: light speed in vacuum $[2.997\,924\,58\cdot10^{8}\ \mathrm{m}\cdot\mathrm{s}^{-1}]$, [1];
$\hbar$: reduced Planck constant ($\hbar = \frac{h}{2\pi}$) $[1.054\,571\,726\cdot10^{-34}\ \mathrm{J}\cdot\mathrm{s}]$, [1];
μ_0: permeability of vacuum $[4\pi\cdot10^{-7}\ \mathrm{V}\cdot\mathrm{s}\cdot\mathrm{A}^{-1}\cdot\mathrm{m}^{-1}]$, $[4\pi]$;
ϵ_0: dielectric constant of vacuum $[8.854\,187\,817\cdot10^{-12}\ \mathrm{A}\cdot\mathrm{s}\cdot\mathrm{V}^{-1}\cdot\mathrm{m}^{-1}]$, $[\frac{1}{4\pi}]$;
e: electron charge $[1.602\,176\,565\cdot10^{-19}\ \mathrm{A}\cdot\mathrm{s}]$, $[0.085\,424\,546]$;
m_e: mass of the electron at rest $[9.109384\cdot10^{-31}\ \mathrm{kg}]$, $[0.510\,998\,946\ \cdot\ 10^{6}\ \mathrm{eV}]$;
λ_c: electron Compton wavelength $[2.426\,310\,2389\cdot10^{-12}\ \mathrm{m}]$, $[1.229\,588\,259\cdot10^{-5}\ \mathrm{eV}^{-1}]$;
r_e: reduced Compton wavelength of electron (Compton radius) $r_e = \frac{\lambda_c}{2\pi}$;
$\omega_e = \frac{c}{r_e}$: *Zitterbewegung* angular frequency;
T: Zitterbewegung period $T = \frac{2\pi}{\omega_e}$;
$\boldsymbol{P}_{\square}$: energy-momentum four-vector $[\mathrm{kg}\cdot\mathrm{m}\cdot\mathrm{s}^{-1}]$, [eV];
$\boldsymbol{P}_{\triangle}$: momentum vector $[\mathrm{kg}\cdot\mathrm{m}\cdot\mathrm{s}^{-1}]$, [eV];
U, W: energy $[J = \mathrm{kg}\cdot\mathrm{m}^2\cdot\mathrm{s}^{-2}]$, [eV].

3.1. Introduction

This chapter is based on reference [**1**]: mostly the same methodology and calculations are followed, and the main difference is the novel electron charge topology model introduced in this work. Building onto the results of chapters 1 and 2, a new and particularly simple model of the electron is proposed in this chapter.

One of the most detailed and interesting Zitterbewegung electron models to date has been proposed by David Hestenes [**2**]. He rewrote the Dirac equation for the electron using the four dimensional real Clifford algebra $Cl_{1,3}(\mathbb{R})$ of space-time with Minkowski signature "$+---$", eliminating unnecessary complexities and redundancies arising from the traditional use of matrices. The Dirac gamma matrices γ_μ and the associated algebra can be seen as an isomorphism of the four-basis vector of space-time geometric algebra. This simple isomorphism allows a full encoding of the geometric properties of the Dirac algebra, and a rewriting of Dirac equation that does not require complex numbers or matrix algebra. In this context, the wave function ψ is characterized by the eight real values of the even grade

multivectors of space-time algebra $Cl_{1,3}(\mathbb{R})$. Even grade multivectors can encode ordinary rotations as well as Lorentz transformations in the six planes of the space-time. Hestenes associates the rotations encoded by the wave function with an intrinsic very rapid rotation of the electron, the "Zitterbewegung", that is considered to generate the electron spin and magnetic moment. The word Zitterbewegung was originally used by Schrödinger to indicate a fast movement attributed to an hypothetical interference between "positive" and "negative" energy states. Kerson Huang later, more realistically, interpreted the Zitterbewegung as a circular motion [**3**].

In particular, B. Sidharth states that *"The well-known Zitterbewegung may be looked upon as a circular motion about the direction of the electron spin with radius equal to the Compton wavelength (divided by 2π) of the electron. The intrinsic spin of the electron may be looked upon as the orbital angular momentum of this motion. The current produced by the Zitterbewegung is seen to give rise to the intrinsic magnetic moment of the electron."* [**4**].

Hestenes considers the complex phase of the wave function solution of the traditional Dirac equation as the phase of the Zitterbewegung rotation, showing "*the inseparable connection between quantum mechanical phase and spin*" consequently rejecting the *"conventional wisdom that phase is an essential feature of quantum mechanics, while spin is a mere detail that can often be ignored"* [**5**]. Using the space-time algebra in reference [**6**], Hestenes defines the *"canonical form"* of *the real wave function* ψ:

$$\psi(x) = \left(\varrho e^{i\beta}\right)^{\frac{1}{2}} R.$$

In the above equation, x is a generic space-time point, $\varrho = \varrho(x)$ is a scalar function interpreted as a probability density proportional to charge density, i is the spatial bivector $i = \gamma_y\gamma_z$, $\beta = \beta(x)$ is a function representing the value of a rotation phase in the plane $\gamma_y\gamma_z$ and R is a rotor valued function that encodes a Lorentz transformation. The imaginary unit i is replaced by a bivector that generates rotation in a well-defined space-like plane, and not in a generic undefined "complex plane". Essentially, this work shows how the electron wavefunction is generated from its Zitterbewegung wave.

Based on the results of chapters 1 and 2, the electron characteristics may be explained by an electromagnetic wave that rotates at the speed of light along a circumference with a radius equal to the reduced electron Compton wavelength ($\approx 0.386159\ pm$). This radius corresponds to speed of light rotation at the $\omega = \frac{mc^2}{\hbar}$ De Broglie frequency. The electron mass-energy, expressed in natural units, is then equal to the angular speed of the Zitterbewegung rotation and to the inverse of the orbit radius (i.e. $\approx 511\ keV$), whereas the angular momentum is equal to the reduced Planck constant $\hbar$. Consequently, unlike the Hestenes prediction, our model proposes a relativistic contraction of the Zitterbewegung radius and a corresponding instantaneous Zitterbewegung angular speed that increases as the electron speed increases.

By using the electromagnetic four-potential as a "*Materia Prima*" a natural connection between electromagnetic concepts and Newtonian and relativistic mechanics seems to be possible. The vector potential should not be viewed only as a pure mathematical tool to evaluate spatial electromagnetic field distributions but as a real physical entity, as suggested by the Aharonov-Bohm effect, a quantum mechanical phenomenon in which a charged particle is affected by the vector potential in regions in which the electromagnetic fields are null [**7**].

The present chapter is structured in the following manner: Section 3.2 deals with a brief presentation of Maxwell's equations that does not use Lorenz gauge; Section 3.3 presents a new simple Zitterbewegung model of the electron with a list of the main parameters that can be deduced by applying this model; Section 3.5 describes an original method to easily derive the Lorentz force law from the electromagnetic field.

In this chapter all equations enclosed in square brackets with subscript "NU" have dimensions expressed in natural units.

3.2. Maxwell's Equations in $Cl_{3,1}$

The Space-time algebra is a four dimensions Clifford algebra with *Minkowski signature* $Cl_{1,3}$ ("west coast metric") or $Cl_{3,1}$ ("east coast metric") [**8, 9**].

In $Cl_{3,1}$ algebra, used in this work, calling $\{\gamma_x, \gamma_y, \gamma_z, \gamma_t\}$ the four unitary vectors of an orthonormal base the following rules apply:

$$\gamma_i\gamma_j = -\gamma_j\gamma_i \quad \text{with} \quad i \neq j \text{ and } i,j \in \{x,y,z,t\}, \tag{3.2.1}$$

$$\gamma_x^2 = \gamma_y^2 = \gamma_z^2 = -\gamma_t^2 = 1. \tag{3.2.2}$$

Maxwell's equations can be rewritten considering all the derivatives of the electromagnetic four-potential $\boldsymbol{A}_{\square}$:

$$\boldsymbol{A}_{\square}(x,y,z,t) = \gamma_x A_x + \gamma_y A_y + \gamma_z A_z + \gamma_t A_t. \tag{3.2.3}$$

Each of the vector potential components A_x, A_y, A_z and A_t is a function of space and time coordinates and has dimension in SI units equal to $[\mathrm{V}\cdot\mathrm{s}\cdot\mathrm{m}^{-1}]$. $\boldsymbol{A}_{\square}$ is a *harmonic* function that can be seen as the unique source of all concepts-entities in Maxwell's equations. We recall from chapter 1 that using the following definition of the operator $\boldsymbol{\partial}$ in space-time algebra (where $\nabla = \gamma_x\frac{\partial}{\partial x} + \gamma_y\frac{\partial}{\partial y} + \gamma_z\frac{\partial}{\partial z}$ and $c = 1/\sqrt{\epsilon_0\mu_0}$)

$$\boldsymbol{\partial} = \gamma_x\frac{\partial}{\partial x} + \gamma_y\frac{\partial}{\partial y} + \gamma_z\frac{\partial}{\partial z} + \gamma_t\frac{1}{c}\frac{\partial}{\partial t} = \nabla + \gamma_t\frac{1}{c}\frac{\partial}{\partial t}, \tag{3.2.4}$$

the following expression can be written (see Table 1):

$$\boldsymbol{\partial}\boldsymbol{A}_{\square} = \boldsymbol{\partial}\cdot\boldsymbol{A}_{\square} + \boldsymbol{\partial}\wedge\boldsymbol{A}_{\square} = S + \boldsymbol{F} = \boldsymbol{G}, \tag{3.2.5}$$

where

$$S = \nabla\cdot\boldsymbol{A}_{\triangle} - \frac{1}{c}\frac{\partial A_t}{\partial t} \tag{3.2.6}$$

is the scalar field,

$$\boldsymbol{F} = \frac{1}{c}\boldsymbol{E}\gamma_t + I\boldsymbol{B}\gamma_t = \frac{1}{c}\left(\boldsymbol{E} + Ic\boldsymbol{B}\right)\gamma_t \tag{3.2.7}$$

the electromagnetic field and

$$I = \gamma_x\gamma_y\gamma_z\gamma_t \tag{3.2.8}$$

is the pseudoscalar unit.

TABLE 1. Relation between electromagnetic entities and the vector potential.

$\boldsymbol{\partial}\boldsymbol{A}_{\square}$	$\gamma_x A_x$	$\gamma_y A_y$	$\gamma_z A_z$	$\gamma_t A_t$
$\gamma_x\frac{\partial}{\partial x}$	S_1	B_{z1}	$-B_{y1}$	$\frac{1}{c}E_{x1}$
$\gamma_y\frac{\partial}{\partial y}$	B_{z2}	S_2	B_{x1}	$\frac{1}{c}E_{y1}$
$\gamma_z\frac{\partial}{\partial z}$	$-B_{y2}$	B_{x2}	S_3	$\frac{1}{c}E_{z1}$
$\gamma_t\frac{1}{c}\frac{\partial}{\partial t}$	$\frac{1}{c}E_{x2}$	$\frac{1}{c}E_{y2}$	$\frac{1}{c}E_{z2}$	S_4

The electromagnetic field $\boldsymbol{G}$ can be expressed in the following compact form

$$\boldsymbol{G}(x,y,z,t) = \nabla\cdot\boldsymbol{A}_{\triangle} - \frac{1}{c}\frac{\partial A_t}{\partial t} + \nabla A_t\gamma_t - \frac{1}{c}\frac{\partial\boldsymbol{A}_{\triangle}}{\partial t}\gamma_t + I\nabla\times\boldsymbol{A}_{\triangle}\gamma_t, \tag{3.2.9}$$

and the expression

$$\boldsymbol{\partial}\boldsymbol{G} = \boldsymbol{\partial}^2\boldsymbol{A}_{\square} = 0, \tag{3.2.10}$$

represents the four Maxwell's equations. This is the mathematically simplest formulation of Maxwell's equation, and it is a proper field equation.

By applying, now, the $\boldsymbol{\partial}$ operator to the scalar field S, we obtain the expression of the four-current as

$$\frac{1}{\mu_0}\boldsymbol{\partial}S = \frac{1}{\mu_0}\left(\gamma_x\frac{\partial S}{\partial x} + \gamma_y\frac{\partial S}{\partial y} + \gamma_z\frac{\partial S}{\partial z} + \gamma_t\frac{1}{c}\frac{\partial S}{\partial t}\right) = \boldsymbol{J}_{\square e}, \tag{3.2.11}$$

where $\boldsymbol{J}_{\square e} = \gamma_x J_{ex} + \gamma_y J_{ey} + \gamma_z J_{ez} - \gamma_t c\rho = \boldsymbol{J}_{\triangle} - \gamma_t c\rho = \rho\left(\boldsymbol{v} - \gamma_t c\right)$ is the four-current vector and $\boldsymbol{v}_{\square} = \gamma_x v_x + \gamma_y v_y + \gamma_z v_z - \gamma_t c = \boldsymbol{v} - \gamma_t c$ is a four-velocity vector. The $\boldsymbol{\partial}$ operator applied to the four-current gives the charge-current conservation law

$$\frac{1}{\mu_0}\boldsymbol{\partial}\cdot(\boldsymbol{\partial}S) = \boldsymbol{\partial}\cdot\boldsymbol{J}_{\square e} = \frac{\partial J_{ex}}{\partial x} + \frac{\partial J_{ey}}{\partial y} + \frac{\partial J_{ez}}{\partial z} + \frac{\partial\rho}{\partial t} = 0, \tag{3.2.12}$$

which can be written alternatively as

$$\boldsymbol{\partial}\cdot(\boldsymbol{\partial}S)=\boldsymbol{\partial}^2S=\frac{\partial^2S}{\partial x^2}+\frac{\partial^2S}{\partial y^2}+\frac{\partial^2S}{\partial z^2}-\frac{1}{c^2}\frac{\partial^2S}{\partial t^2}=\nabla^2S-\frac{1}{c^2}\frac{\partial^2S}{\partial t^2}=0. \tag{3.2.13}$$

The charge is related to the scalar field according to

$$\frac{1}{c}\frac{\partial S}{\partial t}=\mu_0 J_{et}=-\mu_0 c\frac{\partial q}{\partial x\partial y\partial z}=-\mu_0 c\rho, \tag{3.2.14}$$

so that, by applying the time derivative to (3.2.13) and remembering (3.2.14), the wave equation of the charge density field $\rho(x,y,z,t)$ can be deduced:

$$\frac{\partial}{\partial t}\left(\boldsymbol{\partial}^2S\right)=\boldsymbol{\partial}^2\left(\frac{\partial S}{\partial t}\right)=\boldsymbol{\partial}^2\left(-\mu_0c^2\rho\right)=-\mu_0c^2\boldsymbol{\partial}^2\rho=0, \tag{3.2.15}$$

whose last equality gives

$$\boldsymbol{\partial}^2\rho=\nabla^2\rho-\frac{1}{c^2}\frac{\partial^2}{\partial t^2}\rho=0. \tag{3.2.16}$$

A more detailed development of the above equations was discussed in chapter 1.

3.3. Electron Zitterbewegung Model

The concept of charge that emerges from this rewriting of Maxwell's equations, has a non trivial implication: the analysis of (3.2.13) and (3.2.16) shows that the time derivative of a field S which propagates at the speed of light, must necessarily represent charges that are also moving at the speed of light.

This observation advises a pure electromagnetic model of elementary particles based on the Zitterbewegung interpretation of quantum mechanics [**2, 10**]. According to this interpretation, the electron structure consists of a massless charge that rotates at the speed of light along a circumference equal to electron Compton wavelength λ_c [**11, 12**]. Calling r_e the Zitterbewegung radius, ω_e the angular speed and T its period we have:

$$r_e=\frac{\lambda_c}{2\pi}\approx 3.861\,593\cdot10^{-13}\ \text{m}, \tag{3.3.1}$$

$$\omega_e=\frac{c}{r_e}=2\pi\cdot\frac{c}{\lambda_c}\approx 7.763\,440\cdot10^{20}\ \text{rad}\cdot\text{s}^{-1}, \tag{3.3.2}$$

$$T=\frac{2\pi}{\omega_e}=\frac{2\pi r_e}{c}\approx 8.093\,300\cdot10^{-21}\ \text{s}. \tag{3.3.3}$$

The value of the electron mass, expressed in SI units, can be derived from the following energy equations [**2**]

$$W_{tot}=m_ec^2=\hbar\omega_e=\frac{\hbar c}{r_e}, \tag{3.3.4}$$

from which

$$m_e=\frac{\hbar\omega_e}{c^2}=\frac{\hbar}{cr_e}=\frac{h}{c\lambda_c}\approx 9.109\,383\cdot10^{-31}\ \text{kg} \tag{3.3.5}$$

is obtained. Using natural units with $\hbar=c=1$ the electron mass (in eV) is equal to the angular speed ω_e and to the inverse of r_e:

$$\left[m_e=\omega_e=\frac{1}{r_e}\approx 0.511\cdot10^6\ \text{eV}\right]_{NU}.$$

3.3.1. Simple Electron Model. A charge rotating at the speed of light generates a current I_e that is equal to the ratio of the elementary charge e and its rotation period T [**13**]:

$$I_e = \frac{e}{T} = \frac{ec}{2\pi r_e} = \frac{e\omega_e}{2\pi} \approx 19.796\,331 \text{ A}. \tag{3.3.6}$$

Neglecting the electron's charge radius, the electron magnetic moment μ_B (Bohr magneton) is equal to the product between the current I_e and the enclosed area $\mathcal{A}_e$

$$\mu_B = I_e \mathcal{A}_e = \frac{e\omega_e}{2\pi}\pi r_e^2 = \frac{ec}{2} r_e = \frac{ec^2}{2\omega_e} = \frac{e\hbar}{2m_e} \approx 9.274\,010 \cdot 10^{-24} \text{ A} \cdot \text{m}^2. \tag{3.3.7}$$

Occam's razor is an effective epistemological instrument that imposes to avoid as much as possible the introduction of exceptions. Following this rule, a pure electromagnetic origin of the electron's "intrinsic" angular momentum should be found. Consequently, the canonical momentum P_t of the rotating massless charge may be seen as the cause of the intrinsic angular momentum:

$$\Omega = P_t r_e,$$

where the canonical momentum P_t of e, in presence of a vector potential A, generated by the current I_e, is

$$P_t = eA.$$

Imposing the constraint that $\Omega = \hbar$ we can compute A as function of I_e

$$\Omega = eAr_e = \frac{eAc}{\omega_e} = \frac{e^2 cA}{2\pi I_e} = \hbar, \tag{3.3.8}$$

from which it is possible to calculate the vector potential A seen by the spinning charge

$$A = \| \boldsymbol{A}_{\square} \| = \frac{2\pi\hbar}{e^2 c} I_e = \frac{\hbar}{er_e} = \frac{\hbar\omega_e}{ec} = \frac{m_e c}{e} \approx 1.704\,509 \cdot 10^{-3} \text{ V} \cdot \text{s} \cdot \text{m}^{-1}. \tag{3.3.9}$$

From (3.3.9) it is possible to derive the Fine Structure Constant (FSC)

$$\alpha = \frac{\mu_0}{4\pi} \cdot \frac{ce^2}{\hbar} = \frac{\mu_0}{4\pi} \cdot \frac{e\omega_e}{A} \approx 7.297\,352 \cdot 10^{-3} \tag{3.3.10}$$

Using natural units we get these simple relations:

$$\left[A = 2\pi\alpha^{-1} I_e\right]_{NU}$$

$$\left[eA = \omega_e = r_e^{-1} = m_e = P_t\right]_{NU}$$

where α^{-1}, the inverse of the FSC, is a pure number and e is the elementary charge expressed in natural units

$$\left[\alpha^{-1} = e^{-2} \approx 137.035989\right]_{NU}.$$

3.3.2. Spin and Intrinsic Angular Momentum. The intrinsic angular momentum $\hbar$ of the electron model (see (3.3.8)) is compatible with the spin value $\frac{\hbar}{2}$ if we consider the electron interaction with the external magnetic field $\boldsymbol{B}_E$, as in the Stern-Gerlach experiment. We can interpret the spin value $\pm\frac{\hbar}{2}$ as the component of the intrinsic angular momentum $\boldsymbol{\Omega} = \hbar$ aligned with the external magnetic field $\boldsymbol{B}_E$. In this case the angle between the $\boldsymbol{B}_E$ vector and the angular momentum has only two possible values, namely $\frac{\pi}{3}$ and $\frac{2\pi}{3}$ while the electron is subjected to a Larmor precession with angular frequency $\omega_p = \frac{d\vartheta_p}{dt}$. The Larmor precession is generated by the mechanical momentum

$$\tau = |\boldsymbol{\mu}_B \times \boldsymbol{B}_E| = B_E \mu_B \sin\left(\frac{\pi}{3}\right). \tag{3.3.11}$$

But

$$d\Omega = \Omega_{\perp} d\vartheta_p = \Omega \sin\left(\frac{\pi}{3}\right) d\vartheta_p,$$

where $\Omega_\perp$ is the component of the intrinsic angular momentum orthogonal to $\boldsymbol{B}_E$ and, therefore, it is possible to write

$$\tau = \frac{d\Omega}{dt} = \Omega \sin\left(\frac{\pi}{3}\right) \frac{d\vartheta_p}{dt}. \tag{3.3.12}$$

By equating (3.3.11) and (3.3.12) we get

$$B_E \mu_B = \Omega \omega_p,$$

from which it is possible to determine the precession angular frequency

$$\omega_p = \frac{B_E \mu_B}{\Omega} = \frac{B_E \mu_B}{\hbar}. \tag{3.3.13}$$

We note that the Larmor spin-precession's frequency is half of the "electron spin resonance" frequency [**14**]: $\omega_{esr} = 2\omega_p$. The ω_{esr} value is the experimentally measurable angular frequency of resonant flipping between the parallel and anti-parallel spin precession orientations with respect to a sinusoidally varying applied magnetic field. A consequence of Larmor spin-precession phenomenon: the measured $\frac{\hbar}{2}$ spin angular moment, measured via an applied B field, is only that component of the total angular momentum vector which is pointing along the applied B field.

3.3.3. Larmor spin-precession angle. In the preceding section we discussed the Larmor spin-precession phenomenon. Without noise interference, we get the classical mechanics analogue of Larmor precession. In the absence of vacuum noise, the angle between $\boldsymbol{B}_E$ and $\boldsymbol{\mu}_B$ may be arbitrarily close to π, and the measured spin angular momentum could be arbitrarily close to zero in that hypothetical case. However, the presence of vacuum noise establishes an energy noise floor. Let us check how this measured spin angular momentum relates to the magnetic field energy noise floor. We equate the measured angular momentum with the circulation of an electromagnetic wave:

$$\Omega_\perp = P \cdot r = P \frac{c}{\omega} \tag{3.3.14}$$

where P is the electromagnetic momentum, and r is the circulation radius.

With the angle between $\boldsymbol{B}_E$ and $\boldsymbol{\mu}_B$ being $\frac{\pi}{3}$ and $\frac{2\pi}{3}$, we obtained $\Omega_\perp = \frac{\hbar}{2}$ in the preceding section. The above equation therefore becomes:

$$Pc = \frac{\hbar\omega}{2} \tag{3.3.15}$$

On the other hand, the mean magnetic energy density of vacuum noise is $\frac{\bar{B}^2}{\mu_0} = \frac{1}{V}\frac{\hbar\omega}{2}$ at each frequency. A detailed study of the electromagnetic vacuum noise is found in chapter 6. This correspondence between Pc and $\frac{\bar{B}^2}{\mu_0}$ suggests that the Larmor precession angle is defined by the magnetic noise floor, so that we cannot measure a smaller magnetic energy density than the noise floor limit.

3.3.4. Value of the Vector Potential, Cyclotron Resonance and Flux Density Field. The pure electromagnetic momentum eA of the spinning charge of an electron at rest can be seen as if it were the momentum of a particle of mass m_e and speed c in classical Newtonian mechanics. Considering ω_e as the cyclotron angular frequency (which is coincident with the Zitterbewegung angular speed) given by the flux density field B generated by the current I_e

$$\omega_e = \frac{eB}{m_e} = \frac{eBc^2}{\hbar\omega_e}$$

it is possible to deduce the magnetic flux density produced by the electron

$$B_e = \frac{\hbar\omega_e^2}{ec^2} = \frac{m_e^2}{e} \approx 4.414\,004 \cdot 10^9 \ \mathrm{V \cdot s \cdot m^{-2}}. \tag{3.3.16}$$

This very high flux density value is also known as the *Schwinger limit value*. In traditional quantum field theory, the Schwinger limit is interpreted as the boundary above which the electromagnetic field is expected to become nonlinear, i.e. no longer conforming to the linear Maxwell equation. Our work presents a completely different interpretation of the Schwinger limit value: it is defined by the electron structure. The linear versus nonlinear limit of Maxwell's equation is discussed in chapter 7.

It is also possible to calculate the flux density at the center of the electron orbit by the following expression derived from the Biot-Savart law

$$B_o = \frac{\mu_0}{2} \cdot \frac{I_e}{r_e} \approx 32.210\,548 \cdot 10^6 \text{ V} \cdot \text{s} \cdot \text{m}^{-2}. \tag{3.3.17}$$

Considering that

$$dA = Ad\vartheta \Rightarrow \frac{dA}{dt} = A\omega_e, \tag{3.3.18}$$

where $d\vartheta = \omega_e dt$ is the differential of the Zitterbewegung phase, and considering that the magnetic force F_B must be equal to the time derivative of the canonical momentum, it is possible to write

$$F_B = B_e ec = e\frac{dA}{dt} = eA\frac{d\vartheta}{dt} = eA\omega_e \approx 0.212\,014 \text{ N}. \tag{3.3.19}$$

Finally, by manipulating the previous equation, it is possible to recompute by another method the norm of the vector potential

$$A = \frac{B_e c}{\omega_e} = \frac{\hbar\omega_e}{ec} = \frac{\hbar}{er_e}.$$

3.3.5. Electron structure, and the electromagnetic field energy that comprises the electron mass. Once we obtain the expression for the vector potential it is possible to determine the magnetic flux produced by the rotating elementary charge by applying the circulation of the vector potential A:

$$\phi_e = \oint_{\lambda_c} Ad\lambda = \int_0^{2\pi} \frac{\hbar}{er_e} r_e d\vartheta = 2\pi\frac{\hbar}{e} = \frac{h}{e} \approx 4.135\,667 \cdot 10^{-15} \text{ V} \cdot \text{s}, \tag{3.3.20}$$

i.e. the magnetic flux crossing the surface described by the charge trajectory is quantized (*flux quantum*). Now it is possible to estoimate the magnetic energy stored in the field produced by the spinning charge

$$W_m = \frac{1}{2}\phi_e I_e = \frac{1}{2} \cdot 2\pi\frac{\hbar}{e} \cdot \frac{ec}{2\pi r_e} = \frac{\hbar c}{2r_e} \approx 4.093\,553 \cdot 10^{-14} \text{ J} \tag{3.3.21}$$

which is equal to half the electron rest energy W_{tot} as can be seen from (3.3.4). Since electromagnetic induction requires equal amount of electric and magnetic field energies, the other half of the electron energy can be attributed to electric field energy, *i.e.*

$$W_{tot} - W_m = W_e = \iiint_V w_e \, dV, \tag{3.3.22}$$

where w_e is the electrostatic energy per unit of volume and V is the volume in which the whole energy W_e is stored. In essence, we our simple $\left[eA = \omega_e = r_e^{-1} = m_e = P_t\right]_{NU}$ electron model choice implies that the electron mass comprises electric and magnetic field energy, which form the electron wave. In the following, we further refine this simple electron model.

The $\frac{\phi_e}{T}$ ratio has the dimension of a voltage:

$$V_e = \frac{\phi_e}{T} = \frac{h}{e} \cdot \frac{c}{2\pi r_e} = \frac{\hbar c}{er_e} \approx 5.109\,989 \cdot 10^5 \text{ V}, \tag{3.3.23}$$

where T is defined by (3.3.3). Now, dividing the above voltage by the current generated by the rotating charge expressed by means of (3.3.6), we find the von Klitzing constant or *quantum of resistivity*, related to the quantum Hall effect

$$R_K = \frac{V_e}{I_e} = \frac{h}{e} \cdot \frac{c}{2\pi r_e} \cdot \frac{2\pi r_e}{ec} = \frac{h}{e^2} = \frac{2\pi\hbar}{e^2} \approx 25812.807\ \Omega. \tag{3.3.24}$$

Finally, it is possible to deduce the values of two interesting electrical parameters, namely the inductance L_e, the capacitance C_e of the electron and the frequency f_e. In fact

$$L_e = \frac{\phi_e}{I_e} = 4\pi^2\frac{\hbar r_e}{e^2 c} \approx 2.089\,108 \cdot 10^{-16}\ \Omega \cdot \text{s}, \tag{3.3.25}$$

(3.3.26) $$C_e = \frac{e}{\varphi_e} = 4\pi\epsilon_0 r_{cl} \approx 3.135\,381 \cdot 10^{-25}\ \mathrm{F}$$

and

(3.3.27) $$f_e = \frac{1}{\sqrt{L_e C_e}} \approx 1.235\,590 \cdot 10^{20}\ \mathrm{Hz}$$

which is indeed the electron's Zitterbewegung frequency. This relationship demonstrates the electromagnetic induction that generates the electron wave.

The remaining question is to understand what that volume is, within which the electron charge is located. Equation 3.3.9 informs that the electric charge density is distributed in such a way that the electron charge experiences a constant vector potential value. Such a constant vector potential value is a pre-condition to a well-defined Zitterbewegung frequency value. Suppose that the Zitterbewegung current is circulating within a toroidal volume, whose major radius is r_e. From (3.3.9) and (3.3.6), with the hypothesis that the electron is characterized by a uniform current density, we get the first term of the interaction part of the Lagrangian density

(3.3.28) $$L_{int1} = \boldsymbol{J}_{\triangle} \cdot \boldsymbol{A}_{\triangle} = JA = \frac{I_e}{\pi r_{cl}^2} \cdot \frac{m_e c}{e} \approx 1.352\,604 \cdot 10^{27}\ \mathrm{J \cdot m^{-3}}$$

where r_{cl} is the minor toroidal radius.

By integration over the volume described by the electron toroidal trajectory it is possible to validate our electron mass calculation:

(3.3.29) $$W_{tot} = m_e c^2 = \iiint_V JA\,dV = \frac{I_e}{\pi r_{cl}^2} \cdot \frac{m_e c}{e} \cdot 2\pi^2 r_e r_{cl}^2 \approx 8.187\,106 \cdot 10^{-14}\ J = 510.998\,946\ \mathrm{keV}$$

The match with the correct electron mass validates the chosen geometry: the Zitterbewegung current is circulating within a toroidal volume, whose major radius is r_e. We note that the r_{cl} minor toroidal radius remains yet undetermined. The above integral corresponds to a longitudinal electromagnetic wave, whose formulation is given by equation 2.2.1: half of such a longitudinal wave energy comprises scalar field energy. Therefore, the electron's energy comprises electric, magnetic, and scalar field energy components.

3.3.6. Electron charge topology. In this section, we aim to determine the electron's charge and current distribution topology in more details. We estimate r_{cl} from electron-light interaction experiments. At fm-scale photon wavelength, which allows fm-scale spatial resolution of the electron structure, electrons scatter light via the Compton scattering process. In Compton scattering, the scattering cross section is set by the 2.82 fm classical electron radius of the Klein-Nishina formula. Therefore, r_{cl} is approximately given by the classical electron radius formula [**15**]:

(3.3.30) $$r_{cl} = \frac{e^2 r_e}{4\pi\epsilon_0 \hbar c} \approx 2.817\,940 \cdot 10^{-15}\ \mathrm{m}$$

The obtained electron geometry is illustrated in figure 3.3.1. The circulating current distribution has a finite dimension, i.e. the electron is not point-like. The condition of light-speed current circulation implies that, everywhere within the torus, electric currents move along EXACTLY the same r_e radius. This leads to a Hopf-fibration type current topology, where each point moves around a slightly different circulation center. This Zitterbewegung current topology is illustrated in figure 3.3.2. The inherent symmetry of each current loop ensures that they experience the same electric potential, as required for obtaining a single Zitterbewegung frequency.

It is interesting to note that the ratio $\frac{r_e}{r_{cl}}$ is equal to the inverse of the fine structure constant, *i.e.*

(3.3.31) $$\frac{r_e}{r_{cl}} = \frac{4\pi\epsilon_0\hbar c}{e^2 r_e} r_e = \frac{4\pi\epsilon_0\hbar c}{e^2} = \alpha^{-1} \approx 137.035\,999.$$

3.3.7. Summary of electron parameters. We identified the electron's toroidal structure. Its toroidal volume is filled by a longitudinal electromagnetic wave, whose circulation pattern is illustrated in figure 3.3.2. The quantum mechanical wavefunction is the spatial component of the Lorentz-transformed longitudinal electromagnetic wave, hence the Zitterbewegung phase and quantum mechanical phase are everywhere identical. This longitudinal wave induces electric and magnetic fields, which extend outside

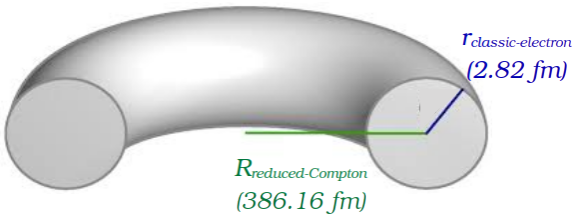

FIGURE 3.3.1. An illustration of the electron's particle aspect. The electric current circulates at the speed of light within a torus whose major radius is the reduced Compton radius, and whose minor radius is classical electron radius. This circular Zitterbewegung motion generates the electron's spin.

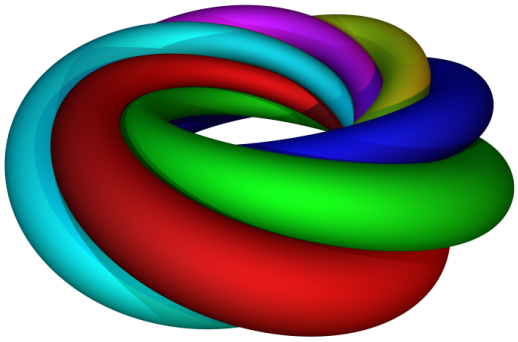

FIGURE 3.3.2. A more detailed illustration of the Zitterbewegung current trajectories within the electron torus.

of its toroidal volume. The electron mass is identified with the integrated energy density of these induced electric and magnetic fields.

Numerous quantitative parameters that can be deduced from our electron Zitterbewegung model; these are summarized in Table 2, where the first three rows are the model's input parameters.

3.3.8. Zitterbewegung and a Simple Derivation of the Relativistic Mass. With the Zitterbewegung model it is possible to show a simple, original and intuitive explanation of the relativistic mass concept. Let us consider the above calculated $r_e^{-1} = m_e$ relation from a boosted reference frame perspective. When a particle having rest mass m_0 is observed from a reference frame boosted by a Lorentz boost factor γ_L, its mass becomes $\gamma_L m_0$ from the perspective of the boosted reference frame. Keeping in mind that circular Zittebewegung comprises electromagnetic waves that are perpendicular to the axial direction of particle motion, the transversal relativistic Doppler shift will change these electromagnetic wavelengths by γ_L^{-1} factor. In the axial direction, the particle size changes also by γ_L^{-1} factor because of Lorentz contraction. Therefore, from the perspective of the boosted reference frame, the particle size changes by γ_L^{-1} factor, leading to the $r^{-1} = m$ relation remaining valid in the boosted reference frame:

$$r = r_e\sqrt{1 - \frac{v_z^2}{c^2}}, \tag{3.3.32}$$

$$m = \frac{m_e}{\sqrt{1 - \frac{v_z^2}{c^2}}}. \tag{3.3.33}$$

where m_e is the electron mass at rest. With reference to equation 3.3.21, the relativistic mass increase is a direct consequence of the shrinking Zitterbewegung radius in a boosted reference frame. Fig. 3.3.3 represents the Zitterbewegung trajectory of the circulating charge of an electron subjected to an acceleration directed along the positive z axis. Due to its acceleration, the Zitterbewegung radius reduces itself according to (3.3.32). In particle accelerator experiments, where electrons gain GeV-range kinetic energy, the energetic electron charge is indeed concentrated into a very tiny region of space.

TABLE 2. Parameters of the Zitterbewegung electron model. The spin is the component of the angular momentum that points along the external magnetic field B_E (see (3.3.11))

Item	Symbol	Value	Unit
charge	e	$1.602\,176\,565 \cdot 10^{-19}$	$\mathrm{C} = \mathrm{A} \cdot \mathrm{s}$
Zitterbewegung orbit radius	$r_e = \frac{\lambda_c}{2\pi}$	$3.861\,593 \cdot 10^{-13}$	m
intrinsic angular momentum	$\Omega = \hbar = \frac{h}{2\pi}$	$1.054\,571\,726 \cdot 10^{-34}$	$\mathrm{J} \cdot \mathrm{s}$
spin*	$\frac{\hbar}{2}$	$0.527\,285\,863 \cdot 10^{-34}$	$\mathrm{J} \cdot \mathrm{s}$
angular speed	ω_e	$7.763\,440 \cdot 10^{20}$	$\mathrm{rad} \cdot \mathrm{s}^{-1}$
mass	m_e	$9.109\,384 \cdot 10^{-31}$	kg
current	I_e	19.796 331	A
magn. moment (Bohr magn.)	μ_B	$9.274\,010 \cdot 10^{-24}$	$\mathrm{A} \cdot \mathrm{m}^2$
vector potential	A	$1.704\,509 \cdot 10^{-3}$	$\mathrm{V} \cdot \mathrm{s} \cdot \mathrm{m}^{-1}$
magnetic flux density	B_e	$4.414\,004 \cdot 10^{9}$	$\mathrm{V} \cdot \mathrm{s} \cdot \mathrm{m}^{-2}$
magnetic flux	$\phi_e = \frac{h}{e}$	$4.135\,667 \cdot 10^{-15}$	$\mathrm{V} \cdot \mathrm{s}$
magnetic energy	W_m	$4.093\,553 \cdot 10^{-14}$	J
electric energy	W_e	$4.093\,553 \cdot 10^{-14}$	J
electron energy at rest	$W_{tot} = m_e c^2$	$8.187\,106 \cdot 10^{-14}$	J
classic electron radius	r_{cl}	$2.817\,940 \cdot 10^{-15}$	m
inverse of the FSC	$\alpha^{-1} = \frac{r_e}{r_0}$	137.035 999	1
Von Klitzing constant	$R_K = \frac{h}{e^2} = \frac{\mu_0 c}{2\alpha}$	25812.807	Ω
inductance	$L_e = \frac{4\pi^2 \hbar r_e}{e^2 c}$	$2.089\,108 \cdot 10^{-16}$	$\Omega \cdot \mathrm{s}$
capacitance	$C_e = 4\pi\epsilon_0 r_0$	$3.135\,381 \cdot 10^{-25}$	F
1-st part of L_{int}	JA	$1.352\,604 \cdot 10^{27}$	$\mathrm{J} \cdot \mathrm{m}^{-3}$
electron energy at rest	$\iiint_V JA\,dV$	510.998 946	keV
electron energy at rest	$\iiint_V \rho\varphi_e\,dV$	510.998 946	keV
memristance	$\frac{\phi_e}{e} = \frac{h}{e^2}$	25812.807	Ω

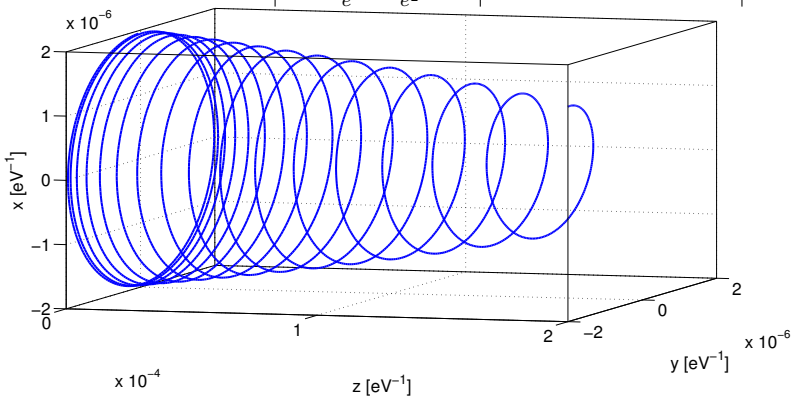

FIGURE 3.3.3. Zitterbewegung trajectory during an acceleration of the electron in the z direction.

3.4. A precise magnetic moment calculation

The magnetic moment is traditionally given by the $\mu_B = \frac{e\hbar}{2m_e}$ formula, where the only non-constant parameter is the electron mass. This magnetic moment formula was calculated via equation 3.3.7.

Measurements indicate that there is a small deviation between the experimental magnetic moment and the above formula. According to equation 3.3.7, the measurement of the electron's magnetic moment can be interpreted as a measurement of its mass. The presence of the small anomalous part means that the formula is not exactly correct, and the implicit assumptions going into this formula must be checked. It has the implicit assumption that the dipole magnetic field is created by the electric charge, upon exactly one full rotation. Let us check whether this assumption is valid.

Starting from the fundamentals, the $\boldsymbol{\partial}^2 \boldsymbol{A}_{\square} = 0$ Maxwell equation describes how electric and magnetic fields induce each other. In this chapter, we showed that the electron mass comprises electric and magnetic field energies, that induce each other.

But let us consider the circular Zitterbewegung of an electron, as illustrated in figure 3.4.1. During one Zitterbewegung cycle at circulation radius R_e, the induction is influenced by electromagnetic signals

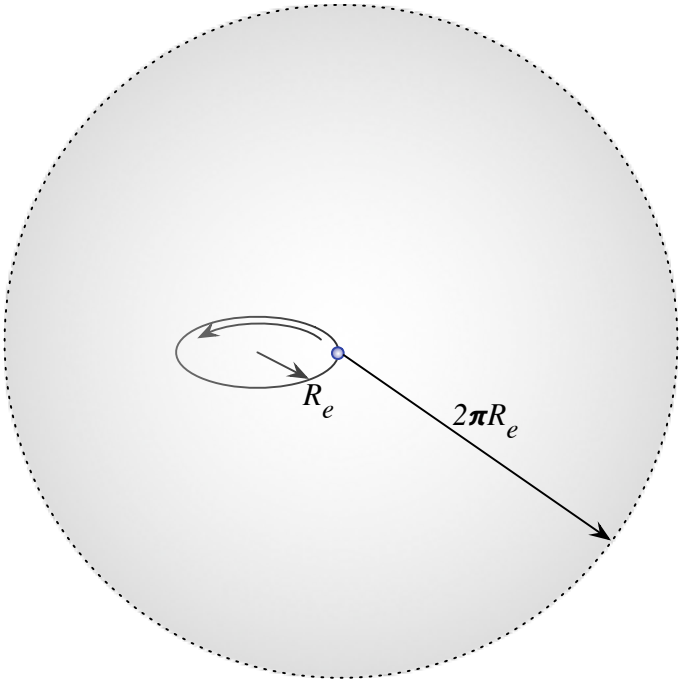

FIGURE 3.4.1. The spherical volume element within the reach of electromagnetic signals during one full Zitterbewegung circulation

propagating at the speed of light from within a sphere of $2\pi R_e$ radius. The total electric field energy of the electron is:

$$W_e = \frac{1}{2} m_e c^2 \tag{3.4.1}$$

However, the electric field energy outside of a sphere of $2\pi R_e$ radius is:

$$W_{2\pi R} = \frac{e^2}{32\pi^2\epsilon_0}\int_{2\pi R_e}^{\infty}\frac{1}{r^4}\cdot 4\pi r^2 dr = \frac{e^2}{8\pi\epsilon_0}\int_{2\pi R_e}^{\infty}\frac{1}{r^2}dr = -\frac{e^2}{8\pi\epsilon_0}\,\frac{1}{r}\Big|_{2\pi R_e}^{\infty} = \frac{e^2}{8\pi\epsilon_0 2\pi R_e} \tag{3.4.2}$$

The above equation means that only a part of the total electric field could exert its magnetic-field-inducing effect during a Zitterbewegung rotation by 2π phase. The unaccounted ratio of electric field energy is:

$$\frac{W_{2\pi R}}{W_e} = \frac{e^2}{4\pi\epsilon_0 2\pi R_e m_e c^2} = \frac{r_{cl}}{2\pi R_e} \tag{3.4.3}$$

where we used the $r_{cl} = \frac{1}{4\pi\varepsilon_0}\frac{e^2}{m_e c^2}$ definition of the classical electron radius.

It follows from the above result that the ratio of single loop account electric field energy is $1 - \frac{W_{2\pi R}}{W_e} = 1 - \frac{r_{cl}}{2\pi R_e}$.

In order to calculate the correct magnetic dipole field strength, we must account the induction of the total electric field energy. Therefore, the anomalous magnetic moment is just the inverse of the single loop accounted electric field energy ratio:

$$g = \left(1 - \frac{r_{cl}}{2\pi R_e}\right)^{-1} \approx 1 + \frac{\alpha}{2\pi} \tag{3.4.4}$$

The approximation part in the above formula corresponds to the Schwinger factor. It can be observed from the above result that the correct $g = \left(1 - \frac{r_{cl}}{2\pi R_e}\right)^{-1}$ formula is just slightly different from the Schwinger factor when $\frac{r_{cl}}{R_e}$ is small, but becomes significantly different when r_{cl} and R_e are similar in size.

3.5. Electron kinematics from electromagnetic momentum

Our preceding results mapped out the electromagnetic field structure of an electron particle. The electron mass and energy have purely electromagnetic field origin. The "pure electromagnetic" vector $e\boldsymbol{A}_{\square}$ may be interpreted as the momentum-energy $\boldsymbol{P}_{\square}$ of a particle with electric charge e, momentum $\boldsymbol{P}_{\triangle}$ and energy $U = P_t c$:

$$\boldsymbol{P}_{\square} = e\boldsymbol{A}_{\square}, \tag{3.5.1}$$

$$\boldsymbol{P}_{\square} = \gamma_x P_x + \gamma_y P_y + \gamma_z P_z + \gamma_t \frac{U}{c} = \boldsymbol{P}_{\triangle} + \gamma_t \frac{U}{c}. \tag{3.5.2}$$

For a particle that moves with speed $\boldsymbol{v}$ along a direction z orthogonal to the Zitterbewegung rotation plane, the momentum $\boldsymbol{P}_{\triangle}$ can be decomposed in two vectors: parallel component to the Zitterbewegung plane and an orthogonal component to it. The parallel component is a rotating vector, that indicates the component of the momentum due to the angular frequency ω_e:

$$\boldsymbol{P}_{\triangle} = \boldsymbol{P}_{\parallel} + \boldsymbol{P}_{\perp}, \tag{3.5.3}$$

where

$$|\boldsymbol{P}_{\parallel}| = \frac{\hbar\omega_e}{c} = m_e\omega_e r_e = m_e c$$

$$\left[|\boldsymbol{P}_{\parallel}| = \frac{1}{r_e} = \omega_e = m_e\right]_{NU}.$$

The $\boldsymbol{P}_{\perp}$ component can bee seen as the usual kinetic momentum of a particle with rest mass m_e. For simplicity of notation, from now, we shall refer to this component as $\boldsymbol{P}$, so that

$$P_{\square}^2 = e^2 A_{\square}^2 = P_{\triangle}^2 - \frac{U}{c^2}^2 = P^2 + m_e^2 c^2 - \frac{U}{c^2}^2.$$

The relativistic mass m can be expressed as:

$$m^2 c^2 = m_e^2 c^2 + P^2 = m_e^2 c^2 + m^2 v^2.$$

Consequently this electromagnetic four-momentum $\boldsymbol{P}_{\square}$, for electrons moving with uniform velocity, is a light-like vector:

$$P_{\square}^2 = m^2 c^2 - \frac{U}{c^2}^2 = 0$$

An electron that moves with velocity $v \ll c$ has an approximate momentum P given by

$$P = eA_{\perp} \simeq P_{\parallel}\frac{v}{c} = m_e v,$$

and an acceleration $a = \frac{dv}{dt}$ implies a force $f = \frac{dP}{dt} = e \cdot \frac{dA_{\perp}}{dt} = m \cdot \frac{dv}{dt}$.

Now recalling that the bivector part of (3.2.5) is

$$\boldsymbol{\partial} \wedge \boldsymbol{A}_{\square} = \boldsymbol{F}$$

after multiplying both sides by the charge e, it becomes

$$e\boldsymbol{\partial} \wedge \boldsymbol{A}_{\square} = \boldsymbol{\partial} \wedge e\boldsymbol{A}_{\square} = e\boldsymbol{F}. \tag{3.5.4}$$

By considering (3.5.1) and (3.5.2) this equation can be rewritten as

$$\boldsymbol{\partial} \wedge \left(\boldsymbol{P}_{\triangle} + \gamma_t \frac{U}{c}\right) = e\boldsymbol{F}, \tag{3.5.5}$$

or, by means of (3.5.3), as

$$\boldsymbol{\partial} \wedge \left[\left(\boldsymbol{P}_{\parallel} + \boldsymbol{P}\right) + \gamma_t \frac{U}{c}\right] = e\boldsymbol{F}. \tag{3.5.6}$$

The term $\boldsymbol{\partial} \wedge \boldsymbol{P}_{\parallel}$ can be carried out because the average value of $\boldsymbol{P}_{\parallel}$, in a scale time much larger than the Zitterbewegung period, is zero:

$$\boldsymbol{\partial} \wedge \left(\boldsymbol{P} + \gamma_t \frac{U}{c} \right) = e\boldsymbol{F}, \tag{3.5.7}$$

$$\boldsymbol{\partial} \wedge \left(\boldsymbol{P} + \gamma_t \frac{U}{c} \right) = \frac{e}{c} \boldsymbol{E} \gamma_t + eI\boldsymbol{B}\gamma_t.$$

Equating only the components that contain bivectors with γ_t terms we obtain

$$\left(\frac{\partial \boldsymbol{P}}{\partial t} \right)_{EU} \gamma_t + \nabla U \gamma_t = e\boldsymbol{E}\gamma_t$$

or

$$\left(\frac{\partial \boldsymbol{P}}{\partial t} \right)_{EU} = e\boldsymbol{E} - \nabla U. \tag{3.5.8}$$

In (3.5.8) $\left(\frac{\partial \boldsymbol{P}}{\partial t}\right)_{EU}$ is the force acting on the charge e due both to the electric field $\boldsymbol{E}$ (Coulomb force) and to the gradient of the "potential energy" U. Instead, by equating only the components that contain pure spatial bivectors we get

$$\nabla \wedge \boldsymbol{P} = eI\boldsymbol{B}\gamma_t = -eI\gamma_t \boldsymbol{B} = eI_{\triangle}\boldsymbol{B}, \tag{3.5.9}$$

where the term $-I\gamma_t = \gamma_x\gamma_y\gamma_z = I_{\triangle}$ is the unitary volume of the three dimensional space. Left-multiplying both sides of (3.5.9) by $I_{\triangle}$ gives

$$I_{\triangle} \nabla \wedge \boldsymbol{P} = -e\boldsymbol{B}, \tag{3.5.10}$$

which is equivalent to the following equation in the ordinary algebra:

$$\nabla \times \boldsymbol{P} = e\boldsymbol{B}. \tag{3.5.11}$$

As an example, the component of the above equation along the x axis is

$$\gamma_x \left(\frac{\partial P_z}{\partial y} - \frac{\partial P_y}{\partial z} \right) = \gamma_x e B_x.$$

Now, by applying the cross product of the velocity $\boldsymbol{v}$ of charge e to both terms in (3.5.11) we obtain

$$\boldsymbol{v} \times (\nabla \times \boldsymbol{P} - e\boldsymbol{B}) = 0. \tag{3.5.12}$$

The components of (3.5.12) are represented in Table 3 considering that

$$\begin{aligned} v_i \frac{\partial P_j}{\partial i} &= \frac{\partial i}{\partial t} \frac{\partial P_j}{\partial i} = \frac{\partial P_j}{\partial t} \\ v_j \frac{\partial P_j}{\partial i} &= \frac{\partial j}{\partial t} \frac{\partial P_j}{\partial i} = \frac{\partial j}{\partial i} \frac{\partial P_j}{\partial t} = 0 \quad \text{for } i \neq j, \end{aligned}$$

where $i, j \in \{x, y, z\}$.

For these reasons (3.5.12) leads to the usual form of the force contribution due to the magnetic flux density field $\boldsymbol{B}$

$$\left(\frac{\partial \boldsymbol{P}}{\partial t} \right)_{B} = e\boldsymbol{v} \times \boldsymbol{B}. \tag{3.5.13}$$

Finally, we get the whole force contribution by summing up the forces $\frac{d\boldsymbol{P}}{dt} = \left(\frac{\partial \boldsymbol{P}}{\partial t}\right)_{EU} + \left(\frac{\partial \boldsymbol{P}}{\partial t}\right)_{B}$ given respectively by (3.5.8) and (3.5.13)

$$\frac{d\boldsymbol{P}}{dt} = e\left(\boldsymbol{E} + \boldsymbol{v} \times \boldsymbol{B}\right) - \nabla U. \tag{3.5.14}$$

TABLE 3. Products $\boldsymbol{v} \times (\nabla \times \boldsymbol{P} - e\boldsymbol{B})$.

$\boldsymbol{v} \times (\nabla \times \boldsymbol{P} - e\boldsymbol{B})$	$\gamma_x \left(\frac{\partial P_z}{\partial y} - \frac{\partial P_y}{\partial z} - eB_x \right)$	$\gamma_y \left(\frac{\partial P_x}{\partial z} - \frac{\partial P_z}{\partial x} - eB_y \right)$
$\gamma_x v_x$	0	$\gamma_z \left(- \frac{\partial P_z}{\partial t}\Big\vert_{xy} - ev_x B_y \right)$
$\gamma_y v_y$	$-\gamma_z \left(\frac{\partial P_z}{\partial t}\Big\vert_{yx} - ev_y B_x \right)$	0
$\gamma_z v_z$	$-\gamma_y \left(- \frac{\partial P_y}{\partial t}\Big\vert_{zx} - ev_z B_x \right)$	$-\gamma_x \left(\frac{\partial P_x}{\partial t}\Big\vert_{zy} - ev_z B_y \right)$

$\boldsymbol{v} \times (\nabla \times \boldsymbol{P} - e\boldsymbol{B})$	$\gamma_z \left(\frac{\partial P_y}{\partial x} - \frac{\partial P_x}{\partial y} - eB_z \right)$
$\gamma_x v_x$	$\gamma_y \left(\frac{\partial P_y}{\partial t}\Big\vert_{xz} - ev_x B_z \right)$
$\gamma_y v_y$	$\gamma_x \left(- \frac{\partial P_x}{\partial t}\Big\vert_{yz} - ev_y B_z \right)$
$\gamma_z v_z$	0

3.6. Wave-particle duality and the electron mass concept

Treating the electron as a particle, various interpretations of the electron mass are based on Einstein's $mc^2 = \epsilon$, De Broglie's $mc^2 = \hbar\omega$, and Newton's $ma = F$ formulas. Taking the electron wave perspective, a realistic electron wave model must precisely define the electron mass from its electromagnetic wave parameters. Applying the results established so far, the following list summarizes the electron wave perspective based interpretations of the electron mass:

(1) Einstein's $mc^2 = \epsilon$ definition, which equates mass with energy. According to this definition, the electron mass is the total energy of the electromagnetic field constituting it. The energy density of the electromagnetic field is given by equation 1.3.26, which follows directly from Maxwell's equation. Electron wave models that leave any electromagnetic field energy uncounted are violating Maxwell's equation. As a first estimation, the magnetic field energy of the electron wave is given by equation 3.3.21, which yields half the electron mass. Maxwell's equation ensures that any electromagnetic wave comprises equal amounts of electric and magnetic field energy. This simplest model equates the electron mass with electric and magnetic field energy. Regarding a more precise energy accounting, we showed at the end of section 3.3.5 that the electron's mass comprises electric, magnetic, and scalar field energy components. The ratio of scalar field energy is left undetermined in our work.

(2) De Broglie's $mc^2 = \hbar\omega$ definition, which equates mass with a wave frequency. We have identified ω with the angular frequency of the electromagnetic wave, which comprises the electron. We demonstrated in chapter 2 that the quantum mechanical wavenumber is just the Lorentz transformed component of this electromagnetic angular frequency. In this chapter, we identified ω with the angular frequency of the electron wave's circular Zitterbewegung. The proportionality between m and ω follows from $r^{-1} = m$ relation between mass and Zitterbewegung radius, and we showed that this relation originates from a relativistic Doppler effect on the electron wave.

(3) The Schrödinger equation based mass definition, where mass is a Hamilton–Jacobi equation's single free parameter. We showed in chapter 2 that the Schrödinger equation converges to the classical Hamilton–Jacobi equation in the $\hbar \to 0$ limit. The Lagrangian of this Hamilton–Jacobi equation is defined by $\boldsymbol{J}_{\square} \cdot \boldsymbol{A}_{\square}$; the corresponding electromagnetic wave solution was also shown in chapter 2. Equation 3.3.29 integrates the amplitude of $J \cdot A$ over the toroidal Zitterbewegung region where it is non-zero; this integral indeed evaluates to mc^2. For a stationary electron, the Hamilton–Jacobi action is obtained by this Lagrangian over time. This means that the electron mass evolves with time, and in this case the electron mass can be interpreted as a vector pointing along the time axis. For a moving electron, its mass vector is pointing along its spacetime trajectory. This concept of vectorial mass dimensionality shows up also in the Dirac equation context, and shall be further discussed in chapter 5.

(4) Newton's $ma = F$ definition, which equates mass with resistance to acceleration. Equation 3.5.14 shows that the electron-comprising electromagnetic wave momentum evolves according to the usual Lorentz force. Since the Schrödinger equation converges to the classical Hamilton–Jacobi equation, Newton's $ma = F$ relation is fulfilled.

These four complementing electron mass interpretations nicely illustrate how the electron mass arises from its microscopic wave structure. A successful electron model explains why the same mass term appears in the the above-listed four formulas. In contrast to particle-oriented perspectives, where the electron mass

remains a black-box parameter, our wave-oriented electron model reveals the tangible origin of electron mass.

3.7. Preceding Spinning Charge Models

In 1915 Alfred Lauck Parson published "A Magneton Theory of the Structure of the Atom"[**19**] where he proposed a spinning ring model of the electron. Various forms of the spinning charge model of electrons have been rediscovered by many authors. However, the incompatibility with the most widely accepted interpretations of quantum mechanics prevented them from receiving proper attention.

Using geometric algebra and starting from Dirac theory, David Hestenes has proposed a Zitterbewegung model according to which "*the electron is a massless point particle executing circular motion in the rest system*" and "*with an intrinsic orbital angular momentum or spin of fixed magnitude* $s = \frac{\hbar}{2}$" [**2**]. The phase of the wave function is related to the Zitterbewegung rotation phase; a concept usually hidden in the traditional mathematical formalism of quantum mechanics, which is based on complex numbers and matrices. However, we should remark that the concept of point-like charge in quantum mechanics should be considered unrealistic. It violates Occam's razor principle and may be used only as a first approximation. Reference [**20**] is a good example of working with such a "center of charge" approximation, and it arrives at a toroidal geometry that is similar to our electron model. We note also that in our model the value of intrinsic angular momentum for a free electron is $\hbar$ and that the "spin" is interpreted as the component of the angular momentum along an external magnetic field, as in the Stern-Gerlach experiment. Another interesting electron model has been proposed by David L. Bergman [**11, 12**]. According to this model the electron is a very thin, torus shaped, rotating charge distribution with intrinsic angular momentum of the electron equal to its spin value $s = \frac{\hbar}{2}$. The torus radius has a length $R = \frac{\hbar}{mc}$ and half thickness $r = 8Re^{-\frac{\pi}{\alpha}}$, where α is the fine structure constant.

In our work, we calculated the parameters and relations that characterize the electron, but did not derive an electromagnetic field distribution for each point in space. Some recent Zitterbewegung models, such as [**21**], aim to calculate the spatial distribution of the electromagnetic field. In particular, reference [**21**] derives a circulating wave formula that is a solution of Maxwell's equation; this may help to answer the question of how the electromagnetic Zitterbewegung wave curls up.

3.8. Conclusions

We developed a realistic description of the electron structure. We used the language of geometric algebra, and recognized the fundamental role of the electromagnetic four-vector potential.

The application of Occam's Razor principle to Maxwell's equations suggests a Zitterbewegung interpretation of quantum mechanics. The obtained results are similar but not identical to the electron model proposed by D. Hestenes. According to this model, the electron structure consists of a current distribution that is carried by a longitudinal electromagnetic wave: it circulates at the speed of light along a circumference with a length equal to electron Compton wavelength. Inertia has a pure electromagnetic origin related to the vector potential generated by the Zitterbewegung current.

"It is a delusion to think of electrons and fields as two physically different, independent entities. Since neither can exist without the other, there is only one reality to be described, which happens to have two different aspects; and the theory ought to recognize this from the outset instead of doing things twice!" - A. Einstein, cited in [**17**]

"In atomic theory, we have fields and we have particles. The fields and the particles are not two different things. They are two ways of describing the same thing, two different points of view" - P. A. M. Dirac, cited in [**18**]

Acknowledgements

The author thanks Giorgio Vassallo for helpful discussions and suggestions.

Bibliography

[1] G. Vassallo et al "The Electron and Occam's razor", Journal of Condensed Matter Nuclear Science, volume 25.1 (2017)

[2] David Hestenes. Quantum Mechanics from Self-interaction. Foundations of Physics, 15(1):63–87, 1985.

[3] Kerson Huang. On the zitterbewegung of the dirac electron. American Journal of Physics, 20(8):479–484, 1952.

[4] B. G. Sidharth. Revisiting Zitterbewegung. International Journal of Theoretical Physics, 48:497–506, February 2009.

[5] David Hestenes. Mysteries and insights of dirac theory. In Annales de la Fondation Louis de Broglie, volume 28, page 3. Fondation Louis de Broglie, 2003.

[6] D. Hestenes. Hunting for Snarks in Quantum Mechanics. In P. M. Goggans and C.-Y. Chan, editors, American Institute of Physics Conference Series, volume 1193 of American Institute of Physics Conference Series, pages 115–131, December 2009.

[7] Aharonov, Y. and Bohm, D. Significance of Electromagnetic Potentials in the Quantum Theory. Physical Review, 115:485–491, aug 1959.

[8] David Hestenes. Reforming the Mathematical Language of Physics. Oersted Medal Lecture 2002, 2002.

[9] David Hestenes. Spacetime Physics with Geometric Algebra. American Journal of Physics, 71(3):691–714, July 2003.

[10] David Hestenes. Zitterbewegung Modeling. Foundations of Physics, 23(3):365–387, 1993.

[11] David L. Bergman and J. Paul Wesley. Spinning Charged Ring Model of Electron Yielding Anomalous Magnetic Moment. Galilean Electrodynamics, 1(5):63–67, 1990.

[12] D. L. Bergman and C. W. Lucas. Credibility of Common Sense Science. Foundations of Science, pages 1–17, 2003.

[13] F. Santandrea and P. Cirilli. Unificazione elettromagnetica, concezione elettronica dello spazio, dell'energia e della materia, 2006. Atlante di numeri e lettere, http://www.atlantedinumerielettere.it/energia2006/labor.htm

[14] A. Schweiger and G. Jeschke "Principles of Pulse Electron Paramagnetic Resonance" (2001)

[15] R. P. Feynman, R. B. Leighton, and M. Sands. The Feynman Lectures on Physics: Mainly electromagnetism and matter. Volume 2. Basic Books. Basic Books, 2011.

[16] David L. Bergman. The real proton. Foundations of Science, 3(4), November 2000.

[17] C. Mead. Collective Electrodynamics: Quantum Foundations of Electromagnetism. MIT Press, 2000.

[18] A. Babin and A. Figotin. Neoclassical Theory of Electromagnetic Interactions: A Single Theory for Macroscopic and Microscopic Scales. Theoretical and Mathematical Physics. Springer London, 2016.

[19] A. L Parson. A Magneton Theory of the Structure of the Atom. Smithsonian Miscellaneous Collection, Pub 2371. 1915.

[20] O. Consa. The Zitter Electron Model and the Anomalous Magnetic Moment. (2025)

[21] C. A. M. dos Santos and M. Fleury "An electromagnetic model of the electron", Annales de la fondation Louis de Broglie, volume 49 (2025)

CHAPTER 4

The Aharonov-Bohm equations, flux quantization, and the Zitterbewegung Lagrangian

Giorgio Vassallo[1,2] and **Antonino Oscar Di Tommaso**[2]
[1] International Society for Condensed Matter Nuclear Science (ISCMNS)-UK.
[2] Università degli Studi di Palermo - Engineering Department, viale delle Scienze, 90128 Palermo, Italy. E-mail: antoninooscar.ditommaso@unipa.it, giorgio.vassallo@unipa.it.

Nomenclature

Symbol, name, SI units, natural units (NU).

$\boldsymbol{A}_{\square}$: electromagnetic four-potential $[V \cdot s \cdot m^{-1}]$, $[eV]$;
$\boldsymbol{A}_{\triangle}$: electromagnetic vector potential $[V \cdot s \cdot m^{-1}]$, $[eV]$;
A: the norm of the electromagnetic vector potential $[V \cdot s \cdot m^{-1}]$, $[eV]$;
A_t: time component of electromagnetic four potential $[V \cdot s \cdot m^{-1}]$, $[eV]$;
$\boldsymbol{a}_{\square}$: the four-vector Proca field $[V \cdot s \cdot m^{-1}]$, $[eV]$;
$\boldsymbol{a}_{\triangle}$: spatial components of the Proca field $[V \cdot s \cdot m^{-1}]$, $[eV]$;
a: the norm of the Proca field, not to be confused with acceleration $[V \cdot s \cdot m^{-1}]$, $[eV]$;
a_t: time component of the Proca field $[V \cdot s \cdot m^{-1}]$, $[eV]$;
m: mass $[kg]$, $[eV]$;
$\boldsymbol{F}$: electromagnetic field bivector derived from $\boldsymbol{A}_{\square}$ $[V \cdot s \cdot m^{-2}]$, $[eV^2]$;
$\boldsymbol{f}$: field bivector derived from $\boldsymbol{a}_{\square}$ $[V \cdot s \cdot m^{-2}]$, $[eV^2]$;
$\boldsymbol{B}$: flux density field $[V \cdot s \cdot m^{-2}] = [T]$, $[eV^2]$;
$\boldsymbol{E}$: electric field $[V \cdot m^{-1}]$, $[eV^2]$;
V: potential energy $[J = kg \cdot m^2 \cdot s^{-2}]$, $[eV]$;
$\boldsymbol{J}_{\square}$: four current density field, $[A \cdot m^{-2}]$, $[eV^3]$;
$\boldsymbol{J}_{\triangle}$: current density field, $[A \cdot m^{-2}]$, $[eV^3]$;
ρ: charge density $[A \cdot s \cdot m^{-3} = C \cdot m^{-3}]$, $[eV^3]$;
x, y, z: space coordinates $[m]$, $[eV^{-1}]$, $[1.9732705 \cdot 10^{-7}\ m \simeq 1\ eV^{-1}]$;
t: time variable $[s]$, $[eV^{-1}]$, $[6.5821220 \cdot 10^{-16}\ s \simeq 1\ eV^{-1}]$;
c: light speed in vacuum $[2.997\,924\,58 \cdot 10^{8}\ m \cdot s^{-1}]$, $[1]$;
$\hbar$: reduced Planck constant $(\hbar = \frac{h}{2\pi})$ $[1.054\,571\,726 \cdot 10^{-34}\ J \cdot s]$, $[1]$;
μ_0: permeability of vacuum $[4\pi \cdot 10^{-7}\ V \cdot s \cdot A^{-1} \cdot m^{-1}]$, $[4\pi]$;
ϵ_0: dielectric constant of vacuum $[8.854\,187\,817 \cdot 10^{-12}\ A \cdot s \cdot V^{-1} \cdot m^{-1}]$, $[\frac{1}{4\pi}]$;
e: electron charge $[1.602\,176\,565 \cdot 10^{-19}\ A \cdot s]$, $[0.085\,424\,546]$;
α: fine structure constant $[7.2973525664 \cdot 10^{-3}]$, $[7.2973525664 \cdot 10^{-3}]$;
m_e: electron rest mass $[9.10938356 \cdot 10^{-31} kg]$, $[0.5109989461 \cdot 10^{6} eV]$;
λ_c: electron Compton wavelength $[2.426\,310\,2389 \cdot 10^{-12}\ m]$, $[1.229\,588\,259 \cdot 10^{-5}\ eV^{-1}]$;
K_J: Josephson constant $[0.4835978525 \cdot 10^{15}\ Hz\, V^{-1}]$, $[2.71914766 \cdot 10^{-2}]$
r_e: reduced Compton electron wavelength (Compton radius) $r_e = \frac{\lambda_c}{2\pi}$;
r_c: electron charge radius $r_c = \alpha r_e$;
T_e: Zitterbewegung period $T_e = \frac{2\pi r_e}{c}$;
ω_e: Zitterbewegung angular frequency $\omega_e = \frac{2\pi}{T_e}$;
γ_i: $\gamma_x^2 = \gamma_y^2 = \gamma_z^2 = -\gamma_t^2 = 1$, where $\{\gamma_x, \gamma_y, \gamma_z, \gamma_t\}$ are the four basis vectors of $Cl_{3,1}(\mathbb{R})$ Clifford algebra, isomorphic to Majorana matrices algebra;
$\boldsymbol{\partial}$: $\boldsymbol{\partial} = \gamma_x \frac{\partial}{\partial x} + \gamma_y \frac{\partial}{\partial y} + \gamma_z \frac{\partial}{\partial z} + \gamma_t \frac{1}{c} \frac{\partial}{\partial t}$;
I: $I = \gamma_x \gamma_y \gamma_z \gamma_t$;
$I_{\triangle}$: $I_{\triangle} = \gamma_x \gamma_y \gamma_z$;

4.1. Introduction

According to Carver Mead, mainstream physics literature has a long history of hindering fundamental conceptual reasoning, often *"involving assumptions that are not clearly stated"* [**1**]. One of these is the unrealistic assumption of point-like shaped elementary particles with *intrinsic* properties as mass, charge, angular momentum, magnetic moment and spin. According to the laws of mechanics and electromagnetism, a point-like particle cannot have an "intrinsic angular momentum". A magnetic moment must necessarily be generated by a current loop, which cannot exist in a point-like particle. Furthermore, the electric field generated by a point-like charged particle should have an infinite energy. Therefore, an alternative realistic approach that fully addresses these *very basic* problems is indispensable. We developed a *Zitterbewegung* solution of the electron structure in chapter 3, according to which charged elementary particles can be modeled by a current ring generated by a charge distribution rotating at light speed along a circumference whose length is equal to the particle's Compton wavelength. As a consequence, every elementary charge is always associated with a magnetic flux quantum and every charge is coupled to all other charges on its light cone by time-symmetric interactions [**1, 9**]. The aim of this chapter is to further develop the electron Zitterbewegung model of chapter 3.

N.B. all equations enclosed in square brackets with subscript "*NU*" have dimensions expressed in natural units.

4.2. The inter-related concepts of Energy, Mass, Frequency and Information

The concept of measurement plays a fundamental role in all scientific disciplines based on experimental evidence. The most used measurement units (such as the international system, SI) are based mainly on human conventions not directly related to fundamental constants. To simplify the conceptual understanding of certain physical quantities it is convenient to adopt in some cases a measurement system based on universal constants, such as the speed of light c and the Planck's quantum $\hbar$.

Considering that a measurement is an event localized in space and time, the quantum of action can be seen, in some cases, as an objective entity in some respects analogous to a bit of information located in the space-time continuum. In accordance with Heisenberg's uncertainty principle, the result of the measurement of some values (such as angular momentum) cannot have an accuracy less than half a single Planck's quantum. Therefore, to simplify the interpretation of physical quantities, it may be useful to adopt a system in which both the speed of light and the quantum of action are dimensionless quantities (pure numbers) having a unit value, *i.e.*: $c = 1$ and $\hbar = 1$. In this system, the constancy of light speed makes possible to use a single measurement unit for space and time, simplifying, in many cases, the conceptual interpretation of physical quantities. The energy of a photon, a "particle of light", is equal to Planck's quantum multiplied by the photon angular frequency. By using the symbol T to indicate the period of a single complete oscillation and λ the relative wavelength, it is, therefore, possible to write

$$E = \hbar\omega = \frac{2\pi\hbar}{T} = \frac{2\pi\hbar c}{\lambda}. \tag{4.2.1}$$

By using natural units, period and wavelength coincide and the above expression is simplified in

$$\left[E = \omega = \frac{2\pi}{T} = \frac{2\pi}{\lambda}\right]_{NU}. \tag{4.2.2}$$

The NU subscript highlights the use of natural units for expressions contained within square brackets. This equation indissolubly links some fundamental concepts, as space, time, energy and mass, giving the possibility to express an energy value simply as a frequency or as the inverse of a time, or even as the inverse of a length. *Vice versa*, it allows to use as a measurement unit of both space and time a value equal to the inverse of a particular energy value as the electron-volt. Therefore, to compute a photon wavelength in vacuum with natural units it is sufficient to divide the constant 2π by its energy. This value will correspond exactly to the period of a complete oscillation. Hence, in natural units the inverse of an eV can be used as a measurement unit for space and time:

$$L_{(1eV)} = 1\ \mathrm{eV}^{-1} \approx 1.9732705 \cdot 10^{-7}\ \mathrm{m} \approx 0.2\ \mu\mathrm{m},$$

$$T_{(1eV)} = 1\ \mathrm{eV}^{-1} \approx 6.582122 \cdot 10^{-16}\ \mathrm{s} \approx 0.66\ \mathrm{fs}.$$

Consequently, an angular frequency can be measured in electron volts:

$$1\ \mathrm{eV} \approx 1.519268 \cdot 10^{15}\ \mathrm{rad\,s}^{-1}.$$

Following these concepts, it is possible to define a link between fundamental concepts of information, space, time, frequency and energy. A "quantum of information" carried by a single photon will have a "necessary reading time" and a "spatial dimension" inversely proportional to its energy. A simple example is given by radio antennas (dipoles), whose length is proportional to the received (or transmitted) "radio photons" wavelength and inversely proportional to their frequency and to the number of bits that can be received in a unit of time. In this perspective, the concept of energy is closely linked to the "density" of measurable information in space and in time.

4.3. The Aharonov-Bohm equations, flux quantization, and the Zitterbewegung Lagrangian

4.3.1. Magnetic flux quantization. Einstein's famous $E = mc^2$ formula becomes particularly explanatory if expressed in natural units:

$$[E = m]_{NU} .$$

Mass is energy and it is, therefore, possible to associate a precise amount of energy to a particle having a given mass. Taking up the considerations made on the deep bond existing between the concepts of space, time, frequency and energy, it is interesting trying to associate the electron rest mass m_e to an angular frequency ω_e, a length r_e and a time T_e. In fact Einstein's formula can be expressed as

$$E_e = m_e c^2 = \hbar\omega_e = \frac{\hbar c}{r_e} = \frac{h}{T_e}, \tag{4.3.1}$$

or adopting natural units

$$\left[E_e = m_e = \omega_e = \frac{1}{r_e} = \frac{2\pi}{T_e}\right]_{NU} . \tag{4.3.2}$$

These constants have a simple and clear interpretation under our electron model consisting of a current ring generated by a massless charge rotating at the speed of light along a circumference whose radius is equal to the electron reduced Compton wavelength, defined as $r_e = \frac{\lambda_c}{2\pi} \approx 0.38616 \cdot 10^{-12}$ m . According to the model described in the preceding chapters, the charge is not a point-like entity. In equation (4.3.2), ω_e is the angular frequency of the circulating current, r_e is its circulation radius and T_e its period. The current loop is associated with a quantized magnetic flux Φ_M equal to Planck's constant ($h = 2\pi\hbar$) divided by the elementary charge e (see eq. 3.3.20 in chapter 3):

$$\Phi_M = h/e,$$

or in natural units

$$[\Phi_M = 2\pi/e]_{NU} .$$

The above relation demonstrates that understanding magnetic flux quantization leads to understanding elementary charge quantization, and vice versa.

The charge circulation is caused by the centripetal Lorentz force due to the magnetic field associated with the current loop generated by the elementary rotating charge. The value of this elementary charge, in natural units, is a pure number and is equal to the square root of the ratio between the charge radius r_c and the the orbit radius r_e (see eq. 3.3.30, 3.3.31 in chapter 3):

$$\left[e = \sqrt{\frac{r_c}{r_e}} = \sqrt{\alpha} \approx 0.0854245\right]_{NU} . \tag{4.3.3}$$

Similar models, based on the concept of "current loop", have been proposed by many authors, but have often been ignored for their incompatibility with the most widespread interpretations of Quantum Mechanics [**2, 3, 4, 5, 6, 7**]. It is interesting to remember how, already in his Nobel lecture of 1933, P.A.M. Dirac referred to an internal high-frequency oscillation of the electron: "*It is found that an electron which seems to us to be moving slowly, must actually have a very high frequency oscillatory motion of small amplitude superposed on the regular motion which appears to us. As a result of this oscillatory motion, the velocity of the electron at any time equals the velocity of light. This is a prediction which cannot be directly verified by experiment, since the frequency of the oscillatory motion is so high and its amplitude is so small*". In the scientific literature, the German word *Zitterbewegung* (ZBW) is often

used to indicate this rapid oscillation/rotation of the electron charge. The circulating electric current is characterized by a momentum p_c of purely electromagnetic nature:

$$p_c = eA = e\frac{\Phi_M}{2\pi r_e} = \frac{\hbar\omega_e}{c} = \frac{\hbar}{r_e} = m_e c.$$

As defined in equation 3.3.9 of chapter 3, in this formula $A = \frac{\hbar}{er_e}$ refers to the magnitude of the vector potential seen by the rotating charge.

Multiplying the above defined charge momentum p_c by the radius r_e we obtain the "intrinsic" angular momentum $\hbar$ of the electron:

$$p_c r_e = \hbar. \tag{4.3.4}$$

Using natural units the momentum p_c has the dimension of energy and it is exactly equal to the electron mass-energy at rest m_e:

$$\left[p_c = eA = E_e = \frac{1}{r_e} = m_e = \omega_e\right]_{NU}.$$

Magnetic flux quantization applies to any stable charge circulation, including electron orbitals. Let r_{orb} be the mean radius of an electron orbital. The wavefunction's continuity requires that:

$$k\,(2\pi r_{orb}) = n2\pi \tag{4.3.5}$$

where n is positive integer number. It follows from the $p_c = eA$ relation that the kinetic momentum defines the vector potential component along the Zitterbewegung axis:

$$p_{kinetic} = eA_{\perp} \tag{4.3.6}$$

Recaling the derivation of $p_{kinetic} = \hbar k$ from chapter 2, it is now possible to determine the magnetic flux of an electron orbital by applying the circulation of the vector potential $A_{\perp}$:

$$\phi_{orb} = \oint A_{\perp} d\lambda = \int_0^{2\pi} \frac{\hbar k}{e} r_{orb} d\vartheta = k\,(2\pi r_{orb})\,\frac{\hbar}{e} = n\frac{h}{e} \tag{4.3.7}$$

Therefore, the magnetic flux of electron orbitals is also quantized by elementary magnetic flux $\Phi_M = h/e$. This result further illustrates the fundamental nature of magnetic flux quantization.

4.3.2. Aharonov-Bohm equations in the Zitterbewegung electron model context. The magnetic Aharonov-Bohm effect is described by a quantum law that gives the phase variation φ of the "electron wave function" starting from the integral of the vector potential $\boldsymbol{A}_{\triangle}$ along a path [**8**], *i.e.*

$$\varphi = \frac{e}{\hbar}\int \boldsymbol{A}_{\triangle} \cdot d\boldsymbol{l}. \tag{4.3.8}$$

In the proposed Zitterbewegung model, the "wave function phase" of the electron has a precise geometric meaning and indicates the charge rotation phase. By using (4.3.8), one may verify that the phase shift φ along the circumference of the Zitterbewegung orbit is equal exactly to 2π radians. In fact

$$\varphi = \frac{e}{\hbar}\oint \boldsymbol{A}_{\triangle} \cdot d\boldsymbol{l} = \frac{e}{\hbar}\int_0^{2\pi r_e} A dl = \frac{e}{\hbar}\int_0^{2\pi r_e} \frac{\hbar}{er_e} dl = \frac{e}{\hbar}\frac{\hbar}{er_e} 2\pi r_e = 2\pi, \tag{4.3.9}$$

because the vectors $\boldsymbol{A}_{\triangle}$ and $d\boldsymbol{l}$ have the same direction tangent to the elementary charge trajectory.

This result is also consistent with the prediction of the *electric* Aharonov-Bohm effect, a quantum phenomenon that establishes the variation of phase φ as a function of the integral of electric potential V in a time interval T, *i.e.*:

$$\varphi = \frac{e}{\hbar}\int_T V dt. \tag{4.3.10}$$

Applying the electric Aharonov-Bohm effect formula to compute the phase shift φ within a Zitterbewegung time interval $T_e = \frac{2\pi}{\omega_e}$, we must obtain the expected result, *i.e.* $\varphi = 2\pi$. Let us define an effective electron charge radius r_c via the electrostatic potential formula:

$$V = \frac{e}{4\pi\varepsilon_0 r_c} = \left[\frac{e}{r_c}\right]_{NU}$$

The corresponding Zitterbewegung time interval is:

$$T_e = \frac{2\pi r_e}{c} = [2\pi r_e]_{NU}\,.$$

Applying equation 4.3.10, yields the following phase shift:

$$\varphi = \frac{e}{\hbar}\int_0^{T_e} V dt = \frac{e}{\hbar} V T_e = \frac{e}{\hbar} V \frac{2\pi r_e}{c} = \left[\frac{e^2}{r_c} 2\pi r_e\right]_{NU}. \tag{4.3.11}$$

Recalling equations 3.3.31 and 4.3.3, we recognize that $\varphi = 2\pi$ if $r_c = r_{cl}$, i.e. the classical electron radius. This result demonstrates that the classical electron radius, which was illustrated in figure 3.3.1, is an effective radius of the electron charge distribution. However, we must keep in mind that the actual electron charge distribution is not spherical, but has a toroidal topology shown in figure 3.3.1.

Now, by equating the $\frac{e}{\hbar}\frac{\hbar}{er_e}2\pi r_e$ term of (4.3.9) and the $\frac{e}{\hbar}V\frac{2\pi r_e}{c}$ term of (4.3.11) it is possible to demonstrate that

$$A_t = \frac{V}{c} = A = |\boldsymbol{A}_\triangle|\,,$$

$$[A_t = V = A = |\boldsymbol{A}_\triangle|]_{NU}\,,$$

$$\boldsymbol{A}_\square^2 = \left(\boldsymbol{A}_\triangle + \gamma_t A_t\right)^2 = \boldsymbol{A}_\triangle^2 - A_t^2 = 0. \tag{4.3.12}$$

The obtained electromagnetic wave-like expression further demonstrates the electron's wave nature. We emphasize that the above relationships pertain to the electromagnetic potential field seen by the electron charge distribution. By introducing the differential form of (4.3.10) we obtain

$$d\varphi = \frac{e}{\hbar} V dt$$

and this yields the phase speed

$$\frac{d\varphi}{dt} = \omega_e = \frac{e}{\hbar}V = \frac{e^2}{4\pi\varepsilon_0\hbar r_c} = \frac{c\alpha}{r_c} = \frac{c}{r_e} = \frac{m_e c^2}{\hbar} = \frac{ce}{\hbar}A$$

In natural units, the above phase speed is expressed as:

$$\left[\frac{d\varphi}{dt} = \omega_e = m_e = eV = eA\right]_{NU} \tag{4.3.13}$$

4.3.3. The Zitterbewegung Lagrangian. Transversal electromagnetic waves are trivial solutions of Maxwell's equation. Such transversal electromagnetic waves may travel millions of kilometers across vacuum. Upon entering the curved space-time region in the vicinity of a nucleus, the trivial electromagnetic wave may generate an electron-positron particle pair. The electromagnetic four-potential can thus be seen as the field, a "*Materia Prima*", from which the physical entities that we call "electrons" and "positrons" are generated.

To calculate electron dynamics from first principles, we must start from the electromagnetic Lagrangian density, which was introduced in chapter 1:

$$\begin{aligned}\mathscr{L} =& \frac{1}{2\mu_0}\boldsymbol{\partial}\boldsymbol{A}_\square\widetilde{\boldsymbol{\partial}\boldsymbol{A}_\square} = \frac{1}{2\mu_0}\boldsymbol{G}\widetilde{\boldsymbol{G}} = \frac{1}{2\mu_0}\|\boldsymbol{G}\|^2 = \frac{1}{2\mu_0}(S+\boldsymbol{F})(S-\boldsymbol{F}) = \frac{1}{2\mu_0}\left(S^2-\boldsymbol{F}^2\right) = \\ &= \frac{1}{2\mu_0}\left(-\frac{E^2}{c^2} + B^2 + S^2 - \frac{2}{c}\mathcal{I}\boldsymbol{E}\cdot\boldsymbol{B}\right)\end{aligned} \tag{4.3.14}$$

where $\mathcal{I}$ is the Clifford pseudo-scalar, $\boldsymbol{G}$ is the generalized electromagnetic field, S is the electromagnetic scalar field, and $\boldsymbol{F}$ is the usual scalar-free electromagnetic field.

The $\widetilde{\ }$ operator denotes Clifford reversion, which reverses the order of base vectors.

Essentially, equation 4.3.14 expresses that the electromagnetic Lagrangian density is the square of the generalized electromagnetic field strength.

As can be seen in the above expression, the electromagnetic Lagrangian density comprises two parts:

$$\mathscr{L} = \mathscr{L}_{\perp} + \mathscr{L}_{\parallel}$$

where $\mathscr{L}_{\perp} = \frac{1}{2\mu_0}\left(-\frac{E^2}{c^2} + B^2\right)$ is the Lorentz-invariant Lagrangian density of a transversal electromagnetic wave, and $\mathscr{L}_{\parallel} = \frac{1}{2\mu_0}\left(S^2 - \frac{2}{c}\mathcal{I}\boldsymbol{E}\cdot\boldsymbol{B}\right)$ is the Lorentz-invariant Lagrangian density of a longitudinal electromagnetic wave. The transversal electromagnetic wave is well known, and has been the focus of electromagnetism studies over the past 150 years. A pioneering exploration of the longitudinal electromagnetic wave solution was undertaken in chapter 2.

The $\mathscr{L}_{\parallel} = \frac{1}{2\mu_0}\left(S^2 - \frac{2}{c}\mathcal{I}\boldsymbol{E}\cdot\boldsymbol{B}\right)$ Lagrangian density can be also written as $\mathscr{L}_{\parallel} = \boldsymbol{J}_{\square}\cdot\boldsymbol{A}_{\square}$. This equivalence was derived in equation 1.3.19. The $\mathscr{L}_{\perp} = \frac{1}{2\mu_0}\left(-\frac{E^2}{c^2} + B^2\right)$ and $\mathscr{L}_{\parallel} = \boldsymbol{J}_{\square}\cdot\boldsymbol{A}_{\square}$ terms are well-known in the scientific literature, and are referred to as the "field term" and "interaction term" of the electromagnetic Lagrangian density[1].

In the following paragraphs, we show that the elementary charge is characterized by a simple Zitterbewegung Lagrangian $L_{\parallel}$ that defines the action $\mathscr{S}$:

$$L_{\parallel} = \int \boldsymbol{J}_{\square}\cdot\boldsymbol{A}_{\square}\, dv\, dt = e\boldsymbol{A}\cdot\boldsymbol{c} - eV \tag{4.3.15}$$

$$\mathscr{S} = \int L_{\parallel} dt$$

where the $e\boldsymbol{A}$ term describes the Zitterbewegung momentum of the elementary charge, eV term describes its electric energy, and $\boldsymbol{J}_{\square}$ is the averaged internal four-current density of the particle. The dv and dt terms represent the infinitesimal volume and time elements of the space-time integral.

The stationary action condition $\delta\mathscr{S} = 0$ is can be written as:

$$\mathscr{S} = \int (e\boldsymbol{A}\cdot\boldsymbol{c} - eV)\, dt = e\int \boldsymbol{A}\cdot\boldsymbol{dl} - e\int V dt = 0 \tag{4.3.16}$$

$$\delta\mathscr{S} = 0$$

The stationary action condition is satisfied when the elementary charge's electromagnetic four potential $\boldsymbol{A}_{\square} = \boldsymbol{A} + \gamma_t V$ is a nilpotent vector: $\boldsymbol{A}_{\square}^2 = 0$. We showed in the preceding section that this $\boldsymbol{A}_{\square}^2 = 0$ condition leads to the well-known magnetic and electric Aharonov-Bohm relations between the electromagnetic phase φ and the electromagnetic four potential:

$$\varphi = \frac{e}{\hbar}\int \boldsymbol{A}\cdot d\boldsymbol{l} \tag{4.3.17}$$

$$\varphi = \frac{e}{\hbar}\int_T V dt \tag{4.3.18}$$

Considering circular Zitterbewegung, we now show that identifying φ with the Zitterbewegung phase also leads to the Aharonov-Bohm relations. As $\boldsymbol{A}$ and $\boldsymbol{c}$ are parallel vectors for a freely moving charge, it's possible to substitute the dot product with the product of their norm:

$$L_{\parallel} = eAc - eV = eA\frac{dl}{dt} - eV$$

If the radius of the charge's Zitterbewegung trajectory is r, the differential of the displacement dl can be substituted by the $rd\varphi$ product:

$$dl = rd\varphi$$

$$L_{\parallel} = eAr\frac{d\varphi}{dt} - eV$$

[1] In the following, we also use the $\mathscr{L}_{\parallel} = \boldsymbol{J}_{\square}\cdot\boldsymbol{A}_{\square}$ formulation. The significance of knowing the $\mathscr{L}_{\parallel} = \frac{1}{2\mu_0}\left(S^2 - \frac{2}{c}\mathcal{I}\boldsymbol{E}\cdot\boldsymbol{B}\right)$ formulation is that it reveals the connection with longitudinal electromagnetic waves.

Consequently, the following simple conditions guarantee that the action $\mathscr{S}$ is always zero:

$$eAr = \hbar = 1$$

$$\frac{d\varphi}{dt} = eV = eA = \frac{1}{r}$$

$$r^{-1} = \frac{d\varphi}{dt} = \omega = m$$

In natural units, the electron's or positron's mass-energy is equal to its Zitterbewegung angular speed, to the inverse of its Zitterbewegung radius, and to the absolute value of its Zitterbewegung momentum eA.

The $eV = eA$ condition is equivalent to the $\boldsymbol{A}_{\square}^2 = 0$ condition on the electromagnetic four potential, and it is easy to see that the above listed three conditions directly lead to the Aharonov-Bohm relations. It follows that the circulating charge is characterized by a momentum p and energy E_e of purely electromagnetic nature:

$$(E_e\gamma_t, \boldsymbol{p})_{\square} = eA_{\square} \tag{4.3.19}$$

where $A_{\square}$ is the four-vector potential seen by the electron's charge, and $(E_e\gamma_t, \boldsymbol{p})_{\square}$ is the energy-momentum four-vector. Considering the general case of a moving electron, $A_{\square}$ has the following components:

$$A_{\square} = V\gamma_t + \boldsymbol{A}_{\perp} + \boldsymbol{A}_{\parallel} \tag{4.3.20}$$

where $\boldsymbol{A}_{\parallel}$ is the vector potential along the Zitterbewegung circle, $\boldsymbol{A}_{\perp}$ is the axial vector potential perpendicular to the Zitterbewegung circle, V is the electric potential, γ_t is the basis vector along the time axis, and $\gamma_t^2 = -1$.

In the classical field scenario, the electromagnetic field evolution is governed by the above-stated $\delta\mathscr{S} = 0$ condition of stationary action. However, elementary particles reside in an electromagnetic vacuum noise environment. This noise effect is captured by the path integral formulation of quantum mechanics. Specifically, the Feynman path integral is defined by the exponentiation of electromagnetic action, which is given by equation 4.3.16. The probability of each path is defined according to the $e^{i\mathscr{S}}$ probability factor. It can be shown [**13, 14**] that quantum mechanics can be understood as a vacuum noise effect over the $\delta\mathscr{S} = 0$ condition of stationary action. However, given that the vacuum contains the same noise energy at all frequencies, one may wonder why this noise effect is not infinitely large. This topic is addressed in chapter 6.

4.4. Practical applications of the Zitterbewegung Lagrangian

Reference [**10**] proves in great detail that superconductivity is the Bose-Einstein condensation of conduction band electrons. However, the conventional formulation of quantum mechanics does not help to answer the question of how and why do electrons Bose-Einstein condense. In this context, a practical application of the Zitterbewegung Lagrangian - as defined by equation 4.3.15 - can be found in reference [**10**], where it is used to find the equilibrium state of Bose-Einstein condensing electrons.

The appearance of coherent electrons may be possible not only in condensed matter, but also in vacuum environment. For example, Johan F. Prins has observed the formation of a stable superconductive electron structure in 10^{-6} mbar vacuum, in a micrometric gap between an oxygen-doped diamond cathode, which has negative electron affinity, and a gold-plated steel anode [**11**]. As a second example, Kenneth Shoulders has reported the observation of high density charged plasma clusters, in special spark gap devices [**12**]. He found that such plasma clusters comprise $\sim 10^{10} - 10^{14}$ electrons, with a cation content ratio of $<10^{-6}$. We anticipate the Zitterbewegung Lagrangian - as defined by equation 4.3.15 - to become a useful tool for modeling coherent electron clusters, where the Coulomb repulsion is apparently compensated by a previously unrecognized attractive force.

4.5. ESR, NMR, Spin and "Intrinsic" angular momentum

As shown in the previous paragraph, in the proposed model, the electron has an angular momentum $\boldsymbol{\hbar}$ and a magnetic moment $\boldsymbol{\mu}_B$, equal to the Bohr magneton. It is, therefore, reasonable to assume that, in presence of an external magnetic field, the electron is subjected, as a small gyroscope, to a torque $\boldsymbol{\tau}$ and to a Larmor precession with frequency ω_p. The only difference with a classical gyroscope is the

quantization of the $\hbar_{\parallel}$ component of the angular momentum $\boldsymbol{\hbar}$ along the external flux density field $\boldsymbol{B}_E$. This component can take only two possible spin values, namely $\hbar_{\parallel} = \pm\frac{1}{2}\hbar$ (see chapter 3 , section 3.3.2). The two spin values will correspond to two possible values for the angle θ formed between the angular momentum vector and the external magnetic field vector: $\theta \in \left\{\frac{\pi}{3}, \frac{2\pi}{3}\right\}$:

$$\hbar_{\parallel}^2 + \hbar_{\perp}^2 = \hbar^2,$$

$$\hbar_{\parallel} = \pm\frac{1}{2}\hbar.$$

The torque exerted by the external flux density field $\boldsymbol{B}_E$ is

$$\tau = |\boldsymbol{\mu}_B \times \boldsymbol{B}_E| = \mu_B B_E \sin(\theta)$$

and the related Larmor precession angular frequency is

$$\omega_p = \frac{B_E \mu_B}{\hbar}. \tag{4.5.1}$$

The precession angular frequency will correspond to two possible energy levels:

$$E_H = \hbar\omega_p \qquad \text{if } \theta = \frac{2\pi}{3}$$

and

$$E_L = -\hbar\omega_p \qquad \text{if } \theta = \frac{\pi}{3}.$$

The difference of energy levels corresponds to the Spin Electronic Resonance (ESR) frequency ν_{ESR}:

$$\Delta E = E_H - E_L = 2\hbar\omega_p = \hbar\omega_{ESR} = h\nu_{ESR}. \tag{4.5.2}$$

From (4.5.2) and (4.5.1) it is possible to determine the ESR frequency as

$$\nu_{ESR} = 2\frac{B_E \mu_B}{h}. \tag{4.5.3}$$

For instance, an external magnetic flux density field equal to $B_E = 1.5\,\mathrm{T}$ yields a frequency $\nu_{ESR} \approx 42$ GHz. The ESR method is already used for various applications, such as quantum computing or chemical analysis, even though its theoretical foundations have been lacking. With a proper understanding of the ESR theory, scientists will have a solid foundation to guide their progress.

By calling s the spin value and μ the nuclear magnetic moment we can also generalize (4.5.3) for particles other than the electron. In this case the term used is Nuclear Magnetic Resonance (NMR) frequency, which is equal to

$$\nu_{NMR} \approx \frac{B_E \mu}{hs}. \tag{4.5.4}$$

For instance, for isotope ${}^{7}_{3}Li$, with $s = \frac{3}{2}$, $\mu \approx 1.645 \cdot 10^{-26}$ and $B_E = 1.5$ T, the NMR frequency is $\nu_{NMR} \approx 24.8$ MHz, whereas for isotope ${}^{11}_{5}B$ we have $s = \frac{3}{2}$, $\mu \approx 1.36 \cdot 10^{-26}\ \mathrm{J \cdot T^{-1}}$ and NMR frequency is $\nu_{NMR} \approx 20.5$ MHz. Another example deals with isotope ${}^{87}_{38}Sr$ with $s = \frac{9}{2}$ and $\mu \approx 5.52 \cdot 10^{-27}\ \mathrm{J \cdot T^{-1}}$. In this case NMR frequency is $\nu_{NMR} \approx 278\,\mathrm{kHz}$ for $B_E = 0.15$ T with a Larmor frequency $\frac{\omega_p}{2\pi} = \frac{1}{2}\nu_{NMR} \approx 139\,\mathrm{kHz}$.

The electron, in the presence of an external magnetic field, is subjected to Larmor precession and its spin value $\pm\frac{\hbar}{2}$ is interpreted as the intrinsic angular momentum component parallel to the magnetic field. It is interesting to note that a hypothetical technology, able to align the intrinsic angular momentum of a sufficient number of electrons, could favor the formation of a coherent superconducting and super-fluid condensate state. This possibility is explored in reference [**10**].

4.6. Conclusions

In this chapter a simple Zitterbewegung electron model has been introduced, where the concepts of mass-energy, momentum, magnetic momentum and spin naturally emerge from its geometric and electromagnetic parameters, thus avoiding the obscure concept of "intrinsic property" of a "point-like" particle. Using only electromagnetic and geometric concepts, an insightful interpretation of the Aharonov-Bohm equations has been presented. The results of this chapter further demonstrate that the phase of a quantum mechanical wave-function is derived from the Zitterbewegung wave.

The Electronic Spin Resonance (ESR) frequency has been computed starting from a spin model based on the Larmor precession frequency of Zitterbewegung rotation plane.

Acknowledgements

The authors thank Giuliano Bettini for helpful discussions and suggestions.

Bibliography

[1] Carver Mead. The nature of light: what are photons? Proc.SPIE, 8832:8832 – 8832 – 7, 2013.

[2] David Hestenes. Quantum Mechanics from Self-interaction. Foundations of Physics, 15(1):63–87, 1985.

[3] A. L. Parson and Smithsonian Institution. A magneton theory of the structure of the atom (with two plates). Number v. 65 in Publication (Smithsonian Institution). Smithsonian Institution, 1915.

[4] J. Paul Wesley David L. Bergman. Spinning charged ring model of electron yielding anomalous magnetic moment. Galilean Electrodynamics, 1:63–67, Sep/Oct 1990.

[5] D. L. Bergman and C. W. Lucas. Credibility of Common Sense Science. Foundations of Science, pages 1–17, 2003.

[6] David Hestenes. The zitterbewegung interpretation of quantum mechanics. Foundations of Physics, 20(10):1213–1232, 1990.

[7] Richard Gauthier. The electron is a charged photon. Volume 60 of APS April Meeting 2015, 2015.

[8] Aharonov, Y. and Bohm, D. Significance of Electromagnetic Potentials in the Quantum Theory. Physical Review, 115:485–491, 1959.

[9] R. P. Feynman. QED: The Strange Theory of Light and Matter. Penguin Books. Penguin, 1990.

[10] A. Kovacs et al. The Bose-Einstein condensation of electrons: a long overdue discovery of how superconductors really work. Zitter Institute, 2025.

[11] J. F. Prins. The diamond-vacuum interface: Electron extraction from n-type diamond, evidence for superconduction at room temperature. Semiconductor Science and Technology, volume 18(3), (2003)

[12] K. Shoulders. EV, A Tale of Discovery. (1987)

[13] V. Yordanov “Revisiting the Bohr Model of the Atom through Brownian Motion of the Electron”, arXiv:2412.19918v4 (2025)

[14] J. Lindgren et al. “The Heisenberg uncertainty principle as an endogenous equilibrium property of stochastic optimal control systems in quantum mechanics”, Symmetry, volume 12.9 (2020)

CHAPTER 5

The Dirac equation and Occam's razor

Andras Kovacs[1]
[1] Exafuse. E-mail: andras.kovacs@broadbit.com

5.1. Introduction

The Dirac equation is considered to be the most important equation of quantum mechanics because its solutions allow precise calculation of electron orbitals' binding energies. The Dirac equation is generally known to be "spinor field" valued, but the intuitive physical meaning of this statement remains unclear in most textbooks. It also remains unclear why Nature would choose to operate with such complex-looking Dirac gamma matrices. The challenge is to develop a clear interpretation of the Dirac equation.

Important progress was made in this field by David Hestenes and William Baylis, who recognized that a spinor field represents Lorentz boost and spatial rotations of the particle orientation. With their approach, the spinor value factorizes into a scalar valued probability density, and representations of a Lorentz boost and a spatial rotation. All of these factors have a well-understood physical meaning. The corresponding formulations of the Dirac equation are referred to as the Dirac-Hestenes and Dirac-Baylis equations. These approaches are discussed in references [**1, 2**], along with applications that demonstrate the utility these new insights.

We showed in chapter 4 that the electron's probability distribution is defined by a path integral, formulated via an exponentiated Lagrangian action. In reference [**3**], the Schrödinger equation is derived from this exponentiated Lagrangian action. Similarly, reference [**4**] shows that the path integral formulation corresponds to a maximum entropy random walk process, and also derives the Schrödinger equation via this approach. All these results imply a scalar valued probability density representation.

Starting from the $\epsilon^2 - (pc)^2 = \left(mc^2\right)^2$ energy-momentum relationship, we demonstrate a simple formulation of the Dirac equation, where the probability density field is scalar valued and represents the electron's energy and momentum density. Most importantly, we show how the Dirac equation's mass term also demonstrates the previously developed concept of electromagnetic field energy based electron mass.

5.2. A simple formulation of the Klein-Gordon and Dirac equations

5.2.1. Conceptual formulation. Macroscopically, the acceleration of charges produces transversal electromagnetic waves. This macroscopic situation changes when the energy of a harmonically oscillating charge coincides with the noise floor, which is represented by the Heisenberg uncertainty relation. Under such a quantum mechanical scenario, a radiationless equilibrium state is obtained. In the 1920s, Dirac discovered that these radiationless equilibrium states can be found by solving the equation named after him, which is a differential equation over the so-called "four-component spinor field".

In the conventional Dirac equation context, a complex valued spinor wavefunction is denoted by ψ. The spinor field is defined as the quantum mechanical wavefunction whose time-wise derivative yields the particle energy, and whose spatial derivative in a certain direction yields canonical momentum along that direction. Since ψ is a quantum mechanical field, the quantity $\psi\bar{\psi}$ gives the particle's probability density distribution.

Consider a plane-wave spinor field: $\psi = \psi_0 e^{i(\Omega t - \mathbf{K}\cdot\mathbf{r})}$. The Dirac equation's main concept is that spinor field's differentiation along the time coordinate gives $\hbar\partial_t\psi = i\hbar\Omega\psi_0 e^{i(\Omega t - \mathbf{K}\cdot\mathbf{r})} = i\epsilon\psi$, where $i\epsilon$ represents an imaginary energy eigenvalue of the wavefunction. Similarly, differentiation along a space coordinate gives the imaginary momentum eigenvalue.

For any wavefunction, the $\epsilon^2 - (pc)^2 = \left(mc^2\right)^2$ energy-momentum relation turns into the Klein-Gordon equation:

$$i^2\hbar^2\left(\frac{1}{c^2}\partial_t^2 - \partial_x^2 - \partial_y^2 - \partial_z^2\right)\psi = -\left(mc\right)^2\psi \tag{5.2.1}$$

Using the above stated ψ formulas, it is easy to see that the Klein-Gordon equation is equivalent to the $\epsilon^2 - (pc)^2 = \left(mc^2\right)^2$ energy-momentum relation.

Now let us find a linear equation for ψ, whose solution is also a solution of the above Klein-Gordon equation. We write this linear equation using the following matrix notation:

$$i\hbar\left(\gamma_0\frac{1}{c}\partial_t - \gamma_1\partial_x - \gamma_2\partial_y - \gamma_3\partial_z\right)\psi = mc\psi \tag{5.2.2}$$

The above equation is the Dirac equation. It implies the Klein-Gordon equation if the γ_μ matrices satisfy the following properties:

$$\gamma_0^2 = \mathbf{I}, \gamma_1^2 = \gamma_2^2 = \gamma_3^2 = -\mathbf{I} \tag{5.2.3}$$

$$\gamma_i\gamma_j = -\gamma_j\gamma_i \; (i \neq j) \tag{5.2.4}$$

It is recognized that the above relations are the same as the Clifford commutation relations. The spinor geometry of the ψ field is equivalent to the Clifford geometry. There are several possible choices to write the Dirac γ_μ matrices. Dirac originally discovered the following matrix representation of Clifford algebra:

$$\gamma_0 = \begin{pmatrix} \mathbf{I} & 0 \\ 0 & -\mathbf{I} \end{pmatrix}, \gamma_1 = \begin{pmatrix} 0 & -\sigma_x \\ \sigma_x & 0 \end{pmatrix}, \gamma_2 = \begin{pmatrix} 0 & -\sigma_y \\ \sigma_y & 0 \end{pmatrix}, \gamma_3 = \begin{pmatrix} 0 & -\sigma_z \\ \sigma_z & 0 \end{pmatrix} \tag{5.2.5}$$

where $\mathbf{I}$ is the identity matrix and σ_i are the Pauli spin-matrices. This establishes the equivalence between the Dirac and Klein-Gordon equations.

Instead of working with a matrix representation of base elements, we can choose to write the Dirac equation using Clifford bases, using the same notation as in previous chapters:

$$I\hbar\boldsymbol{\partial}\psi = mc\psi \tag{5.2.6}$$

where I is the Clifford pseudo-scalar, and the $\boldsymbol{\partial}$ operator is defined according to equation 1.2.2: i.e. it is used in the same way as in the preceding chapters. This analysis of the Dirac equation also sheds light on why the imaginary unit i appears in the Dirac equation; it is the Clifford pseudo-scalar $\gamma_t\gamma_x\gamma_y\gamma_z$. The traditional way of treating i just as an imaginary number occults its geometric meaning of being the unit of space-time volume.

In summary, we obtained a mathematically simple formulation of the Dirac equation, which has a clear geometric meaning, and established the equivalence between the Dirac and Klein-Gordon equations.

5.2.2. The dimensionality of the mass term. We established that the space-time differential of ψ yields the energy-momentum eigenvalues of a particle. It was shown in the previous chapters that the energy-momentum $\boldsymbol{P}_\square$ of a particle with electric charge e is given by the $\boldsymbol{P}_\square = e\boldsymbol{A}_\square$ relationship, where $\boldsymbol{A}_\square$ is the vector potential seen by the electric charge. Since $\boldsymbol{A}_\square$ means here the vector potential seen by the electric charge, an externally applied vector potential adds onto this vector potential seen by the electric charge, and thus we directly obtain the effect of external electromagnetic fields on the Dirac equation:

$$I\hbar\boldsymbol{\partial}\psi = mc\psi + IeA_{applied} \tag{5.2.7}$$

The above equation was historically validated by comparing the calculated energy levels of electron orbitals against experimental transition energy measurements.

Term	Dimension
ψ	Scalar
$I\partial\psi$	Tri-vector
eA	Vector
IeA	Tri-vector
mc	Tri-vector

TABLE 1. The dimension of terms appearing in the Dirac equation

Let us look at the dimension of the terms appearing in equation 5.2.7. ψ is a scalar, $\boldsymbol{\partial}\psi$ becomes Clifford vector, and thus we get a tri-vector upon further multiplication by the pseudoscalar I. On the right hand side $eA_{applied}$ is a Clifford vector, and thus $IeA_{applied}$ also becomes tri-vector. These relationships are summarized in table 1, and show that the dimensionality of the mass term m is a tri-vector. In this way, equation 5.2.7 is yet again telling us that the particle mass m is the result of field energy integration over a volume element, as derived in chapter 3, and not just some "inherent scalar property of an abstract point particle". I.e. this dimensional analysis confirms that particle mass is the integral of the electromagnetic energy density.

Instead of a tri-vector mass representation, we can switch to a vectorial mass representation:

$$I\hbar\partial\psi = mc\psi \;\Leftrightarrow\; \hbar\partial\psi = -\boldsymbol{m}c\psi \tag{5.2.8}$$

where $I\boldsymbol{m} \equiv m$ is the tri-vector representation of mass, while $\boldsymbol{m}$ is the vector representation of mass. It follows from the dimensional analysis of the above equations that as long as ψ is scalar, mass must be represented as either a vector or a tri-vector quantity, but certainly can no longer be scalar quantity. The above equations highlight the equivalence between these two mass representations. This might strike the reader as odd: all textbook discussions of the Dirac equation consider mass to be a scalar quantity, even geometric algebra oriented studies.

It is interesting to note that Giorgio Vassallo derives a very similar equation to 5.2.8 in chapter 4 of reference [**5**], but it describes the electron's Zitterbewegung instead of probability distribution and it is expressed in terms of electromagnetic vector potential. Perhaps chapter 4 of reference [**5**] is relevant for learning how to formulate the Dirac equation in terms of electromagnetic waves.

Let us recall that our starting point was the wish to study solutions of the scalar type $\psi = \psi_0 e^{i(\Omega t - \mathbf{K}\cdot\mathbf{r})}$ quantum mechanical wavefunction. We found that working with the Dirac equation implies that either m is not scalar or that ψ is not scalar. Historically, scientists made the "ψ is not scalar" choice, and ψ was understood as a spinor-valued function. Based on the above-presented dimensional analysis, the "m is not scalar" choice has also a strong justification. Therefore, the vectorial representation of $\boldsymbol{m}$ will be pursued further in this chapter.

Into which direction is $\boldsymbol{m}$ pointing? As a particle moves through the four-dimensional spacetime, equation 5.2.8 implies that $\mathbf{m}$ is pointing along the particle's spacetime trajectory. In the particle's rest frame, the $\boldsymbol{m}$ vector is pointing into the time direction. It is clear from this analysis that a hypothetical "negative energy" state represents a particle traveling backwards in time. Schwinger and Feynman indeed modeled positrons as particles traveling backwards in time. However, in reality all particles travel forward in time; the Dirac equation's "negative energy states" are therefore un-physical, and have nothing to do with positrons. This is further demonstrated by the fact that an electron-positron annihilation event releases 2·511 keV energy, implying that the positron energy is +511 keV. The only difference between an electron and a positron is in their electromagnetic waves' scalar components, which correspond to opposite charge values.

5.3. Can the Zitterbewegung frequency be obtained from the Dirac equation?

In quantum theory, a so-called Zitterbewegung term appears in the free electron a solution of the Dirac equation, and it was firstly calculated by Schrödinger [**6**]. Taking the Heisenberg picture, and solving the Dirac equation for the electron position yields a high frequency oscillation term, with the corresponding oscillation velocity being the speed of light. This constant velocity implies a circular Zitterbewegung oscillation at light-speed. The details of this calculation can be found for example on pages 322-323 of [**7**]. Such a calculation yields an oscillation angular frequency of $2mc^2/\hbar$ and oscillation amplitude of $\hbar/2mc$. Such a frequency differs by a factor of two from the $mc^2/\hbar$ De Broglie frequency of electromagnetic wave oscillation; this discrepancy led to a long-standing ambiguity between the two values. In order to clear up this ambiguity, we address the question of whether the Dirac equation based electron position calculation can be extrapolated to the high frequency limit of electromagnetic wave oscillation.

As we saw in the previous section, the physical meaning of the Dirac spinor field is that its differentiation yields energy-momentum eigenvalues. The analogous definition of an electromagnetic spinor is the following:

$$I\hbar\partial\psi_{EM} = \frac{1}{2}G\gamma_t\widetilde{G} \tag{5.3.1}$$

where G is the electromagnetic field, and we used the electromagnetic energy-momentum expression from chapter 1. This is the applicable definition for the high-frequency limit, in which we are directly observing the electromagnetic wave.

A harmonic electromagnetic spinor has $\psi_{EM} = \psi_0 e^{i(\Omega t - \mathbf{k}\cdot\mathbf{r})}$ form. In chapter 1 we showed that each term of the electromagnetic energy-momentum comprises a multiplication between two selections from the S, E, or B field; this can be directly seen also from the $\frac{1}{2}G\gamma_t\widetilde{G}$ expression. When the electromagnetic field oscillates at an angular frequency ω, we have $S \sim e^{i\omega t}$, $E \sim e^{i\omega t}$, and $B \sim e^{i\omega t}$. Therefore, multiplications between any two selections from S, E, or B yield $\partial\psi_{EM} \sim e^{i2\omega t}$, and since a differentiation operator does not change the frequency we get $\psi_{EM} \sim e^{i2\omega t}$. Thereby we obtain an important relationship: $\Omega = 2\omega$. This means that the frequency of the electromagnetic spinor field is twice the electromagnetic wave frequency. In the high frequency limit, the $2mc^2/\hbar$ angular frequency obtained via Dirac equation is NOT a physical oscillation frequency; it is twice the $mc^2/\hbar$ angular frequency of the underlying electromagnetic wave.

We finish this chapter by summarizing the three major quantum theory related clarifications presented in this book. In each case, we corrected a factor of two mistake that went unnoticed for nearly a century:

(1) The Dirac spinor field is considered to describe a "half-spin" particle. Under an applied magnetic field, the electron's angular momentum measurement yields $\frac{\hbar}{2}$. This measured value was interpreted as the internal angular momentum of the electron, despite the obvious contradiction with angular momentum conservation in electron-positron annihilations that produce two circularly polarized photons, each carrying $\hbar$ angular momentum. Regarding measurements, one must realize that under an applied magnetic field the electron's angular momentum is precessing around magnetic field lines, and the measured $\frac{\hbar}{2}$ value is only its projection onto the direction of the applied magnetic field. The equations of this precession are described in chapter 3. The electron's internal angular momentum value is $\hbar$. Our interpretation is in line with the operating principle of NMR devices, while the traditional interpretation of the measured $\frac{\hbar}{2}$ value is contradictory also to the operating principle of commercial NMR technology.

(2) Schrödinger suggested in 1930 to interpret the high frequency extrapolation of the Dirac equation as a real spatial $2mc^2/\hbar$ oscillation frequency of an elementary particle [**6**]. However, the above presented analysis reveals that the correct Zitterbewegung frequency of the electromagnetic wave is $mc^2/\hbar$. There is no spatial oscillation at $2mc^2/\hbar$ angular frequency.

(3) We showed in chapter 4 that an individual electron is associated with an h/e magnetic flux value. However, superconductivity-related measurements show that an externally applied magnetic field penetrates superconductors in steps of $h/2e$ magnetic flux quanta. Such superconductivity related measurements are performed over a multi-electron system; the superconductivity-related $h/2e$ magnetic flux quantum must not be automatically associated with the magnetic flux value of an elementary particle's Zitterbewegung.

Bibliography

[1] A. G. Campos et al “Analytic Solutions to Coherent Control of the Dirac Equation”, Physical Review Letters, volume 119.17 (2017)

[2] A. G. Campos et al “Construction of Dirac spinors for electron vortex beams in background electromagnetic fields”, Physical Review Research, Volume 3.1 (2021)

[3] G. Vassallo "Charge clusters, low energy nuclear reactions and electron structure", Journal of Condensed Matter Nuclear Science, volume 39 (2024)

[4] M. Faber “Stationary Schrödinger Equation and Darwin Term from Maximal Entropy Random Walk”, Particles, volume 7.1 (2023)

[5] A. Kovacs et al “Unified Field Theory and Occam’s Razor”, World Scientific (2022)

[6] E. Schrödinger “Über die kräftefreie Bewegung in der relativistichen Quantenmechanik”, Sitz.ber. Preuss. Akad. Wiss. Phys.-Math., volume XXIV (1930), Pages 418–428

[7] P. Milonni “The Quantum Vacuum”, Academic Press (1994)

CHAPTER 6

The Lamb shift as a spectrometer of electron-noise interaction

Andras Kovacs[1]
[1] Exafuse. E-mail: andras.kovacs@broadbit.com

6.1. Introduction

The electron wavefunction exists not in empty space, but in a vacuum filled by electromagnetic noise. This electromagnetic vacuum noise can be experimentally measured [**5**], and it also produces the well-known Casimir effect. One may ask how the electromagnetic vacuum noise interacts with the electron wavefunction. This question is closely related to a second fundamental issue: why does the oscillating ground state wavefunction not radiate electromagnetic energy, i.e. how to reconcile the existence of non-radiating quantum mechanical states with Maxwell's equation? Taking the Dirac equation based eigenstate calculation at face value, it yields accurate electron binding energy while bypassing both questions. This apparent paradox has puzzled generations of physicists. A recently suggested resolution to these puzzles is that any stable wavefunction state does in fact radiate energy according to Maxwell's equation, but also absorbs vacuum noise energy at the same rate, thus achieving a thermodynamic equilibrium [**6, 7**]. This interpretation is strongly supported by the electromagnetic vacuum noise being defined by Planck's constant; the specific vacuum noise intensity formulas will be given in the next section. It means that the Planck's constant, which we find in the Dirac equation, is in fact defined by the intensity of electromagnetic vacuum noise.

The experimentally observed electron-light interactions depend on whether the incoming light is more intense than the vacuum noise, or whether it is just the vacuum noise. Above the vacuum noise intensity, the bound electron wavefunction interacts with the entire electromagnetic spectrum. The specific process that quantitatively describes electron-light interaction depends on the incoming light frequency: these processes are known as the photo-electric effect (light wavelength is comparable to the Bohr radius), Thomson-scattering (light wavelength is in the x-ray range), and Compton scattering (light wavelength is comparable to the classical electron radius). Regarding low frequencies, a bound electron can be ionized even by microwave radiation, provided that its intensity is sufficiently large [**2**].

The situation is dramatically different for electron-light interactions at the vacuum noise intensity. The standing wave state of any electron wavefunction oscillates at one well-defined frequency. It follows that the electron should radiate energy only at that specific standing wave frequency. Regarding counter-balancing energy absorption from vacuum noise, there is a long history of interpreting quantum mechanics as a stochastic process of such noise energy absorption [**8, 9**]. What is the counter-balancing noise frequency range in which the electron absorbs energy from vacuum noise? Despite the presence of high frequency vacuum noise, the stability of matter around us demonstrates that the Thomson-scattering and Compton scattering cross-sections become zero at the vacuum noise intensity. Despite the presence of low frequency vacuum noise, there is no measurable Stark effect without applied electric fields, demonstrating that the low-frequency interaction cross-section also becomes zero at the vacuum noise intensity. For some reason, the vacuum noise interacts with electrons only in a specific frequency range. Identifying the effective electron-noise interaction frequency range is one objective of this chapter; our main result is that this frequency range can be identified from the Lamb shift effect.

The Lamb shift effect is experimentally observed only for s-state involving transitions, whose the wavefunction probability is non-zero at the nucleus. The Lamb shift effect is therefore generally interpreted as a noise-induced "blurring" of the electron wavefunction; the measurements on the following pages indicate that such a blurring radius is in the tens of femtometers range for hydrogen. The Lamb-shift related blurring radius is thus an order of magnitude smaller than the reduced Compton radius, which defines the electron's Zitterbewegung radius. One might therefore anticipate that the electron's Zitterbewegung structure should also cause a measurable binding energy impact around the nucleus, generating an order of magnitude larger energy shift in s-states than the Lamb shift. However, that anticipation is contradicted by measurements, and to the best of our knowledge this contradiction has

not been addressed in prior studies. A secondary objective of our present work is therefore to resolve this apparent paradox by clarifying what happens to electron Zitterbewegung in the nuclear vicinity.

6.2. Electron-noise interaction based Lamb-shift accounting

6.2.1. Electromagnetic vacuum fluctuations. One way to characterize electromagnetic vacuum fluctuation is to describe its average electric and magnetic field intensity. In a harmonic wave, the average field intesities are related to the energy density as $\frac{1}{2}\left(\varepsilon_0 E^2 + \frac{1}{\mu_0}B^2\right) = \varepsilon_0 \bar{E}^2 = \frac{\bar{B}^2}{\mu_0}$. The average vacuum field intensity is given by the following formula [**5**]:

$$\varepsilon_0 \bar{E}^2 = \frac{\bar{B}^2}{\mu_0} = \frac{\hbar c}{4\pi^2}\int_0^\infty k^3 dk \tag{6.2.1}$$

where k is the wavenumber of the given wave. There is no special wavelength; each electromagnetic wavelength contributes uniformly to the field intensity of the vacuum fluctuation. Such spectral distribution is the only Lorentz invariant possibility - under non-accelerating frame transformations. If there was any other type of spectral distribution in the vacuum, it would be subject to Doppler shift in various reference frames, and our perception of the vacuum would then depend on our frame of reference. We emphasize that equation 6.2.1 is not just a theory for explaining the Casimir force measurements, but was also directly measured in reference [**5**].

We rewrite the above formula as follows:

$$\varepsilon_0 \bar{E}^2 = \frac{\bar{B}^2}{\mu_0} = \frac{\hbar c}{4\pi^2}\int_0^\infty k^3 dk = \frac{\hbar c}{16\pi^3} 4\pi \int_0^\infty k k^2 dk = \tag{6.2.2}$$

$$= \frac{\hbar c}{16\pi^3}\iiint_0^\infty k\, d^3k = \frac{1}{8\pi^3}\iiint_0^\infty \left(\frac{1}{2}\hbar\omega\right) d^3k = \frac{1}{V}\sum_k \frac{1}{2}\hbar\omega$$

where V is a unit volume element. This result implies that each possible vacuum oscillation mode has $\frac{1}{2}\hbar\omega$ energy, which is generally referred to as the "zero-point energy" of the electromagnetic noise floor. The above expression is the field intensity integration over the abstract space of all possible wavenumbers, and this form will be used in the Lamb shift calculation. The overall electric field intensity can also be written as an integration over its spectral components:

$$\varepsilon_0 \bar{E}^2 = \frac{V}{8\pi^3}\iiint_0^\infty \varepsilon_0 \bar{E}_k^2\, d^3k \tag{6.2.3}$$

From the above equations we get the relationship between $\bar{E}_k$ and k:

$$V\bar{E}_k^2 = \frac{\hbar c}{2\varepsilon_0}k \tag{6.2.4}$$

6.2.2. A naive approach to the electron-noise interaction modeling. As the electric field of a harmonic noise component pushes the electron back-and-forth, it "blurs out" the electron's position. To characterize this blurring, we consider a stationary point-particle electron, and calculate the mean distance δr_k into which the noise component with wavenumber k pushes the electron.

The maximum and mean electric field intensities of a harmonic noise component are related by the $E_{max}^2 = 2\bar{E}^2$ relationship. The harmonic noise component accelerates the electron according to the $a = \frac{eE_{max}}{m}\sin(\omega t)$ relationship. Consequently, the displacement generating the electron blur is $x = \frac{eE_{max}}{m}\omega^{-2}\sin(\omega t) = \frac{eE_{max}}{m}(kc)^{-2}\sin(\omega t)$. In a harmonic oscillation, the maximum and mean displacements are related by the $x_{max}^2 = 2\bar{x}^2$ relationship.

As the above relationships hold independently for each spatial direction, we are now able to estimate the mean displacement δr_k as follows:

$$(\delta r_k)_{stationary}^2 = \left(\frac{e\bar{E}_k}{m}\right)^2 (kc)^{-4} \tag{6.2.5}$$

where the k index labels the displacement caused by the k wavenumbered noise component.

While this naive approach is a useful first step, it needs adjustments for the practical purpose of Lamb shift calculation. The Lamb shift applies to a radially oscillating electron, and its effect arises in a close nuclear proximity. In that context, the electron is neither stationary or point-like.

In order to clarify the applicable electron-noise interaction model, we must study the radially oscillating electron's Zitterbewegung dynamics.

6.2.3. The radially oscillating electron's Zitterbewegung topology. Some isotopes are capable of capturing electrons into their nuclear structure; mainly inner-shell electrons are captured. For some isotopes, such as ^{3}He, it only takes a few keV energy to capture electrons: such small energy cannot alter the electron structure prior to its capture. This implies that, near the nucleus, radially oscillating electron converges into a Zitterbewegung structure that enables its capture by a few femtometers sized nucleus.

The electron's total energy remains invariant during radial oscillation: it may be described as the back-and-forth conversion of potential and kinetic energies. Recalling the Aharonov-Bohm equations, given by equations 4.3.8 and 4.3.10, let us apply them in the context of radial oscillation.

Taking the $\frac{1}{T} = \frac{\omega}{2\pi} = \frac{m_0 c^2}{h}$ Zitterbewegung frequency of a free electron, and applying the electric Aharonov-Bohm formula to compute the 2π phase shift within a time interval T, we can evaluate the potential V experienced by the electron charge.

Let us consider the electron's radial oscillation around a proton. When the electron charge is centered around the proton, the electron charge experiences $V \to 0$ as the two charges' potential fields cancel out. The electric Aharonov-Bohm formula implies that the electron's Zitterbewegung frequency goes to zero near the oscillation mid-point. Nevertheless, we showed in chapter 1 that charge conservation requires that the electric charge moves at the speed of light, and therefore in this mid-point region the electron charge moves at the speed of light along a nearly straight line trajectory. In the case of a higher nuclear charge, the region of straight line charge trajectory extends radially further. Figure 6.2.1 illustrates a radially oscillating electron's Zitterbewegung trajectory.

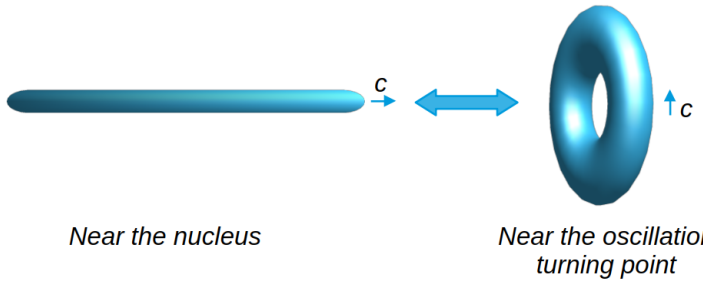

FIGURE 6.2.1. An illustration of a radially oscillating electron's Zitterbewegung trajectory. Away from the nucleus, the electron charge's light-speed trajectory converges to the circular Zitterbewegung movement of a free electron. Near the nucleus, the electron charge's light-speed trajectory converges to a straight line; the nuclear electron's light-speed trajectory is therefore also a straight line in free space.

With this background, we may consider how electromagnetic noise impacts the electron near the nucleus.

6.2.4. Mean electron displacement. As before, maximum and mean electric field intensities of a harmonic noise component are related by the $E_{max}^2 = 2\bar{E}^2$ relationship. Without the noise effect, a radially oscillating electron goes directly through the nucleus. We are interested in the noise component that is perpendicular to the direction of a radially incoming electron; only this perpendicular component causes a deviation of the closest electron-nucleus approach. Therefore, we are ignoring the field component in the electron's direction of motion; the applicable field intensity is $E_{\perp max}^2 = \frac{4}{3}\bar{E}^2$.

In the static electron case, the electric noise component accelerates the electron according to the $a = \frac{eE_{\perp max}}{m}\sin(\omega t)$ relationship. As illustrated in figure 3.3.3, the electron's kinetic acceleration and speed are perpendicular to the static electron's Zitterbewegung trajectory. The key insight is that the acceleration of a static electron is completely analogous to the action of a perpendicular force onto a linear Zitterbewegung trajectory.

Consequently, the electric displacement generating the electron blur is $x = \frac{eE_{\perp max}}{m}\omega^{-2}\sin(\omega t) = \frac{eE_{\perp max}}{m}(kc)^{-2}\sin(\omega t)$. In a harmonic oscillation, the maximum and mean displacements are related by the $x_{max}^2 = 2\bar{x}^2$ relationship.

We are now able to estimate the mean electric displacement as follows:

$$(\delta r_k)_e^2 = \frac{2}{3}\left(\frac{e\bar{E}_k}{m}\right)^2 (kc)^{-4} \tag{6.2.6}$$

In the vicinity of a proton, the electron's linear Zitterbewegung trajectory means that we must consider magnetic displacement as well. In that central region, the magnetic noise component accelerates the electron according to the Lorentz force law: $a = \frac{ecB_{\perp max}}{m}\sin(\omega t)$. The mean magnetic displacement is then calculated analogously to the electric case:

$$(\delta r_k)_m^2 = \frac{2}{3}\left(\frac{ec\bar{B}_k}{m}\right)^2 (kc)^{-4} = \frac{2}{3}\left(\frac{e\bar{E}_k}{m}\right)^2 (kc)^{-4} \tag{6.2.7}$$

where we used equation 6.2.1 for the relation between the mean magnetic and electric field components.

The k wavenumbered electromagnetic noise thus leads to the following mean electron displacement from the nucleus:

$$(\delta r_k)^2 = (\delta r_k)_e^2 + (\delta r_k)_m^2 = \frac{4}{3}\left(\frac{e\bar{E}_k}{m}\right)^2 (kc)^{-4} \tag{6.2.8}$$

6.2.5. Electron-noise interaction based Lamb shift calculation. The s and p electron orbital wavefunctions are calculated from the Dirac equation, according to the well-known methodology explained in [**1**]. The following formulas describe the radial part of the wavefunctions which are relevant to this section:

$$\psi_{1s}(r) = 2\left(\frac{Z}{a_0}\right)^{\frac{3}{2}} e^{-\frac{Z}{a_0}r} \tag{6.2.9}$$

$$\psi_{2s}(r) = \frac{1}{2\sqrt{2}}\left(\frac{Z}{a_0}\right)^{\frac{3}{2}}\left(2-\frac{Z}{a_0}r\right)e^{-\frac{Z}{2a_0}r} \tag{6.2.10}$$

$$\psi_{2p}(r) = \frac{1}{2\sqrt{6}}\left(\frac{Z}{a_0}\right)^{\frac{3}{2}}\frac{Z}{a_0}re^{-\frac{Z}{2a_0}r} \tag{6.2.11}$$

$$\psi_{3s}(r) = \frac{2}{81\sqrt{3}}\left(\frac{Z}{a_0}\right)^{\frac{3}{2}}\left(27-18\frac{Z}{a_0}r+2\left(\frac{Z}{a_0}r\right)^2\right)e^{-\frac{Z}{3a_0}r} \tag{6.2.12}$$

$$\psi_{3p}(r) = \frac{4}{81\sqrt{6}}\left(\frac{Z}{a_0}\right)^{\frac{3}{2}}\left(\frac{6Z}{a_0}r-\left(\frac{Z}{a_0}r\right)^2\right)e^{-\frac{Z}{3a_0}r} \tag{6.2.13}$$

where r is the radial coordinate, Z is the nuclear charge, and a_0 is the Bohr radius parameter. The Bohr radius depends also on the nuclear mass:

$$a_0 = \frac{\hbar}{m_{reduced}c\alpha} = \frac{\hbar}{c\alpha}\frac{m_e+m_n}{m_e m_n}$$

where the $m_{reduced} = \frac{m_e m_n}{m_e+m_n}$ parameter indicates that the m_e electron mass and m_n nuclear mass oscillate around their center of mass.

The electrostatic potential energy of the ψ_{2s} and ψ_{2p} functions is exactly the same. Therefore, according to the virial theorem, the kinetic energy and binding energy should also be the same in both cases. Nonetheless measurements reveal a small difference between the energy of these two states; this difference is referred to as the Lamb shift. Likewise, the electrostatic potential energy of the ψ_{3s} and ψ_{3p} functions is exactly the same, yet there is also a measured Lamb shift. The Lamb shift is a tiny effect; the binding energy of the above mentioned two electron states differs by about one part in a million.

In the following paragraphs we calculate the interaction between the electromagnetic vacuum fluctuations and a radially oscillating electron. The calculation methodology is based on the idea introduced by Welton in [**3**], which we develop into a simpler and assumption-free calculation.

How to add up the contributions of various wavenumbered noise components? Since the various noise wavelengths are independent of each other, their contributions are adding up in quadrature:

$$(\delta r)^2 = \sum_k (\delta r_k)^2 \tag{6.2.14}$$

We now rewrite the above summation as an integration over the possible wave numbers, replacing $\sum_k$ by $\frac{V}{8\pi^3} \iiint d^3k$. Using equation 6.2.8, the integral formula thus takes the following form:

$$(\delta r)^2 = \frac{V}{8\pi^3} \iiint \frac{4}{3} \left(\frac{e\bar{E}_k}{m} \right)^2 (kc)^{-4} \, d^3k = \frac{1}{16\pi^3} \frac{4}{3} \frac{e^2\hbar}{\varepsilon_0 m^2 c^3} \iiint k k^{-4} \, d^3k = \tag{6.2.15}$$

$$= \frac{4}{3} \frac{e^2\hbar}{4\pi^2 \varepsilon_0 m^2 c^3} \int_{k_{min}}^{k_{max}} \frac{1}{k} \, dk = \left(\frac{e}{mc^2} \right)^2 \frac{\hbar c}{3\pi^2 \varepsilon_0} \ln \left(\frac{k_{max}}{k_{min}} \right)$$

In the above equation, we substituted in the average field intensity formula according to equation 6.2.4. The $\left(\frac{e}{mc^2}\right)^2 \frac{\hbar c}{3\pi^2\varepsilon_0}$ factor evaluates to $(21.487 \text{ fm})^2$.

The above displacement formula yields infinity if either k_{min} goes to zero or k_{max} goes to infinity. Recognizing this issue, Welton and Bethe chose $k_{min} = 17.8 \cdot R_H$ and $k_{max} = \frac{m_e c}{\hbar} = \frac{\omega_e}{c}$, where R_H is the hydrogen's Rydberg constant. According to references [**3, 4**], these constants were set to yield the correct Lamb shift energy for hydrogen, which was experimentally measured at that time. As quantum mechanical transitions from the ground state approach towards this continuum, the limiting value of their transition energy is characterized by the Rydberg constant R, which denotes the lowest k value capable of generating a free electron from its ground state. In the heaviest elements, the Rydberg constant becomes the same order of magnitude as $\frac{\omega_e}{c}$, and thus $17.8 \cdot R$ becomes larger than k_{max}, which shows that Welton's and Bethe's formulas cannot be correct.

In our work, we treat $\frac{k_{max}}{k_{min}}$ as an experimentally determined input parameter. As can be seen from equation 6.2.15, only this ratio is relevant for the Lamb shift calculation, not the actual numbers. As will be shown in the following paragraphs, the $\frac{k_{max}}{k_{min}} = 2\pi$ ratio yields the experimentally correct Lamb shift values; that is a surprisingly tight ratio for the noise response. In contrast, the k_{min} and k_{max} values chosen by Welton and Bethe evaluate to $\frac{k_{max}}{k_{min}} = 13265$ for hydrogen; that is very different from the experimentally correct number, and again invalidates their calculation.

With our $\frac{k_{max}}{k_{min}} = 2\pi$ input parameter choice, the $\ln\left(\frac{k_{max}}{k_{min}}\right)$ factor evaluates to $\ln\left(\frac{k_{max}}{k_{min}}\right) = 1.838$. This relatively small number means that the spectral range, where the bound electron responds to vacuum noise in the same way as free particle, is actually quite narrow. From equation 6.2.15, the δr parameter evaluates to 29.125 fm.

In order to evaluate the effect of the δr parameter on the average potential, we calculate the first and second order Taylor expansion terms of the potential at $\vec{r} + \vec{\xi}$, where $\vec{\xi}$ is a small random displacement from $\vec{r}$:

$$U\left(\vec{r} + \vec{\xi}\right) = U\left(\vec{r}\right) + \vec{\xi} \cdot \nabla U\left(\vec{r}\right) + \frac{1}{2} \sum_{ij} \xi_i \xi_j \partial_i \partial_j U\left(\vec{r}\right) \tag{6.2.16}$$

The timewise averages of $\vec{\xi}$ are $\bar{\xi} = 0$ and $\overline{\xi_i \xi_j} = \frac{1}{3} \vec{\xi}^{\,2} \delta_{ij} = \frac{1}{3} (\delta r)^2 \delta_{ij}$, where δ_{ij} is the Kronecker delta symbol. The $\frac{1}{3}$ factor appears since the variance of a random displacement is equally split among the three spatial dimensions. We evaluate the time averaged potential value at some location:

$$\overline{U\left(\vec{r} + \vec{\xi}\right)} = U\left(\vec{r}\right) + \frac{1}{6} (\delta r)^2 \nabla^2 U\left(\vec{r}\right) \tag{6.2.17}$$

The second term of the above equation gives the Lamb shift effect. $\nabla^2 U\left(\vec{r}\right)$ is non-zero only at the nucleus, and we use Gauss' law to evaluate it:

$$\nabla^2 U\left(\vec{r}\right) = -\nabla^2 \frac{Ze}{4\pi\epsilon_0 r} = \frac{\rho\left(\vec{r}\right)}{\epsilon_0} \tag{6.2.18}$$

In the above expression, the $\rho\left(\vec{r}\right)$ symbol denotes the charge density at a given coordinate $\vec{r}$. Now we can evaluate the electron's potential energy by integrating over the radial coordinate:

$$U_p = e \int \psi^2(r) \, \overline{U} 4\pi r^2 dr = e \int \psi^2(r) \, U(r) \, 4\pi r^2 dr + \frac{Ze^2}{6\epsilon_0} (\delta r)^2 \psi^2(0) \tag{6.2.19}$$

The first term of the above formula is the usual Coulomb potential energy, and the second term is the Lamb shift of this potential. The relationship between the electron's potential and kinetic energies is given by the virial theorem. In the non-relativistic limit, the electron's kinetic energy is half of its electrostatic potential, and we may write the Lamb shift of the electron energy as follows:

$$E_{Lamb} = \frac{Ze^2}{12\epsilon_0} (\delta r)^2 \psi^2 (0) \tag{6.2.20}$$

Equation 6.2.20 is remarkable because we already have all the information for evaluating it. The p type wavefunction has a vanishing probability at the origin, while the s type wavefunction has a non-zero probability at the origin. Therefore the Lamb shift influences the potential energy of s type wavefunctions only.

We use the experimental $2s \to 2p$ and $3s \to 3p$ Lamb shift values of hydrogen and muonium for validating our calculation. The results are shown in table 1; our $\frac{k_{max}}{k_{min}}$ parameter choice indeed gives the rather precise Lamb shift values, with less than 2% error. The nuclear mass impacts the binding energy calculation via the a_0 parameter's above-described dependence on the nuclear mass; the correct nuclear mass accounting of our calculation is validated by the muonium entry of table 1.

Orbital transition	Nucleus type	Calculated $s-p$ Lamb shift	Experimental $s-p$ Lamb shift
$2s \to 2p$	p^+	1044 MHz	1058 MHz
$2s \to 2p$	μ^+	1037 MHz	1047 MHz
$3s \to 3p$	p^+	310 MHz	315 MHz

TABLE 1. The calculated and experimental $2s \to 2p$ and $3s \to 3p$ Lamb shift values for atomic hydrogen, and $2s \to 2p$ Lamb shift values for muonium. The calculation is based on equation 6.2.20.

While the Lamb shift of the $1s$ state cannot be directly observed, it can be indirectly measured from the $2s \to 1s$ transition energy, by comparing the experimental transition energy against the Dirac equation based calculation and subtracting $2s$ Lamb shift. Table 2 compares the experimental $1s$ Lamb shift energies against equation 6.2.20 based calculation. The difference between calculation and experiment again has 2% error.

Nucleus type	Calculated $1s$ Lamb shift	Experimental $1s$ Lamb shift
Muonium	8298 MHz	8095 MHz
Hydrogen	8354 MHz	8173 MHz
Deuterium	8358 MHz	8184 MHz

TABLE 2. The calculated and experimental $1s$ Lamb shift values for muonium, hydrogen, and deuterium. The experimental measurement is based on the $2s \to 1s$ transition measurement, and the calculation is based on equation 6.2.20.

Recent measurements [**10**] also reveal the Lamb shift values of an electron around a $Z = 2$ nucleus. Regarding this $Z > 1$ case, equation 6.2.20 implies approximately Z^4 dependence: there is a Z dependence of the first term, a Z^3 dependence of the $\psi^2 (0)$ term. In the $Z = 2$ case, the $2s \to 2p$ Lamb shift estimation with this simple Z^4 dependence yields 16.7 GHz, which compares reasonably well with the measured value of 14.04 GHz. The 14.04 GHz experimental value of $2s \to 2p$ Lamb shift at $Z = 2$ implies $Z^{3.7}$ dependence of the Lamb shift. The $2s \to 2p$ Lamb shift measurement on heavier nuclei, such as oxygen [**11**], indicates that this $Z^{3.7}$ dependence remains fairly constant.

In summary, we showed that the Lamb shift can be accounted for as an electron-noise interaction. Our calculation yields the approximately correct Lamb shift dependence on the nuclear mass, nuclear charge, and orbital quantum number. The experimental Lamb shift data implies $\frac{k_{max}}{k_{min}} \approx 2\pi$ ratio of limiting noise wavenumbers between which the bound electron responds to vacuum noise. This relatively narrow range suggests some type of resonant noise interaction around the electron's wavenumber value, as illustrated in figure 6.2.2. Our result raises the follow-up question of explaining the $\frac{k_{max}}{k_{min}} \approx 2\pi$ ratio.

The obtained δr parameter is an order of magnitude smaller than the electron zitterbewegung radius. For the first time, we clarified why the electron Zitterbewegung structure does not blur the quantum mechanical wavefunction with respect to the nuclear position.

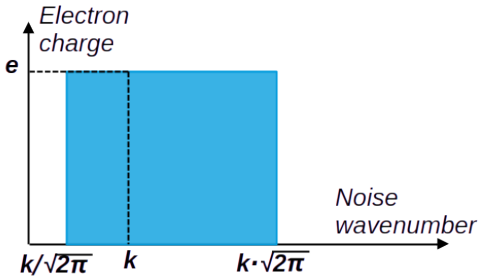

FIGURE 6.2.2. The electron-noise interaction strength for an electron with $p = \hbar k$ momentum. The interaction strength is represented by the shaded area; it is defined by the elementary charge value and by the interacting noise wavenumber range.

6.3. Is QED theory relevant for the Lamb shift calculation?

Historically, two different Lamb shift calculations emerged in the 1940s. Bethe modeled the vacuum noise as random electron-positron charge fluctuations appearing and disappearing [**4**], while Welton modeled vacuum noise as an electromagnetic noise field. In Bethe's model, the appearing "virtual positrons" behave just like real positrons, except for their magical ability of disappearing without any trace, i.e. they should annihilate without producing any 511 keV gamma radiation, which actual positrons always produce upon annihilation. To date, there is no experimental evidence for "virtual positrons", the concept of negative energy remains paradoxical, and we explained why Bethe's k_{min} and k_{max} choices cannot be correct. Bethe's model is also unrealistic in its treating electrons and positrons as point particles, in order to obtain an effect ranging up to tens of femtometers, without giving any consideration to the much larger Zitterbewegung structure of electrons and positrons. There is no reason to give further considerations to Bethe's model.

In contrast, our Lamb shift calculation is based on a realistic electron Zitterbewegung model, and accounts the effect of Lorentz invariant electromagnetic vacuum noise. This electromagnetic vacuum noise has been experimentally measured, as presented for example in [**5**], and also in Casimir–Polder force measurements. Occam's razor principle favors not to add any complicated assumptions about the physical vacuum.

Acknowledgements

This research received partial funding from Marc Fleury (LENR Capital).

Bibliography

[1] W. R. Johnson et al "Accurate Relativistic Calculations Including QED Contributions for Few-Electron Systems", chapter 3 in "Relativistic Electronic Structure Theory" (2004)

[2] T. F. Gallagher "Ionization in linearly and circularly polarized microwave fields", book chapter in "The Electron - New Theory and Experiment" (1991)

[3] T. A. Welton "Some observable effects of the quantum-mechanical fluctuations of the electromagnetic field", Physical Review, Volume 74.9 (1948)

[4] H. A. Bethe "The electromagnetic shift of energy levels", Physical Review, Volume 72.4 (1947)

[5] C. Riek et al Direct sampling of electric-field vacuum fluctuations", Science, Volume 350 (2015)

[6] T. H. Boyer "Any Classical Description of Nature Requires Classical Electromagnetic Zero-Point Radiation", American Journal of Physics, Volume 79.11 (2011)

[7] H. E. Puthoff "Quantum ground states as equilibrium particle–vacuum interaction states", Quantum Studies: Mathematics and Foundations, Volume 3 (2016)

[8] S. Agrawal "A Stochastic View of Quantum Mechanics" (2020)

[9] J. Lindgren et al. "The Heisenberg uncertainty principle as an endogenous equilibrium property of stochastic optimal control systems in quantum mechanics", Symmetry, volume 12.9 (2020)

[10] A. van Wijngaarden et al Lamb shift in He^+", Physical Review A, Volume 63 (2001)

[11] G. P. Lawrence et al Measurement of the Lamb Shift in the O Ion", Physical Review Letters, Volume 28 (1972)

CHAPTER 7

Are space-time curvature effects relevant to electron modeling?

Andras Kovacs[1]
[1] Exafuse. E-mail: andras.kovacs@broadbit.com

7.1. Introduction

What is the role of space-time metrics in the description of fundamental forces and interactions? In preceding chapters, we showed how the linear $\boldsymbol{\partial}^2\boldsymbol{A}_{\square} = 0$ Maxwell equation accounts for particle mass as electromagnetic field energy and accounts for particle spin as the magnetic moment of the circulating electromagnetic wave. However, this linear $\boldsymbol{\partial}^2\boldsymbol{A}_{\square} = 0$ equation cannot account for the elementary charge quantization; a different elementary charge value would be just a scaling factor adjustment for the particle mass and spin calculation. In Natural units, the elementary charge value is $e = \sqrt{\alpha}$, where α is the electromagnetic fine structure constant. The constant value of e and α indicates that they are determined by a nonlinear equation, whose solutions are only stable at a specific value of e and α. Identifying the nonlinear dynamics, which is responsible for charge and mass quantization, requires a proper understanding of spacetime metrics in the context of charged elementary particles. The main goal of this chapter is to establish the methodology of spacetime metrics calculation in the microscopic limit. Specifically, we present the involved concepts in as clear terms as possible, and point interested readers to references where further details can be found.

As mentioned in the book's introduction, the motion of planets was first described and predicted by epicycloid formulas. Newton discovered that planetary motion is caused by gravitational forces, given by the $F_{gravity} = G\frac{mM}{r^2}$ formula. While Newton's formula has the same the accuracy as epicycloids for predicting planetary motion, it represents a deeper understanding of elementary interactions and gives a unified method to calculate the motion of planets, falling apples, and rockets. A next level of understanding gravitational forces was given by Einstein's general relativity theory. As illustrated in figure 7.1.1, general relativity allows us to identify mass with spacetime curvature or more precisely to identify the stress-energy-momentum tensor with the Ricci curvature tensor. In this theory, a planet moves along a straight line (geodesic) in its locally flat spacetime, which corresponds to a trajectory of a closed ellipsoid loop in the globally curved spacetime. Moreover, although one may calculate approximately the same planetary trajectory via Newton's gravitational force over a flat spacetime or via Einstein's spacetime gravitational field equations, nevertheless they are different from both an ontological and physics perspective. The new insights gained through the concepts and equations of general relativity involve a paradigm shift. For example, as illustrated in figure 7.1.1, general relativity gives a unified method to calculate the motion of planets and the gravitational deflection of electromagnetic waves. Thus we gained new knowledge with respect to Newton's theory, which failed to say anything about light deflection.

The Reissner-Nordström metric of general relativity describes how electromagnetic field energy curves spacetime. This suggests the following thought experiment: consider two electrically charged cannon balls

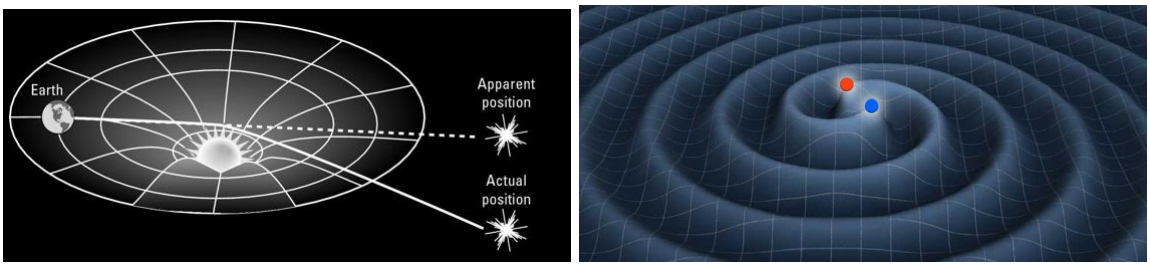

FIGURE 7.1.1. An illustration of gravitational spacetime curvature (top) and electromagnetic spacetime curvature (bottom).

orbiting around their center of mass, such that the gravitational forces are negligible in comparison with electric forces. Applying Maxwell's equations over a flat spacetime, we may calculate the trajectory of these balls spiraling into each other, as well as the radiated electromagnetic wave during this process. Alternatively, we can calculate the space-time curvature, which is not constant in this case, but rather a rotating spiral as shown in figure 7.1.1. Upon lengthy calculations, we would arrive at the same geodesic trajectory result as obtained by applying Maxwell's equations over a flat spacetime metric. So far there is nothing controversial, and the involved relativistic equations are well known. We might now ask: what happens when the balls are scaled down to a microscopic level so that the mass to charge ratio is very small? As the ball radius shrinks, electromagnetic fields get more intense, which generates more curved spacetime. Intuitively, the role of spacetime curvature should be immense in quantum mechanics. However, quantum mechanics yields precise binding energy values without any accounting of spacetime curvature effects. It means that, if spacetime curvature is relevant in the microscopic context, it is already incorporated into the Dirac equation. We address this topic as well in the last section.

7.2. Electromagnetic fields' geometric interpretation via the Riemann metric tensor

Ever since the discovery of general relativity, it remained an open challenge to determine whether its scope can be extended to also include electromagnetic forces and interactions. Such an extension has been Einstein's dream of unifying gravity with electromagnetism. A novel insight of Jussi Lindgren is that the spacetime metric tensor, which defines spacetime distances and curvature, also encodes electromagnetic fields and charges starting from the following simple relationship:

$$g_{\mu\nu} = \eta_{\mu\nu} + CA_\mu \otimes A_\nu \tag{7.2.1}$$

where $g_{\mu\nu}$ is the spacetime metric tensor, $\eta_{\mu\nu}$ is the Minkowski metric, and A is the electromagnetic four-potential, and C is a constant. The dimension of this C constant is the inverse of $A_\mu \otimes A_\nu$, so that $CA_\mu \otimes A_\nu$ becomes dimensionless. The evolution of this metric can be calculated via the methodology of general relativity, and it leads to a nonlinear form of Maxwell's equation. However, according to Jussi Lindgren's calculations, in the limit where the metric approaches the Minkowskian $\eta_{\mu\nu}$ metric, Maxwell's equation takes the same $\boldsymbol{\partial}^2 \boldsymbol{A}_\square = 0$ form that was introduced in chapter 1. Jussi Lindgren also demonstrated to the author that the charge-carrying longitudinal wave of chapter 2 is a longitudinal wave of spatial compression in this context. This methodology is an other perspective that leads to the same results as our present work. The quantized electron mass and charge values imply that, at close proximity to an electron, spacetime curvature sufficiently differs from the Minkowskian $\eta_{\mu\nu}$ metric: electrodynamics is then governed by a non-linear equation in some microscopic regions. We leave it to interested readers to calculate for themselves the timewise evolution of equation 7.2.1.

In hindsight, it is clear that the mistaken imposition of electromagnetic gauges prevented an earlier unification of gravitational and electromagnetic theories.

In the linear regime of Maxwell's equation, electromagnetic waves pass through each other without scattering. In this linear regime, the electron wave does not scatter a photon wave. It follows from equation 7.2.1 that the limit between linear and non-linear regimes depends on the wave intensity.

At the vacuum noise intensity, we saw in chapter 6 that an electron interacts with photons only when the electron and photon wavenumbers match within a $\frac{k_{max}}{k_{min}} = 2\pi$ range. For an electron wave, the generalized Maxwell equation's non-linear terms thus differ from zero only within this specific wavenumber range, and the electron is essentially transparent to photon wavenumbers outside of this range. As noted in chapter 6, the spectrum of non-linear regime extends further at higher photon intensities. The larger the mismatch between electron and photon wavenumbers is, the larger must be the photon intensity to achieve a certain scattering probability. Correspondingly, it is observed in practice that very high frequency gamma radiation and very low frequency radio waves are the most transparent to electrons.

7.3. Electromagnetic fields' geometric interpretation via Clifford rotors

In section 1.3.2, it was shown that the electromagnetic energy-momentum density vector $\boldsymbol{w}$ is obtained by a rotation of the spacetime base vector γ_t :

$$\boldsymbol{w} = \frac{1}{2\mu_0}\left(\boldsymbol{G}\gamma_t\widetilde{\boldsymbol{G}}\right) \tag{7.3.1}$$

where $\boldsymbol{G}$ is the electromagnetic field vector. Essentially, equation 7.3.1 quantifies how the electromagnetic field intensity twists the time coordinate with respect to the spatial axes. The electromagnetic energy-momentum density thus gains a geometric interpretation, as a twisted space-time metric.

Around an electrically charged particle, the electric field's energy density is proportional to e^2 when the electron mass is fixed. The same applies to magnetic field intensity as well. Therefore, e^2 can be interpreted as a parameter of spacetime twisting. Using Natural units, the elementary charge value is $e^2 = \alpha$, where α is the electromagnetic fine structure constant. In this way, α too can be interpreted as a parameter of spacetime twisting. It has been a long-standing mystery to understand what principle determines these electron parameters.

To explore the elementary charge value's origin, we must understand how the electron wave is stabilized against vacuum noise related distortions. Any electron-stabilizing non-linear process is characterized by e^2, which is the above explained parameter of non-linear spacetime twisting. In chapter 6, we also discovered that an electron scatters vacuum noise only within a $\frac{k_{max}}{k_{min}} = 2\pi$ wavenumber range, and it is transparent to noise wavenumbers outside of this range. When normalized to the electron mass, the electron-noise interaction's non-linear term becomes proportional to $2\pi e^2$. When the deviation from linearity is small, the non-linear term is a second order term. Therefore, this second order term of electron-noise interaction is proportional to $2\pi e^2 = \left(\sqrt{2\pi}e\right)^2$.

It is interesting to observe the following phenomenological relationship, which holds at 99.98% accuracy in Natural units:

$$\sqrt{2\pi}e = \delta_F^{-1} \tag{7.3.2}$$

where δ_F is the Feigenbaum constant. The $\delta_F \approx 4.6692016$ Feigenbaum constant is a fundamental mathematical constant of iterative processes, analogous to π in geometry or to e in calculus. It is a universal constant for any single-parameter quadratic map. In the context of dynamic systems, the Feigenbaum constant is associated with superstable periodic orbits and therefore its relevance to electron Zitterbewegung stabilization is anticipated. If equation 7.3.2 is not a coincidence, we are one step closer to understanding the origin of elementary charge value.

7.4. The Dirac equation's geometric interpretation

As mentioned in the introduction section, the Dirac equation's accurate results imply that it already accommodates the effects of spacetime metrics. Writing down the Dirac equation in terms of spacetime metrics has been accomplished by Paul O'Hara: this work can be found in chapter 5 of reference [1], and we summarize its result in table 1. In chapter 5, we clarified the Dirac equation's meaning in simple terms. In particular, equation 5.2.8 shows how to write the Dirac equation in a dual form: this yields two mathematically equivalent equations that have complementing dimensionality. Based on this approach, the key insight of Paul O'Hara is to use Cartan's spinor eigenvalue method to associate the quadratic polynomial of the metric

$$ds^2 = g_{\mu\nu} dx^\mu dx^\nu \tag{7.4.1}$$

with a spinor eigenvalue equation:

$$ds\xi = \gamma_a dx^a \xi \tag{7.4.2}$$

where γ_a are the Clifford basis vectors of space-time, ξ is a spinor, and $g_{\mu\nu}$ is the spacetime metric tensor given by equation 7.2.1. Equation 7.4.2, in a natural way, maps spinors directly to the metrics of general relativity. As a next step, one may derive how the spinor ξ of equation 7.4.2 relates to the dual of space-time vectors.

On the one hand, each vector $\frac{\partial}{\partial x^a}$ can be mapped to a dual one-form dx^a. This produces to the second column of table 1. On the other hand, the Dirac equation is recognized as the linearized form of the Klein-Gordon equation, where the wavefunction is defined to yield the energy eigenvalue upon time differentiation and to yield the momentum eigenvalue upon spatial coordinate differentiation. In the dual eigenvalue equation, the dual basis vectors γ^a are obtained via the $\gamma_a = I\gamma^a$ assignment, where $I \equiv \gamma_{txyz}$ is the Clifford pseudo-scalar. It can be clearly seen from table 1 that the mc^2 term of the Dirac equation corresponds to the $\frac{\partial \psi}{\partial s} = \frac{mc}{\hbar}\psi$ eigenvalue assignment, the $\hbar$ term is a scaling factor defined by the electromagnetic vacuum noise, and the i term corresponds to the Clifford pseudo-scalar. The Dirac equation can be therefore interpreted as a purely geometric equation, where the mc^2 term directly relates to space-time metric.

In table 1, the mass term's dimensionality also matches the dimensional analysis of chapter 5. Considering that ds yields the length of a vector, the m term of its dual expression must represent a volume quantity. This is in line with the equation 5.2.8, that shows the duality between the Dirac equation's vector and tri-vector mass term formulations. We showed in chapter 3 that the electron mass is calculated

	Space-time metrics	Dual of the metric	Dirac spinor definitions	Eigenvalue of the dual metric
Length	ds	$\frac{\partial\psi}{\partial s}$		mc^2
Time difference	dt	$\frac{\partial\psi}{\partial t}$	$\epsilon=\frac{\partial\psi}{\partial t}$	ϵ
Spatial distance	dx	$\frac{\partial\psi}{\partial x}$	$pc=\frac{\partial\psi}{\partial x}$	pc
Eigenvalue eq.	$ds\xi = \gamma_a dx^a \xi$	$\frac{\partial\psi}{\partial s} = \gamma^a \frac{\partial\psi}{\partial x^a}$	$\gamma_a = I\gamma^a$	$\left(mc^2\right)\psi = i\hbar\gamma^a \frac{\partial\psi}{\partial x^a}$

TABLE 1. The relationship between space-time metrics and Dirac's eigenvalue assignments

by electromagnetic field energy integration over a volume of space; the electron mass must indeed have volume dimension.

In summary, the three approaches outlined in this chapter are three perspectives of the same underlying physics. It is fascinating that both the Maxwell and Dirac equations can be compactly expressed as geometric relations of the spacetime metric. We are perhaps a step closer to understanding the origin of the elementary charge value, whose existence implies non-linear dynamics.

Acknowledgements

The author thanks Paul O'Hara and Jussi Lindgren for helpful discussions and suggestions.

References. [1] A. Kovacs, P. O'Hara et al "Unified Field Theory and Occam's Razor", World Scientific (2022)

CHAPTER 8

Do magnetic monopoles exist? Are they excited electron states?

Andras Kovacs[1]
[1] Exafuse. E-mail: andras.kovacs@broadbit.com

8.1. Introduction

This chapter reviews experiments relating to magnetically charged particles. Surprisingly, several experiments indicate that certain particles might be magnetically charged. If magnetic monopoles exist, then the relevant theoretic background for their understanding is in section 1.3.4, where we derived the equations describing magnetic charges and magnetic charge currents.

On the one hand, the title of this chapter contains a question mark because a confirmation of magnetic monopoles' existence requires the elimination of any alternative interpretations to the measurements described in this chapter. On the other hand, the collected set of experiments is compelling.

Prior monopole-related theories considered magnetic monopoles as particles comprising only magnetic charge [**1**]. However, the following experiments show that magnetically charged particles are also electrically charged. Therefore, magnetic monopoles may not be stand-alone particles, but meta-stable excited electron states, which decay back into an ordinary electron.

8.2. Observation of helicoidal particle tracks

Several experimenters reported a direct observation of helicoidal spiraling tracks: examples are shown in figure 8.2.1. The left side of figure 8.2.1 shows a track recorded in a CR-39 detector, which is emitted from a vacuum electrode illuminated by a laser pulse. Its helicoidal radius is 50 microns.

The right side of figure 8.2.1 shows the optical camera recording of a macroscopic particle traveling a low pressure gas, which is emitted from a glowing electrode. This electrically charged particle is moving along the electric field lines between the two electrodes, which have high voltage between them. Surprisingly, it is moving not in a straight line, but along a helicoidal spiraling track: its helicoidal radius is a few millimeters. The simplest explanation for such a helicoidal track is that a magnetic charge is present on the particle; the magnetic equivalent of the Lorentz force then causes it to spiral along an electric field line. This observation inspires to look for direct experimental evidences of magnetic monopoles.

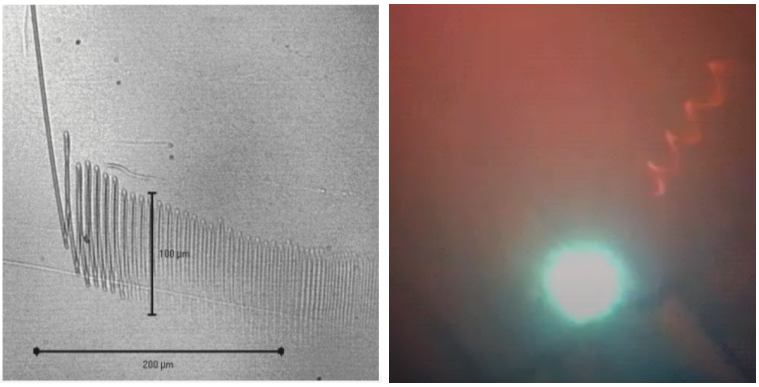

FIGURE 8.2.1. Left: a helicoidal track in a CR-39 detector, reproduced from [**7**]. Right: a helicoidal track emitted from an electrode into low-pressure gas, presented in [**9**].

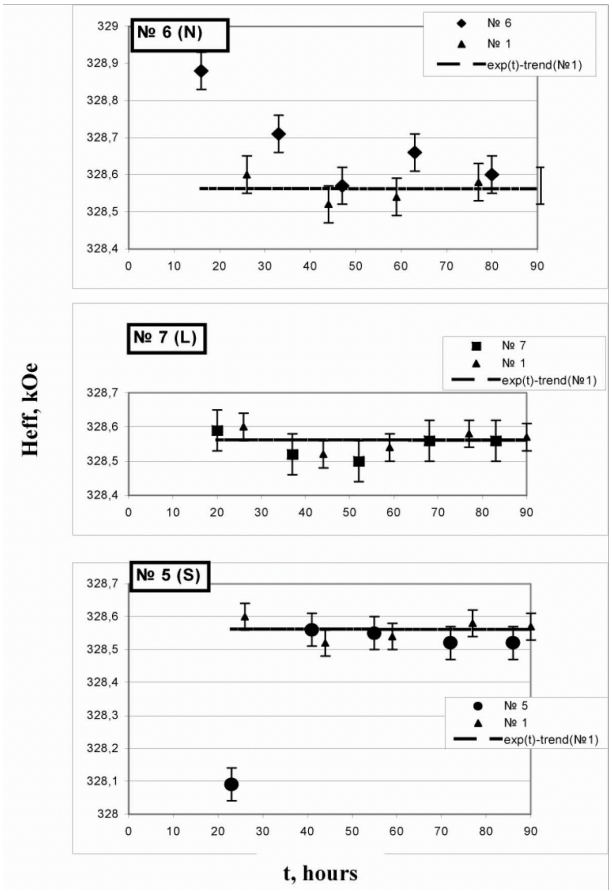

FIGURE 8.3.1. Effective magnetic field (H_{eff}) on the ^{57}Fe nucleus, obtained via Mössbauer spectrum measurements. Samples 5,6,7 were exposed to magnetic monopoles generated by electric discharge, prior to the first measurement. Sample 1 is the unexposed control sample. The N, S, L symbols indicate the North, South, and Lengthwise parallel orientation of a magnet placed behind the iron foil during discharge, with respect to the electric discharge location. Reproduced from [**2**].

8.3. Direct observations of magnetically charged particles

In the following paragraphs we review experiments that could be interpreted as magnetic monopoles' direct observations.

The authors of reference [**2**] placed ^{57}Fe foils near the reactor with underwater exploding titanium wire, and placed a magnet behind the ^{57}Fe foils. As shown in figure 8.3.1, the orientation of the magnet has a measurable effect on the Mössbauer spectrum of ^{57}Fe nuclei, but only in those cases when the foil is placed near the reactor. The authors of [**2**] interpret this effect in the following way: the ^{57}Fe foil captures emitted magnetic monopoles, and opposite magnetic charges shift the effective magnetic field (H_{eff}) on the ^{57}Fe nucleus into opposite directions.

The author of [**7**] observed that the emitted particle tracks form two beams when a magnetic field is applied in his experiment, and they fly towards the two poles of the applied magnet. A photo of these beam-forming tracks is shown in figure 8.3.2. Such tracks are therefore interpreted as magnetic monopole tracks, which separate into two beams according to their magnetic charge.

Vladimir Chizhov placed a container of hydrated nickel powder, that underwent prior heat treatment, into a cloud chamber. There was a magnetic field in the cloud chamber; the red arrows on figure 8.3.3 indicate the magnetic field lines. Figure 8.3.3 contains two frames from a video recording, which shows a particle track emerging from the hydrated nickel powder. The curvature of this track is different than the track of an electrically charged particle, which would spiral around the magnetic field lines. Instead, the emitted particle track may be interpreted as a parabolic curve. The emitted particle initially moves upwards, then the parabola has a peak at a certain height, and subsequently the particle track continues downwards. Such track dynamics is consistent with the movement of a magnetically charged particle.

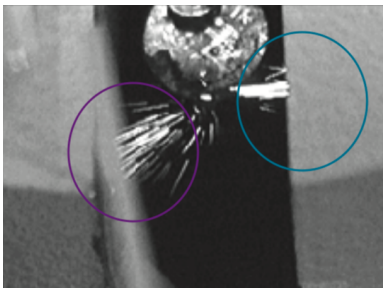

FIGURE 8.3.2. Particle tracks emitted from a laser-pulse illuminated electrode. Two beams are formed, which are flying towards the two poles of a magnet. Reproduced from [**7**].

An other observation of cloud chamber track emission from post-experiment hydrated nickel was also reported in [**8**].

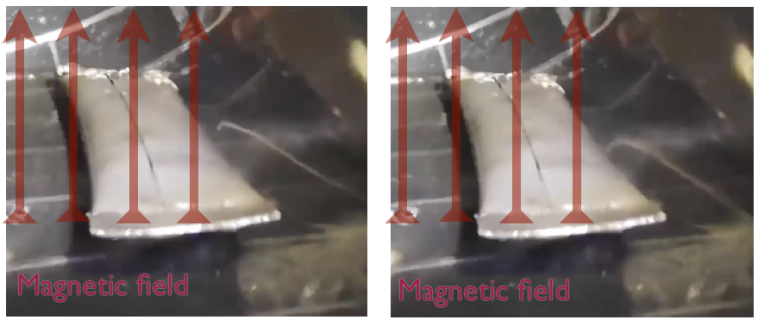

FIGURE 8.3.3. Two frames from a video recording which shows a particle track emerging from a container of hydrated nickel powder, that underwent prior heat treatment. This container is in a cloud chamber, and the red arrows indicate the direction of the applied magnetic field. Data provided by V. Chizhov.

At the JINR institute in Dubna, a group led by Vladimir A. Nikitin analyzed pair creation tracks in a bubble chamber, where particle-antiparticle pairs were generated from energetic photons [**3**]. Upon the analysis of 7000 such tracks, the authors of [**3**] found 47 anomalous lepton tracks. The analysis of these tracks revealed that they are produced by 5-10 MeV mass particles, that eventually decay into an electron or positron. In two cases, the decay event was captured on the track photo. Figure 8.3.4 shows such a particle pair creation event and the subsequent decay of the negatively charged lepton particle. As can be seen in figure 8.3.4, the decay process is actually a two-step decay, and an electron is produced upon the second decay step. The final electron track is a small circle at end of the lepton track. The bubble chamber is under 1.5 T magnetic field, with magnetic field lines being perpendicular to the photographic plane, and electrically charged energetic particles' helicoidal tracks appear as circles from this perspective.

As can be observed in figure 8.3.4, the track of the negatively charged lepton follows an elliptic track. The analysis of reference [**3**] assumes that any deviation from a circular track is caused by the gradual deceleration of an energetic particle; but in this case the curvature radius must be constantly decreasing. However, a deceleration effect is in contradiction with the elliptic track shown in figure 8.3.4. Such a track can be only caused by the particle moving up and down along magnetic field lines, demonstrating that a magnetic charge accelerates the particle in perpendicular direction to the photographic plane. Figure 8.3.4 is therefore a direct evidence of an elementary particle that comprises both electric and magnetic charges.

References [**4, 5, 6**] describe a series of experiments, where magnetic monopole observations were claimed upon illuminating ferromagnetic nano-particles by intense visible light. In these experiments, the tracks of illuminated and falling nano-particles are well visible. The method of magnetic charge measurement is outlined in figure 8.3.5: it is a direct measurement method, and analogous to Millikan's method for measuring the elementary electric charge. Thousands of particle tracks were analyzed in these series of experiments.

These experiments discovered that magnetic monopoles are produced most effectively by circularly polarized light. The sign of the produced magnetic monopole charge depends on the chirality of the

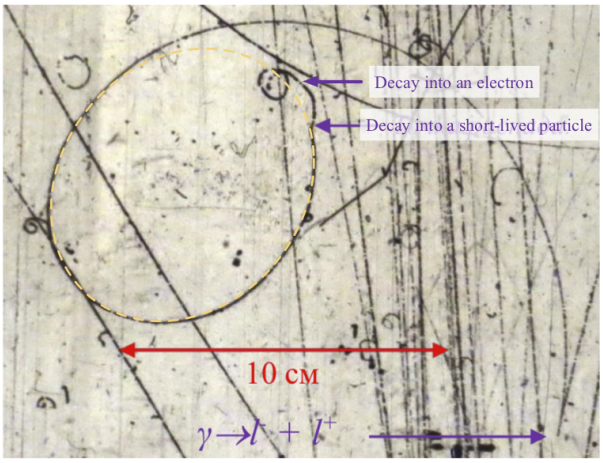

FIGURE 8.3.4. Heavy lepton pair creation in a bubble chamber. A lepton-antilepton pair is created at the bottom right corner. The other two purple arrows indicate the two decay events. The yellow dashed ellipse shows the elliptic track fitting of the negatively charged lepton. Photograph provided by V. A. Nikitin.

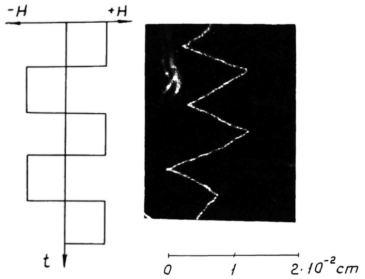

FIGURE 8.3.5. Magnetic charge measurement methodology: a time-varying magnetic field (left) causes a zig-zag pattern of a falling nano-particle's track (right), when it is magnetically charged. The magnetic charge is calculated from the analysis of track photographs. Reproduced from [**6**].

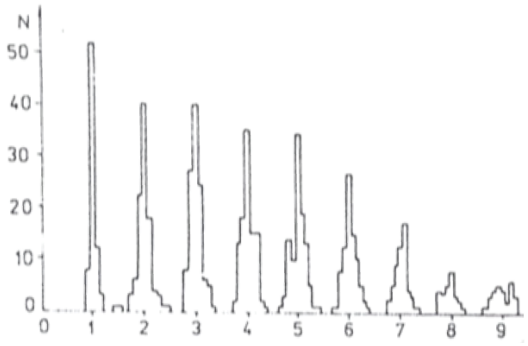

FIGURE 8.3.6. A measurement of the magnetic charge quantum. The vertical scale shows the number of samples in the histogram. The horizontal scale shows the magnetic charge value, where the unit 1 corresponds to the magnetic charge quantum value of $g = 5.84 \times 10^{-13}$ gauss cm^2. Reproduced from [**4**].

applied circularly polarized light; opposite light chiralities produce opposite magnetic charges in the ferromagnetic nano-particles.

The authors of [**4, 5, 6**] succeeded in measuring the magnetic charge quantum, and found its value to be $g = 5.84 \times 10^{-13}$ gauss cm^2. Figure 8.3.6 shows the measured magnetic charge quantization. This magnetic charge quantum value is $g = \frac{\alpha^2}{2.92} g_D = \frac{\alpha^2}{5.84} g_S$, where g_D is the Dirac monopole charge and g_S is the Schwinger monopole charge. This data is unexpected by current mainstream theories, which

anticipate the magnetic monopole charge quantum to be g_D or g_S, which stem from the $\frac{g_D}{e} = \frac{c}{2\alpha}$ and $\frac{g_S}{e} = \frac{c}{\alpha}$ assumptions.

We now compare the above measurement results against the electric charge quantum. Table 1 shows the experimentally measured elementary electric and magnetic charge values, expressed in natural units. We notice their charge ratio to be approximately $2\alpha^{\frac{3}{2}}$.

	elementary electric charge	elementary magnetic charge
Charge	$\left[e = \sqrt{\alpha} \approx 8.543 \cdot 10^{-2}\right]_{NU}$	$\left[g = \frac{\alpha e}{5.84} \approx 2\alpha^2 \approx 1.065 \cdot 10^{-4}\right]_{NU}$

	magnetic/electric charge ratio
Charge ratio	$2\alpha^{\frac{3}{2}}$
Field energy density[1]	$4\alpha^3$

TABLE 1. A comparison between the electron charge and its excited state magnetic charge, expressed in Natural Units.

The surprisingly small magnetic charge quantum of table 1 suggests that, under suitable conditions, it only takes a relatively small energy to add a meta-stable magnetic charge to an electron. This explains why the authors of references **[4, 5, 6]** could use intense light to produce magnetic monopole excitations, where the involved excitation energy is on the order of 1 eV.

Different experiments give varying half-life estimates to magnetic monopoles. References **[4, 5, 6]** report less than 1 sec half-life, while figure 8.3.1 indicates several hours half-life. Apparently, the half-life value depends on the environment in which the monopole charge is embedded.

We leave it for the reader to decide whether the herein reviewed magnetic monopole claims altogether prove the existence of magnetically charged electron states, or whether there is an alternative explanation to these experimental data.

Acknowledgements

The author thanks György Egely for drawing attention to the literature on magnetic charge measurements, and thanks Vladimir Chizhov for making his measurement results available.

[1] measured at a given distance from the charge

Bibliography

[1] G. Lochak "The Equation of a Light Leptonic Magnetic Monopole and its Experimental Aspects", Zeitschrift für Naturforschung, Volume 62a (2007), Pages 231-246

[2] N. G. Ivoilov et al "The influence of strange radiation on Mössbauer spectrum of Fe57 in metallic foils", Annales de la Fondation Louis de Broglie, Volume 29, 3 (2004)

[3] M. Ch. Anikina, V. A. Nikitin, V. S. Rikhvitskiy "Search for New Charged Particle in Mass Interval 2–100 MeV", Communication of the Dubna Joint Institute for Nuclear Research, 1-2022-62 (2022)

[4] V. F. Mikhailov et al "Magnetic charge in the experiments by F. Ehrenhaft and their modern development", Acta Physica Universitatis Comenianae, Volume 29 (1989)

[5] V. F. Mikhailov "Observation of apparent magnetic charges carried by ferromagnetic particles in water droplets", Journal of Physics A, Volume 24, 53 (1991)

[6] V. F. Mikhailov "Six Experiments with Magnetic Charge", in "Advanced Electromagnetism" (editors T. W. Barrett, D. M. Grimes), World Scientific (1995)

[7] V. A. Skvortsov et al "Main Physical Properties of Exotic Quasiparticles", Proceedings of EXON-2014 International Symposium (2015)

[8] E. Campari et al "Photon and particle emission, heat production and surface transformation in Ni–H system", proceedings of the ICCF-11 International Conference on Condensed Matter Nuclear Science (2005)

[9] R. Greenyer "VEGA - Even more extraordinary traces", https://youtu.be/8a4tnh9yCco

[10] P. Ruello et al "Physical mechanisms of coherent acoustic phonons generation by ultrafast laser action", Ultrasonics, Volume 56 (2015)